

https://dspace.org/

Membrane domain localization of HIV-1 subtype C gp41 and receptor proteins in cultured HIV-1 target cell lines

Jamieson, Emma

2010-10-18
http://hdl.handle.net/10539/8835

Downloaded from a DSpace repository. https://dspace.org/

MEMBRANE DOMAIN LOCALIZATION OF HIV-1 SUBTYPE C GP41 AND RECEPTOR PROTEINS IN CULTURED HIV-1 TARGET CELL LINES

Emma Jamieson

A dissertation submitted to the Faculty of Health Sciences, University of the Witwatersrand, in fulfilment of the requirements for the degree of Master of Science in Medicine

JOHANNESBURG, 2009

DECLARATION

I, Emma Jamieson declare that this dissertation is my own work. It is being submitted for the degree of Master of Science in Medicine, in the University of the Witwatersrand, Johannesburg. It has not been submitted before for any degree or examination at this or any other University.

.....

Emma Jamieson

.....

Date

This work is dedicated to my parents, the rest of my family and to Brendon. Thank you for all your love and massive amounts of much needed support.

… so long to devotion

It taught me everything I know

Wave goodbye, wish me well

You've gotta let me go

Are we human or are we dancer?

(The Killers, Human)

ABSTRACT

In recent years there has been much progress in understanding and defining the key protein structure-function relationships that mediate Human Immunodeficiency Virus (HIV-1) entry into host $CD4^+$ cells. This process involves fusion of the virus and host cell membranes, following engagement of corresponding viral (gp120) and target (CD4) receptor proteins. Binding of gp120 to CD4 triggers extensive conformational changes in gp120, exposing binding sites for the co-receptor proteins (CCR5 or CXCR4), and facilitating insertion of gp41, the viral fusion protein, into the target cell membrane. Following insertion of gp41, oligomerisation of fusogenic domains on gp41 is thought to drive the juxtaposition of the virus and host cell and fusion of their membranes. Recent reports suggest that detergent-resistant membrane domains, known as lipid rafts, play a crucial role in orientating the receptor molecules during this step of HIV-1 infection. Lipid rafts are typically rich in cholesterol, sphingolipids and GPI-anchored proteins, and are biophysically distinct from the glycerophosolipid bilayer, which constitutes the bulk of mammalian cell membranes. The role of lipid rafts in virus entry, however, is still controversial, and further experimentation is needed to define their importance in this regard. To provide insight into the role of lipid rafts during HIV-1 entry, we evaluated the natural distribution of the host receptor proteins in HIV-1 target cells (U87.CD4.CCR5/CXCR4). CD4 was detected in membrane samples fractionated by sucrose density gradient centrifugation using immunoblotting techniques, while CCR5 and CXCR4 were detected on whole cells by fluorescence microscopy. We then used a primary CCR5-utilising subtype C HIV-1 isolate (FV5) to characterise dynamic changes in the distribution of these receptors and gp41 during viral entry in real-time. Viral fusion assays were set up by inoculating

target cells with FV5 at 23 °C, a temperature that allows HIV-1 attachment, but is non-permissive for advancement of the fusion reaction. This prefusogenic form of the virus-host receptor complex is defined as the temperature-arrested state (TAS). We found that, under normal, uninfected conditions, CD4, CCR5 and CXCR4 are distributed throughout both raft and non-raft microdomains on the U87 cell surface, and there is little evidence for any significant redistribution of these receptors into lipid rafts during the HIV-mediated fusion reaction. Interestingly, we observed a change in the structure of CD4 during the fusion process, which could describe a functionally important event in HIV-1 entry, or be related to compromises in the integrity of the virally-infected membranes. Moreover, we discovered that gp41 is capable of membrane insertion and oligomerisation at TAS, in contrast to previous reports that suggest the fusion peptide is not capable of breaching the membrane at this temperature. Our results provide valuable novel insights into the HIV-1 subtype C entry process, and the involvement of lipid rafts in this stage of the viral lifecycle, that may be relevant to novel therapy and immunogen design.

ACKNOWLEDGEMENTS

To my supervisor, Dr Alexio Capovilla, thank you for all your support and ambition with this project. You pushed me to the limits of my mental capacity and more, by constantly challenging me and the ideas that were raised during this project. Your invaluable insight ongoing optimism has been much appreciated.

To Catherine Bell and Carol Crowther, thank you for the all your assistance with my fluorescence microscopy experiments. Also, thank you to Dr Clem Penny for the use of your fluorescence microscope and for your help with my experiments, particularly with all the troubleshooting.

Thank you to Kuben Naidoo and the Red Cell Membrane Research Unit for the friendly faces, very useful advice and usage of numerous items of laboratory equipment.

Thank you to the University of the Witwatersrand, PRF and Elevation Biotech for the much needed financial support.

To my lab mates, Maria Antropova, Natasha Pillay, Thenusha Naidoo, Qasim Fish, Mark Killick, Katherine Michler, Naazneen Moolla and Nichole Ceruti, thank you for all the laughs, squash games and general support. Specifically, thanks Kath for your lovely singing in the lab and all your help with my cloning and sequencing, thanks Naaz for your amazing kindness and your willingness to listen and give advice whenever I needed it, and thanks Nichole for dancing with me through the tough times, giving me strong support, brilliant insight and plenty of good giggles.

TABLE OF CONTENTS

DECLARATION ..... **II**

ABSTRACT ..... **IV**

ACKNOWLEDGEMENTS ..... **VI**

TABLE OF CONTENTS ..... **VII**

LIST OF FIGURES ..... **xiii**

LIST OF TABLES ..... **XV**

LIST OF ABBREVIATIONS ..... **XVI**

CHAPTER 1: INTRODUCTION **1**

1.1 HIV and AIDS **2**

1.1.1 Human Immunodeficiency Virus and the Global AIDS Epidemic 2

1.1.2 Genomic Organisation and Classifications of HIV-1 4

1.1.3 Structure and Life-Cycle of HIV-1 5

1.2 Entry of HIV-1 into Host Cells **9**

1.2.1 General Overview of the Entry Process 9

1.2.2 Host Cell Proteins Involved in HIV-1 Entry and Membrane Fusion 10

1.2.2.1 CD4 Receptor 10

1.2.2.2 CCR5 and CXCR4 Co-receptors 11

1.2.3 Viral Proteins Involved in HIV-1 Entry and Membrane Fusion 12
1.2.3.1 gp120 13
1.2.3.2 gp41 14
1.2.3.3 gp41 and the Fusion Process 15

1.3 Lipid Rafts 18
1.3.1 What are Lipid Rafts? 19
1.3.2 Biological Relevance of Lipid Rafts 20
1.3.3 Lipid Rafts and HIV 22
1.3.3.1 Budding of HIV 22
1.3.3.2 Entry of HIV 23
1.3.3.3 Therapeutic Applications 24

1.4 Project Perspective 25

CHAPTER 2: MATERIALS AND METHODS 27

2.1 Cell Culture 28

2.2 Cloning of gp41- and gp160-Expression Plasmids 28
2.2.1 PCR Amplification of gp41-Encoding DNA 29
2.2.2 Preparation of gp160-Encoding DNA for Cloning 30
2.2.3 Generation of Recombinant gp41- and gp160-Expression Vectors 30
2.2.3.1 Digestion and Ligation of pTriEx and gp41/gp160 Fragments 31
2.2.3.2 Colony Screening Procedures 32
2.2.3.3 Sequencing of pTriEx-gp41 and pTriEx-gp160 33

2.3 Expression of gp41 in Bacterial Cell Culture 33

2.4 Protein Purification and Concentration of gp41 34

2.4.1 Analysis of Protein Solubility 34

2.4.2 Preparation of Protein Samples to be Purified 35

2.4.3 Preparation of Columns 35

2.4.4 Purification Procedure 36

2.4.5 Concentration of Recombinant gp41 37

2.5 Expression of gp160 in Mammalian Cell Culture 37

2.6 Total Membrane Isolation 38

2.7 Lipid Raft Isolation 39

2.8 Western Blot Analysis 39

2.9 Immuno-Slot Blot Analysis 40

2.10 Fluorescence Microscopy Analysis of Co-receptor Localization 41

2.10.1 Cell Preparation on Chamber Slides 41

2.10.2 Visualisation of Slides under Fluorescence Microscope 42

2.11 Infections and Fusion Studies 42

2.11.1 Infections 43

2.11.1.1 Amplification of Virus 43

2.11.1.2 Post-Infection Analyses 43

2.11.2 Fusion Studies 44

CHAPTER 3: RESULTS 46

3.1 Generation of Recombinant gp41- and gp160-Expression Vectors 47

3.2 Expression and Purification of gp41 51

3.3 Expression of gp160 54

3.4 Analysis of Membrane Domain Localization of HIV-1 Receptor Proteins CD4, CCR5 and CXCR4 in Uninfected Cells 56

3.4.1 Western Blot Analysis of CD4, CCR5 and CXCR4 Receptors 56

3.4.2 Fluorescence Microscopy Analysis of CXCR4 and CCR5 Receptors 60

3.5 HIV-1 and Fusion Studies 64

3.5.1 Amplification of FV3 and FV5 Viral Isolates 64

3.5.2 Fusion Studies 66

CHAPTER 4: DISCUSSION 72

4.1 Cloning of gp41- and gp160-encoding DNA 73

4.2 gp41 Recombinant Protein 73

4.3 gp160 Expression in HEK 293T Cells 75

4.4 Receptor Localization in Membrane Domains 75

4.4.1 CD4 Localization 76

4.4.2 CXCR4 and CCR5 Localization 77

4.5 HIV-1 and Fusion Studies 79

4.5.1 Amplification of FV3 and FV5 80

4.5.2.1 gp41 Localization at TAS and 3 Hours Post-TAS 82

4.5.2.2 CD4 Localization at TAS and 3 Hours Post-TAS 83

4.5.2.3 CCR5 Localization at TAS and 3 Hours Post-TAS 86

4.5.2.4 Additional Comments on Fusion Studies....87

4.6 Concluding Remarks....88

APPENDICES....90

Appendix A: Standard Protocols and Recipes....91

A1 Bacterial Cell Culture....91

A1.1 Solutions for Bacterial Culture....91

A1.2 Preparation of Competent DH5α Cells....92

A1.3 Transformation of Competent *E. coli* Cells....93

A1.4 Plasmid Preparations of pTriEx-3 and pGA4-gp160....93

A2 Agarose Electrophoresis....94

A2.1 Solutions for Agarose Electrophoresis....94

A2.2 Preparation of Agarose Gels....95

A2.3 Electrophoresis Procedure....95

A3 Mammalian Cell Culture....96

A3.1 Solutions for $CaCl_2$ Transfections....96

A3.2 $CaCl_2$ Transfection Protocol....96

A4 Protein Purification....97

A4.1 Solutions for Protein Purification....97

A4.2 Preparation of Columns for Purification Procedure....98

A5 Cell Counting....99

A6 SDS-PAGE....99

A6.1 Solutions for SDS-PAGE....99

A6.2 Preparation of SDS-PAGE Gels....102

A6.3 Electrophoresis Procedure....102

A7 Staining Procedures 103
A7.1 Solutions for Staining Procedures 103
A7.2 Protocols for Staining Procedures 103
A8 Western- and Immuno-Slot Blotting 104
A8.1 Solutions for Western Blotting 104
A8.2 Solutions for both Western Blotting and Immuno-Slot Blotting 105
A8.3 Western Blotting Procedures 105
A9 Standard Chemiluminescence Methods 107
A10 Fluorescence Microscopy Analysis 108
A10.1 Solutions for Fluorescence Microscopy Analysis 108
A10.2 Antibodies used for Fluorescence Microscopy Analysis 108

Appendix B: Restriction Map Diagrams 110

Appendix C: Nucleotide Sequence Alignment of gp160 and gp41 Clones 111

Appendix D: p24 Results for Infections and Fusion Experiments 113

Appendix E: Viral Load Calculations 114

Appendix F: Western Blot Analysis of CXCR4 and CCR5 Membrane Domain Localization 114

Appendix G: Western Blot Analysis of gp41 During Fusion Experiments 115

Appendix H: Ethics Waiver and Biosafety Clearance 116

REFERENCES 117

LIST OF FIGURES

Figure 1.1: Schematic representation of the HIV-1 genome..... 4

Figure 1.2: Structure of a mature HIV-1 virion. 6

Figure 1.3: HIV-1 lifecycle. 8

Figure 1.4: Ribbon representation of CD4 (PDB File 1CDH).....11

Figure 1.5: Ribbon representation of gp120 (PDB 1GC1).....13

Figure 1.6: Schematic representation of gp41 domains.....15

Figure 1.7: Representation of the coiled coil structure of gp41. 16

Figure 1.8: Schematic representation of HIV-1 fusion process. 17

Figure 1.9: Diagram showing organisation of lipid rafts within cell membranes.....20

Figure 3.1: Agarose gel electrophoresis of PCR products and restriction digestion analysis.49

Figure 3.2: Amino acid sequence alignment of gp41 and gp160 clones. 50

Figure 3.3: Analysis of gp41 expression, solubility and purification.....53

Figure 3.4: Diagram showing the principle of membrane flotation by sucrose density gradient centrifugation.....55

Figure 3.5: Western Blots showing gp160 expression in HEK 293T cells. 55

Figure 3.6: Slot- and Western Blots of U87 X4 and U87 R5 raft and membrane extractions.59

Figure 3.7: Localization of CXCR4 receptor in U87 membrane and lipid raft domains. 62

Figure 3.8: Localization of CCR5 receptor in U87 membrane and lipid raft domains. 63

Figure 3.9: gp41 Western Blot analysis of FV3 and FV5 virus-containing supernatants following amplification in U87 X4 and U87 R5 cell, respectively. 65

Figure 3.10: Slot Blot and Western Blot analysis of FV5 fusion studies. 69

Figure 3.11: Localization of CCR5 receptor in lipid raft domains.....70

Figure 3.12: Localization of CCR5 receptor in membrane domains. 71

Figure D1: p24 analysis of (A) FV3 and FV5 infections for amplification of virus for fusion experiments, and (B) FV5 infections in flasks and on slides for confirmation of infection during fusion experiments. 113
Figure F1: Western Blot analysis of CXCR4 and CCR5 receptor localization. 114
Figure G1: Western Blot analysis of gp41 localization from FV5 fusion studies. 115

LIST OF TABLES

Table A1: Table of Antibodies used in Western Blotting 106

Table A2: Table of Antibodies used for Fluorescence Detection.....108

LIST OF ABBREVIATIONS

AIDS	Acquired Immune Deficiency Syndrome
ATP	Adenosine Triphosphate
BCD	β-Cyclodextrin
BSA	Bovine Serum Albumin
CA	Capsid Protein
CCR5	Chemokine (C-C Motif) Receptor 5
CD^+	CD4 Positive
CD4	Cluster of Differentiation 4
CD59	Complement Regulatory Protein
CO	Codon Optimized
CRFs	Circulating Recombinant Forms
CT	Cholera Toxin
CXCR4	CXC Chemokine Receptor 4
DAPI	4', 6 Diamidino-2-Phenylindole
dH_2O	Distilled Water
DMEM	Dulbecco's Modified Eagle Medium
DNA	Deoxyribonucleic Acid
dNTPs	Deoxynucleotide triphosphates
DRMs	Detergent-Resistant-Membranes
E. coli	*Escherichia coli*
ELISA	Enzyme-Linked Immunosorption Assay
Env	Envelope

FCS	Fetal Calf Serum
FI	Fusion Inhibitor
FITC-Labelled	Fluorescein-Labelled
FP	Fusion Peptide
gp120	Surface Glycoprotein 120
gp160	Envelope Glycoprotein 160
gp41	Transmembrane Glycoprotein 41
GPI	Glycosylphosphatidylinositol
GPL	Glycerophospholipid
HAART	Highly Active Antiretroviral Therapy
HEK 293T Cells	Human Embryonic Kidney 293T Cells
His-Tag	Histidine-Tag
HIV	Human Immunodeficiency Virus
HR	Heptad Repeat
HRP	Horseradish Peroxidase
HTLV	Human T-Cell Leukaemia Virus
IN	Integrase
IPTG	Isopropyl-β-D-Thiogalactopyranoside
kDa	KiloDaltons
LAV	Lymphadenopathy-Associated Virus
LB Broth	Luria-Bertani Broth
Lck	Leukocyte-Specific Protein Tyrosine Kinase
MA	Matrix Protein
MHC	Major Histocompatibility Complex
MOI	Multiplicity Of Infection

MPER	Membrane-Proximal Region
Mw	Molecular Weight Marker
NC	Nucleocapsid Protein
NIAID	National Institute of Allergy and Infectious Diseases
NIH	National Institute of Health
NVC	Non-Virus Control
PBS	Phosphate Buffered Saline
PCR	Polymerase Chain Reaction
PE-Labelled	Phycoerythrin-Labelled
PIC	Preintegration Complex
PR	Protease
PTF Primer	pTriEx-3 Forward Primer
PTR Primer	pTriEx-3 Reverse Primer
R 5	CCR5
RNA	Ribonucleic Acid
RT	Reverse Transcriptase
SDF-1	Stromal Cell Derived Factor 1
SDS-PAGE	Sodium Dodecyl Sulphate Polyacrylamide Gel Electrophoresis
SIV	Simian Immune Deficiency Virus
T-TBS	Tris-Buffered Saline containing 0.1% Tween-20
TAE Buffer	Tris-Acetate-EDTA Buffer
TAS	Temperature-Arrested State
TBS	Tris-Buffered Saline
$TCID_{50}$	50% Tissue Culture Infectious Dose

TCR	T Cell Receptor
TFR	Transferrin
Thy-1	Thymocyte Antigen 1
TUB	Tubulin
U87 R5	U87.CD4.CCR5
U87 X4	U87.CD4.CXCR4
V1/2/3/4/5	Variable Loop 1/2/3/4/5
X4	CXCR4
Zap-70	Zeta-Chain-Associated Protein Kinase 70

CHAPTER 1: INTRODUCTION

1.1 HIV and AIDS

1.1.1 Human Immunodeficiency Virus and the Global AIDS Epidemic

Acquired Immune Deficiency Syndrome (AIDS) was first recognized as a disease in 1981 by the United States Centers of Disease Control (CDC, 1981). It is characterised by a depression in cellular immunity due to a decline in CD4-positive ($CD4^+$) T-lymphocytes (Gottlieb et al., 1981). Homosexual or bisexual males, intravenous drug users, Haitian immigrants to the United States of America, haemophiliacs treated with blood transfusions, and heterosexuals belonging to a high-risk sexual behaviour group and infants born to parents in this group were reported to be at risk for AIDS (CDC, 1982). This specific group of affected patients, as well as the increasing incidence of the disease, led scientists to suggest that AIDS was caused by an infectious agent that could be transmitted sexually or by blood contact (CDC, 1982; Gallo et al., 1984).

The Human Immunodeficiency Virus (HIV) is now known to be the causative agent of AIDS (Barre-Sinoussi et al., 1983; Gallo et al., 1984). The virus was initially isolated from patients showing AIDS or AIDS-like symptoms. It was shown to be a retrovirus and was initially suspected of being related to the human T-cell leukaemia virus (HTLV-I) family (Barre-Sinoussi et al., 1983). Later, it was also shown to have similarities with lymphadenopathy-associated virus (LAV) and HTLV-III (Levy et al., 1984; Popovic et al., 1984). Eventually, in 1986, this AIDS-associated virus was designated the Human Immunodeficiency Virus (Coffin et al., 1986; Palca, 1986). Evidence then surfaced that a second, less virulent HIV existed

(Clavel et al., 1987; Marlink et al., 1994). The nomenclature of HIV was then changed and separated into HIV-1 and HIV-2.

There are approximately 33 million people living with HIV worldwide, with the number of new infections reported annually decreasing from 3 million in 2001 to 2.7 million in 2007. The number of children, under the age of 15, infected annually is 370 000, which has been declining since 2002. The number of annual AIDS deaths of children under the age of 15 has also been dropping. This is thought to be largely due to the expansion of mother-to-child transmission prevention strategies. Globally, Sub-Saharan Africa still remains the region that is most affected by HIV and AIDS, accounting for 67% of all people living with HIV and for 72% of total AIDS deaths in 2007. Moreover, almost 90% of children infected with HIV live in Sub-Saharan Africa[1].

At present there is no vaccine or cure for HIV-1 infection, although a variety of therapeutic agents have been developed against the major proteins involved in the different stages of the HIV-1 lifecycle. Current standard treatment for HIV-1 infection is termed highly active antiretroviral therapy (HAART) (Turpin, 2003; Barbaro et al., 2005), which involves a combination of at least two of the reverse transcriptase (RT) inhibitors plus either a protease (PR) inhibitor or another RT inhibitor. These drugs are, however, expensive and often have serious toxic side effects. In addition, the virus has the potential to mutate and become resistant to the drugs. For these reasons, the development of alternative therapeutic/vaccine approaches is an ongoing priority [Reviewed in (Broder, 2010)].

[1] UNAIDS. 'Report on the Global HIV/AIDS Epidemic 2008: The Executive Summary',.<www.unaids.org> [Accessed May 2009].

1.1.2 Genomic Organisation and Classifications of HIV-1

HIV-1 is a lentivirus that is classed as a T-lymphotropic retrovirus (Barre-Sinoussi et al., 1983). During replication, this retrovirus is able to perform a multitude of biochemical functions with an approximately 9.5 kb genome comprising only nine genes (Figure 1.1), encoding at least sixteen proteins (Leitner et al., 2005). Three of the nine genes encode structural proteins (*gag, pol, env*), two have regulatory functions (*tat, rev*), and four have been designated accessory genes (*vif, vpr, vpu, nef*) (Leitner et al., 2005). Of the genes encoding structural proteins, *gag* encodes the capsid, nucleocapsid and viral matrix proteins, *pol* encodes protease, reverse transcriptase, RNase H and integrase proteins, and *env* codes for the surface glycoprotein gp120 and the transmembrane glycoprotein gp41 (Leitner et al., 2005).

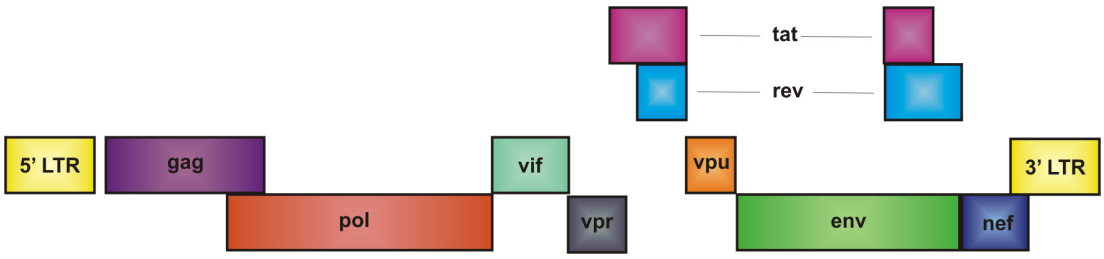

Figure 1.1: Schematic representation of the HIV-1 genome. Figure adapted from Peterlin and Luciw (Peterlin and Luciw, 1988).

HIV-1 has been shown to be closely related to the Simian Immune Deficiency Viruses (SIVs) found in chimpanzees and it is believed that it is from these SIVs that HIV-1 originally diverged (Peeters et al., 1989; Eigen and Nieselt-Struwe, 1990; Gao et al., 1999). HIV-1, has over many years, become genetically diverse and has been classified phylogenetically

into three distantly related groups[2] (Robertson et al., 2000; http://www.hiv.lanl.gov/, 2009). Group M is the 'major' group that is responsible for the global pandemic and phylogenetic analysis of the envelope (e*nv*) and core (*gag*) genes has identified at least eight genetic subtypes within this group (A, B, C, D, F, G, H, J, K) (Robertson et al., 2000). Group O is the 'outlier' group, the viruses of which have been found in low prevalence in West and Central Africa, as well as in Europe (De Leys et al., 1990; Charneau et al., 1994). Group N is the non-M/non-O group and is a rare form of HIV-1 found in Africa (Simon et al., 1998). Numerous circulating recombinant forms (CRFs) have also been identified within group M, which result from the genomes of different subtypes within the same patient recombining (Robertson et al., 2000).

1.1.3 Structure and Life-Cycle of HIV-1

The typical mature HIV-1 virion consists of an envelope, a core and a matrix (Figure 1.2). The envelope is a lipid bilayer that encapsulates the matrix and core of the virus (Goto et al., 1998). Embedded in this bilayer are surface projections comprised of the gp120 surface glycoprotein and the gp41 transmembrane protein (Leis et al., 1988). A matrix shell lines the inner surface of the viral membrane and is made up of p17 matrix protein (MA) (Leis et al., 1988; Marx et al., 1988; Goto et al., 1990; Rao et al., 1995). In the centre of the virus is the conical capsid core particle, comprising the p24 capsid protein (CA), which encapsulates the viral RNA, nucleocapsid protein (NC), protease (PR), reverse transcriptase (RT) and integrase (IN), as well as the accessory proteins nef, vif and vpr (Gelderblom et al., 1987; Goto et al., 1990; Gelderblom, 1991).

[2] '"Los Alamos HIV Sequence Database." <http://.hiv.lanl.gov/> [Accessed intermittently throughout 2007-2009].

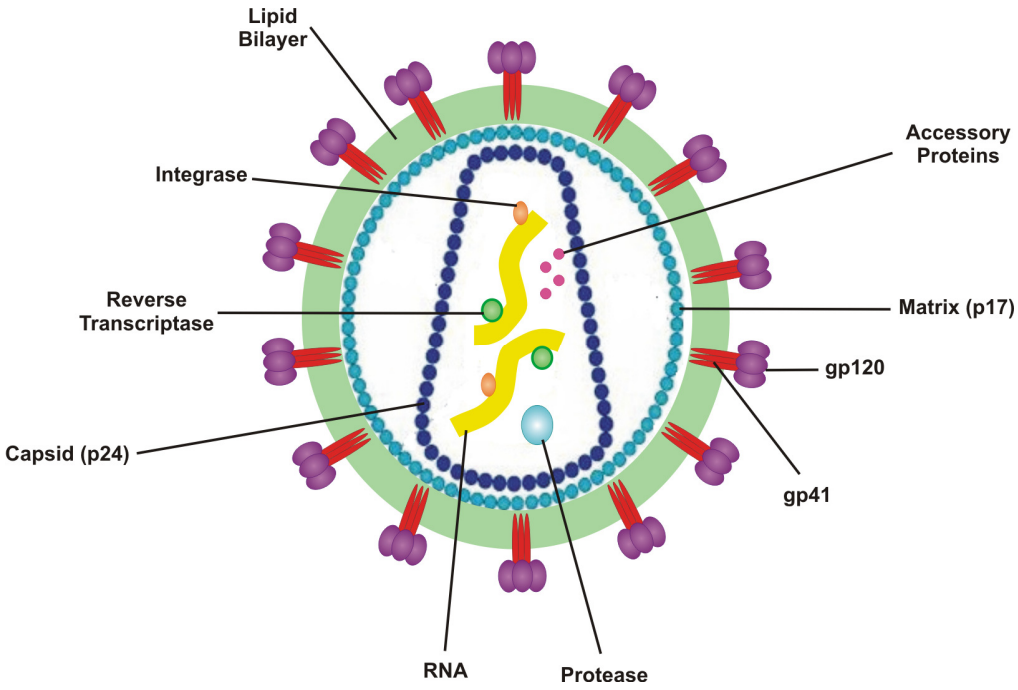

Figure 1.2: Structure of a mature HIV-1 virion.

The replication cycle of HIV-1 (Figure 1.3) involves the initial entry of the virus into the host cell via receptor-mediated endocytosis (Maddon et al., 1986) or cell fusion (Stein et al., 1987). The viral core is then released into the cytoplasm of the host cell and disruption/uncoating of the viral capsid takes place (Grewe et al., 1990). Reverse transcription of the viral RNA then occurs, where double-stranded viral cDNA is synthesized by the reverse transcriptase protein (Fassati and Goff, 2001). The newly synthesized viral cDNA then forms a preintegration complex (PIC) containing viral DNA and integrase (IN), as well as matrix (MA) and reverse transcriptase proteins (Farnet and Haseltine, 1991; Bukrinsky et al., 1993). PICs are transported through the cytoplasm and into the nucleus, using ATP (Bukrinsky et al., 1992), via the cellular cytoskeleton, specifically dynein and the microtubule network (McDonald et al., 2002). Once inside the nucleus, integration of the

PICs into the host cell's genome takes place, which is catalyzed by the IN enzyme (Bowerman et al., 1989; Farnet and Haseltine, 1990).

Once integration is complete, viral messenger RNA (mRNA) is transcribed and transported out of the nucleus (Arya et al., 1985; Feinberg et al., 1986; Nabel and Baltimore, 1987; Tong-Starksen et al., 1987) and the mRNA is translated into viral proteins. Doubly spliced, short viral RNA species are translated into the viral accessory proteins tat, rev and nef. Full-length and singly spliced, long transcripts direct the synthesis of gag, pol and env (Muesing et al., 1985; Sanchez-Pescador et al., 1985), which are then assembled into viral particles together with genomic HIV RNA. The virion matures during budding and release from the host cell surface and then goes on to infect other cells (Varmus, 1988; Goto et al., 1990).

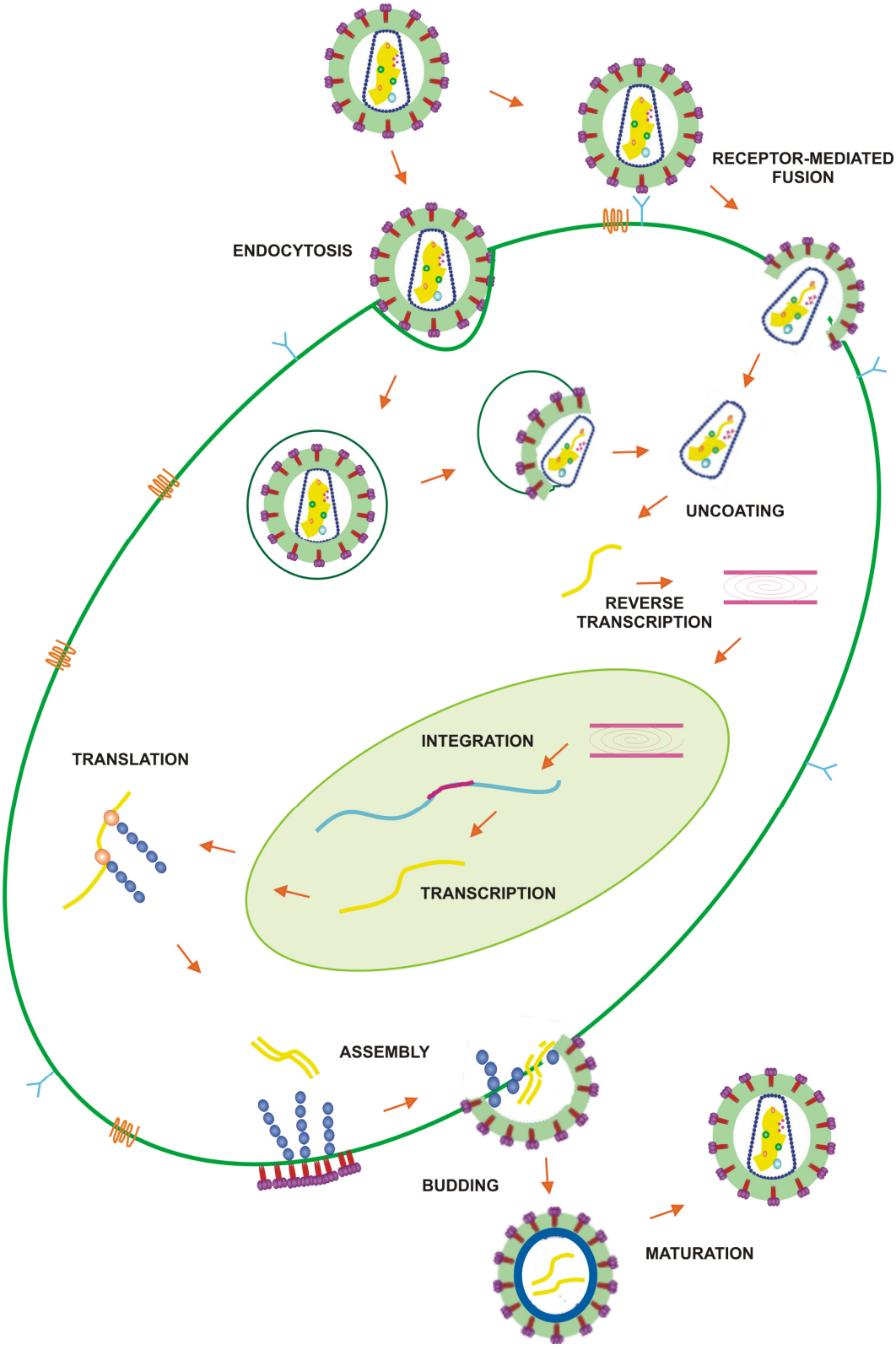

Figure 1.3: HIV-1 lifecycle.

1.2 Entry of HIV-1 into Host Cells

1.2.1 General Overview of the Entry Process

The current model of HIV-1 viral entry describes the coordinated action of the HIV surface envelope glycoprotein (Env) complex and receptors on the host cell (McDougal et al., 1986; Berger et al., 1999; Doms and Moore, 2000). HIV-1 entry into host cells is initiated by the interaction of the gp120 surface glycoprotein on the virus and the CD4 receptor on the host cell surface (Dalgleish et al., 1984; Klatzmann et al., 1984; Maddon et al., 1986; McDougal et al., 1986). This interaction triggers conformational changes in Env that expose gp120 chemokine co-receptor binding sites (Sattentau and Moore, 1991; Trkola et al., 1996; Kolchinsky et al., 2001). The two main chemokine co-receptors utilized by HIV-1 are CCR5 and CXCR4 (Alkhatib et al., 1996; Berson et al., 1996; Deng et al., 1996; Dragic et al., 1996; Feng et al., 1996). Upon gp120-co-receptor binding, further conformational changes occur that result in the exposure of the gp41 N-terminal fusion peptide, believed to be due to shedding of the gp120 subunit caused by the interactions of the gp120 V3 loop with the co-receptor (Moore et al., 1990; Hart et al., 1991; Sattentau et al., 1993; Jones et al., 1998; Huang et al., 2005). The gp41 fusion peptide penetrates the host cell surface, and this leads to the fusion of the viral and host cell membranes and internalisation of the viral capsid (Chan et al., 1997; Tan et al., 1997; Weissenhorn et al., 1997).

1.2.2 Host Cell Proteins Involved in HIV-1 Entry and Membrane Fusion

1.2.2.1 CD4 Receptor

The CD4 (cluster of differentiation 4) receptor is a T-cell surface glycoprotein that associates with major histocompatibility complex (MHC) class II molecules on the surface of antigen-presenting cells to mediate an efficient cellular immune response (Doyle and Strominger, 1987; Gay et al., 1987; Sleckman et al., 1987). It is a 55 kDa protein that consists of an extracellular segment composed of four tandem immunoglobulin-like VJ regions or domains, a transmembrane domain and a cytoplasmic segment (Maddon et al., 1985; Clark et al., 1987; Maddon et al., 1987).

In the mid-80s, it was discovered that CD4 was involved in HIV-1 infection and AIDS, by acting as a target for the interaction with the envelope glycoprotein of HIV-1 and therefore serving as a cellular receptor for HIV-1 entry (Dalgleish et al., 1984; Klatzmann et al., 1984; Maddon et al., 1986; McDougal et al., 1986). Structures for the N-terminal two domains (Figure 1.4) (Ryu et al., 1990; Wang et al., 1990), as well as the entire extracellular segment of CD4 (Wu et al., 1997) have been established. These structures have enabled the determination of the residues on CD4 important for gp120 binding. It has been shown that the gp120 binding site on CD4 is situated in the N-terminus of the first extracellular domain (Arthos et al., 1989; Moebius et al., 1992) and involves the Phe43 residue of CD4 ‘reaching up’ into a large, recessed hydrophobic cavity on gp120 (Arthos et al., 1989; Kwong et al., 1998).

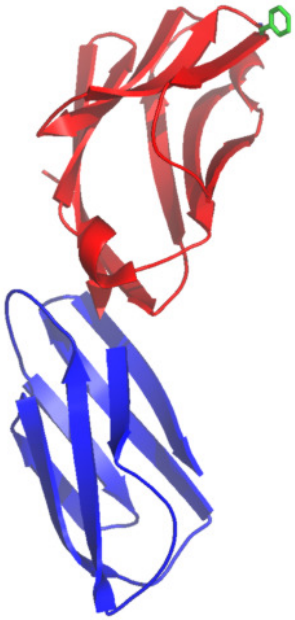

Figure 1.4: Ribbon representation of CD4 (PDB File 1CDH). Domain 1 is shown in red and domain 2 in blue. The Phe43 residue responsible for gp120 binding is shown in stick representation (green) in the first extracellular domain of the CD4 protein. Structure was created using PyMOL.

1.2.2.2 CCR5 and CXCR4 Co-receptors

CXCR4 (Feng et al., 1996), ubiquitously expressed on most haematopoietic cell types, and CCR5 (Raport et al., 1996; Samson et al., 1996), mainly expressed on peripheral blood-derived dendritic cells, T cells and macrophages, are chemokine receptors that belong to the family of seven transmembrane-spanning G protein-coupled receptors. Chemokine receptors are defined by their ability to signal upon binding one or more members of the

chemokine superfamily of chemotactic cytokines (Premack and Schall, 1996; Baggiolini et al., 1997; Yoshie et al., 1997; Luster, 1998; Zlotnik et al., 1999). Feng *et al* first identified CXCR4 as a chemokine receptor that acted as a co-receptor for T cell line-tropic HIV-1 entry (Feng et al., 1996). Lu *et al* thereafter showed how the first and second extracellular loops of CXCR4 were specifically important for gp120 binding and HIV-1 entry (Lu et al., 1997). It was then established that CCR5 also acted as a co-receptor for HIV-1 entry, when it became apparent that macrophage-tropic HIV-1 viral isolates infected cells using CCR5 as a co-receptor (Alkhatib et al., 1996; Deng et al., 1996; Dragic et al., 1996). It has since been determined that it is specifically the second and third extracellular loops of this chemokine receptor that are important in its role as an HIV-1 entry co-receptor (Alkhatib et al., 1997). Dual-tropic viruses have also been shown to exist that can infect both T- and macrophage cell lines (Valentin et al., 1994), using either CXCR4 or CCR5 co-receptors.

1.2.3 Viral Proteins Involved in HIV-1 Entry and Membrane Fusion

The envelope glycoprotein (gp120/gp41) is initially synthesized as a gp160 precursor (Muesing et al., 1985; Ratner et al., 1985; Wain-Hobson et al., 1985) which, in the endoplasmic reticulum, is proteolytically processed into gp120 and gp41 (Veronese et al., 1985) by the cellular protease furin (Gu et al., 1995). A non-covalent gp120-gp41 complex is then positioned on the viral membrane surface (Chatterjee et al., 1992) where the entire gp120 glycoprotein is exposed, anchored to the virus membrane by the gp41 transmembrane subunit (Berman et al., 1988) (Figure 1.2). Functional, fusogenic Env glycoproteins exist as trimers on the viral membrane surface (Weiss et al., 1990).

1.2.3.1 gp120

gp120 is a highly glycosylated and conformationally flexible protein consisting of a recessed and inaccessible conserved core region and five variable regions (V1-V5), which exhibit extensive sequence heterogeneity among different viral isolates (Modrow et al., 1987; Leonard et al., 1990; Profy et al., 1990; Kwong et al., 1999). X-ray crystallography of gp120 demonstrates how the core of this protein is folded into two major domains (Figure 1.5) (Kwong et al., 1998). The domains consist of an inner domain (with respect to the N- and C-termini), from which the V1/V2 loop extends, and a stacked double-barrel outer domain, which includes the V4 and V5 loops (Kwong et al., 1998). These two domains are linked by a four-stranded 'bridging sheet' (Kwong et al., 1998).

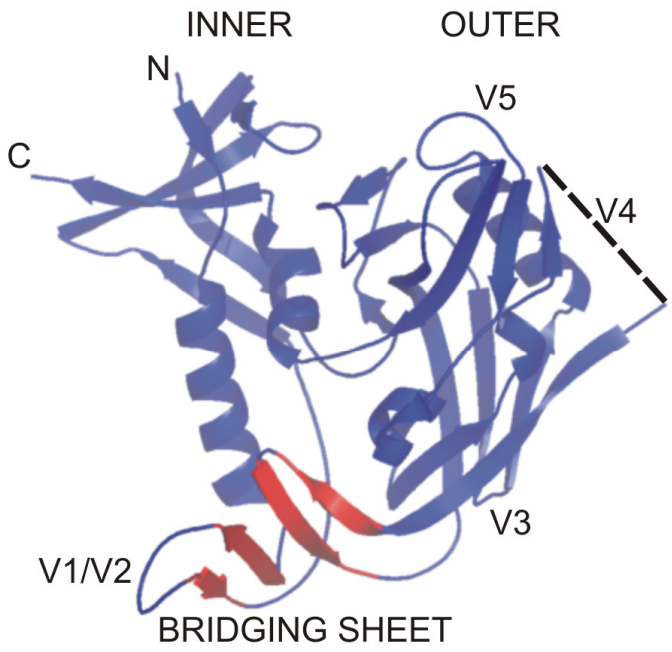

Figure 1.5: Ribbon representation of gp120 (PDB 1GC1). The bridging sheet is shown in red. Structure was created using PyMOL.

Conserved residues on gp120 important for CD4 binding include Trp432, Trp427, Thr257, Asp368, Asp457, and Glu370 (Cordonnier et al., 1989; Olshevsky et al., 1990; Kwong et al., 1998; Wyatt et al., 1998; Kwong et al., 1999). Co-receptor binding and specificity has been shown to be determined by the V3 loop of gp120 (Hwang et al., 1991; Speck et al., 1997; Huang et al., 2005). Binding of gp120 to CD4 and CXCR4/CCR5 then leads to the shedding of gp120, exposing the fusion peptide of the gp41 protein (Moore et al., 1990; Hart et al., 1991; Sattentau et al., 1993; Jones et al., 1998).

1.2.3.2 gp41

The structure of the HIV-1 gp41 transmembrane protein has also been extensively documented. Most of the data accumulated has described the intermediate and post-fusion states of the protein. This transmembrane protein (domain structure shown in Figure 1.6) consists of a hydrophobic fusion peptide (FP) located on the N-terminus (Gallaher, 1987; Gallaher et al., 1989), followed by a N-terminal 'heptad repeat' (N-HR) and C-terminal 'heptad repeat' (C-HR) core structure (Lu et al., 1995; Chan et al., 1997). The Env protein is anchored to the viral membrane by a tryptophan-rich transmembrane domain region and a C-terminal cytoplasmic tail (Gallaher et al., 1989).



Figure 1.6: Schematic representation of gp41 domains. FP = Fusion Peptide, PTM = Proximal to Transmembrane Region, TM = Transmembrane Domain, CT = Cytoplasmic Tail. Adapted from Ingallinella *et al*. (Ingallinella et al., 2009).

Peptides corresponding to the N- and C- terminal regions of the gp41 ectodomain were originally used to generate a stable, soluble gp41 complex (Lu et al., 1995). These peptides, designated N-51 and C-43 respectively, were shown to form a stable, alpha-helical trimer, when mixed together. Lu *et al* proposed that the N-51 peptide 'forms an interior, parallel, homotrimeric, coiled-coil core, against which three C-43 helices pack in an antiparallel fashion' (Lu et al., 1995). They further suggested that this complex is the core that leads to the fusogenic structure of the HIV-1 envelope (Lu et al., 1995). Chan *et al* later identified longer N- and C- terminal regions of gp41, designated N36 and C34 (Figure 1.7) (Chan et al., 1997).

1.2.3.3 gp41 and the Fusion Process

X-ray crystallography has elucidated the mechanism by which gp41 drives membrane fusion (schematic representation shown in Figure 1.8) (Weissenhorn et al., 1997). Weissenhorn *et al* showed how the fusion peptide, which is located at the N-terminus of gp41, inserts into the target membrane. The insertion of the fusion peptide leads to the formation of a 'pre-hairpin intermediate' (Chan and Kim, 1998). This pre-hairpin intermediate consists of the two-

heptad repeat (HR) regions of gp41, N-HR (inserted into the target membrane) and C-HR (anchored to the virus membrane) (Liu et al., 2003). A labile fusion pore is then believed to form before the pre-hairpin intermediate self-assembles into a thermostable 6-helix bundle (Skehel and Wiley, 2000; Markosyan et al., 2003). The formation of the six-helix bundle occurs when the three N-HRs form a parallel, coiled-coil core and the three C-HRs move in between the N-HRs in an antiparallel fashion (Tan et al., 1997; Weissenhorn et al., 1997). This reaction pulls the HIV-1 membrane and the target cell into close proximity therefore allowing for fusion to occur (Weissenhorn et al., 1997).

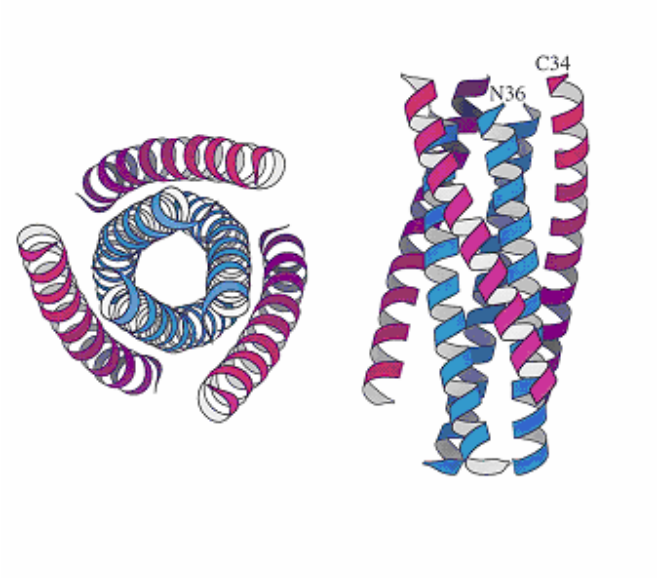

Figure 1.7: Representation of the coiled coil structure of gp41. Blue ribbons represent N36 and pink ribbons represent C34. Taken from Chan *et al.* (Chan et al., 1997).

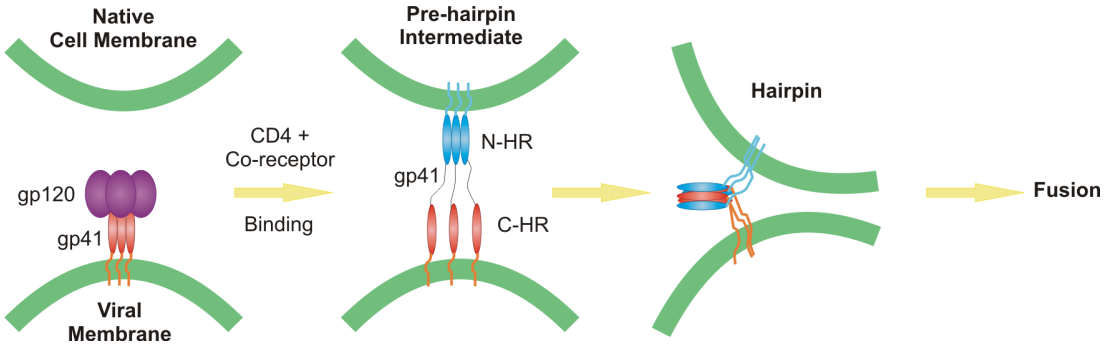

Figure 1.8: Schematic representation of HIV-1 fusion process. Adapted from Koshiba and Chan (Koshiba and Chan, 2003).

The kinetics of HIV/SIV Env-mediated membrane fusion have been extensively studied using fusogenic envelope glycoproteins expressed on the surface of cells (effector cells) interacting with target cells bearing CD4 and appropriate co-receptor (Lifson et al., 1986). A precise measurement of such kinetics was obtained using dye-transfer assays (Dimitrov et al., 1991; Weiss et al., 1996; Munoz-Barroso et al., 1998; Kliger et al., 2001; Lineberger et al., 2002). These assays demonstrate the rapid nature of the fusion process, which is believed to be completed in a time of 20-30 minutes after establishment of the pre-hairpin intermediate (Weiss et al., 1996).

Further insights into gp41 and the fusion process have been gained by the study of temperature dependent fusion intermediates (Munoz-Barroso et al., 1998; Melikyan et al., 2000; Gallo et al., 2001; Golding et al., 2002; Gallo et al., 2004; Mkrtchyan et al., 2005). Intermediate stages of the HIV-1 fusion process have been captured by coincubating effector (E) cells that express fusion proteins on their surfaces and target (T) cells that express appropriate receptors on their surfaces at a temperature (23 ℃), which is slightly below that needed to induce fusion. This state is known as a temperature-arrested stage (TAS)

(Melikyan et al., 2000) and represents the point at which gp120 is engaged with CD4 and the co-receptor (CXCR4/CCR5), prior to formation and maturation of the fusion pore (Melikyan et al., 2000). Increasing the temperature up to 37 ºC then initiates the fusion process. TAS has been used to assess Env interactions with co-receptors and to demonstrate the delay in the late re-folding of gp41 that drives fusion (Mkrtchyan et al., 2005). It has also been utilized to assess entry inhibitor and neutralizing antibody interactions with Env (Munoz-Barroso et al., 1998; Gallo et al., 2001; Golding et al., 2002), as well as to review six-helix bundle and pore formation during fusion (Melikyan et al., 2000; Gallo et al., 2004). Most recently, TAS has been implemented in tracking single virus particle entry via endocytosis, where it was shown that complete HIV-1 fusion occurred in endosomes and that direct viral fusion with the host cell membrane does not progress past the lipid mixing step (Miyauchi et al., 2009).

1.3 Lipid Rafts

Accumulating evidence suggests that certain specialized, plasma membrane components, lipid rafts, play a fundamental role in the HIV-1 entry process. These localized regions of elevated cholesterol within the cellular membrane are believed to be 'hijacked' by HIV-1 and utilized by the virus in both the entry and budding stages of the lifecycle. There are numerous studies showing that HIV-1 buds out of the target cell through these lipid raft microdomains [reviewed in (Campbell et al., 2001; Suomalainen, 2002; Chazal and Gerlier, 2003)]. It is also thought that HIV-1 utilizes lipid rafts in the trafficking or sequestering of CD4 and/or the co-receptors to the point of HIV-1 attachment (Del Real et al., 2002; Nguyen and Taub, 2002; Viard et al., 2002). The latter hypothesis concept is controversial, however, as conflicting evidence has been published (Popik et al., 2002; Percherancier et al., 2003; Popik and Alce, 2004).

1.3.1 What are Lipid Rafts?

The importance of the structure and function of lipid rafts and their role in many biological systems is only beginning to be discovered, and still remains controversial. A great deal of interest surrounds the idea of lipid raft microdomains being present in the cellular membrane, particularly with regard to detection techniques employed. This has led to the questioning of the existence of lipid rafts by some investigators (Jacobson and Dietrich, 1999; Edidin, 2001) and is still an issue of ongoing debate. It is now generally accepted that the cell membrane does not exist as a homogeneous lipid matrix, as initially described by the fluid mosaic model (Singer and Nicolson, 1972). Instead, specialized lipid domains, lipid rafts (Rietveld and Simons, 1998), have been shown to exist in membranes. Lipid rafts are specific detergent-resistant plasma membrane microdomains that are enriched in cholesterol, sphingolipids, glycosylphosphatidylinositol (GPI)-anchored proteins and acetylated signalling molecules (Schroeder et al., 1998).

Sphingolipids are excluded from the cholesterol-poor fluid liquid crystalline (L_C) glycerophospholipid (GPL) bilayer because their acyl chains have a much higher melting temperature than GPLs and are therefore found in much closer association with each other. GPLs are found in a loosely packed disordered state (Thompson and Tillack, 1985). Sphingolipids can therefore organise into specific, cholesterol-rich entities, which form a liquid-ordered (L_O) phase creating lipid raft domains that are situated in and around the more GPL-rich bulk of the plasma membrane (Figure 1.9) (Ahmed et al., 1997). These properties of lipid rafts render them resistant to detergent solubilization (Yu et al., 1973). They are therefore often also referred to detergent-resistant-membranes (DRMs) and have been

isolated from eukaryotic cells by treating the cells with detergents such as Triton-X 100 or Brij 98 (Brown and Rose, 1992; Schroeder et al., 1998; Holm et al., 2003).

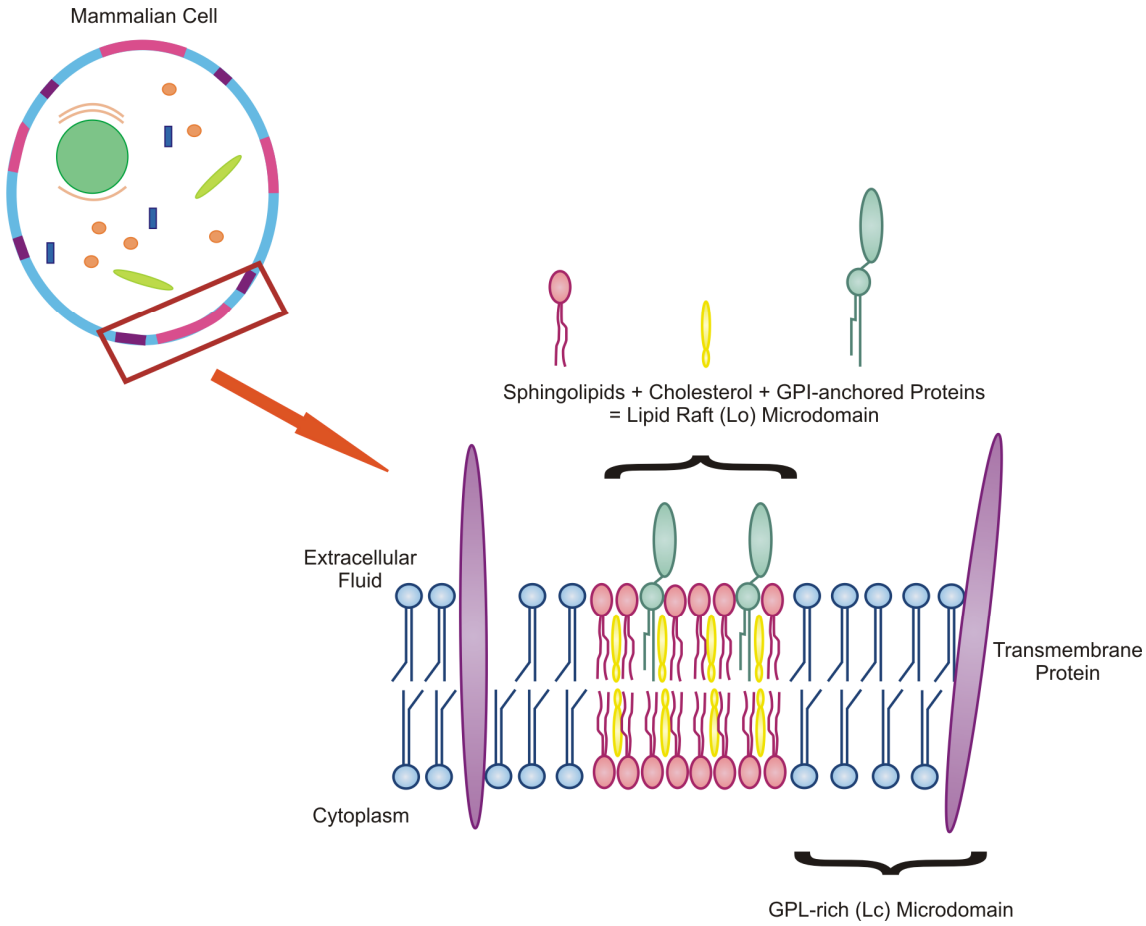

Figure 1.9: Diagram showing organisation of lipid rafts within cell membranes.

1.3.2 Biological Relevance of Lipid Rafts

Several studies have shown that the association of specific membrane proteins with lipid rafts is functionally and physiologically significant (Simons and Ikonen, 1997; Brown and

London, 1998). It has been shown that transmembrane protein receptors associate with lipid rafts during transmembrane signalling events in some haematopoietic cells (Arni et al., 1996; Rodgers and Rose, 1996; Field et al., 1997; Germain, 1997; Isakov, 1997; Kabouridis et al., 1997; Deans et al., 1998). Signalling is also triggered by the clustering or ligation of cell-surface GPI-anchored proteins, which occurs across lipid rafts, particularly, in haematopoietic cells (Thompson and Tillack, 1985; Stefanova and Horejsi, 1991; Brown and Rose, 1992; Cinek and Horejsi, 1992) and neurons (Olive et al., 1995; Zisch et al., 1995). The importance of rafts in exocytic and endocytic transport routes, regulated secretary pathways, cytoskeletal connections, protein transportation between endosomes and the Golgi, and intercompartmental lipid trafficking has been reviewed by Brown and London, 1998; and Ikonen, 2001 (Brown and London, 1998; Ikonen, 2001).

Rafts act as a portal for the entry as well as the assembly and budding of various pathogens. Certain viruses utilize lipid rafts during the entry step of their lifecycles, including simian forest virus and SV40 (Phalen and Kielian, 1991; Nieva et al., 1994). Viruses have also been shown to assemble and bud out of cells through rafts, such as influenza virus, where the virus exits by assembling viral glycoproteins in lipid rafts and trafficking to the point of viral budding at the cell membrane (Zurcher et al., 1994; Keller and Simons, 1998). Rous sarcoma virus (Ochsenbauer-Jambor et al., 2001), murine leukemia virus (Li et al., 2002), measles virus (Manie et al., 2000) and Ebola virus (Bavari et al., 2002) have also been shown to utilize lipid rafts for assembly and budding. Certain bacteria and their toxins exploit lipid rafts to gain entry into their hosts, for example, *Escherichia coli* (Baorto et al., 1997), aerolysin toxin (Abrami et al., 1998), cholera toxin (Tran et al., 1987), and Shiga toxin (Sandvig et al., 1996). Cholera toxin (CT) utilizes lipid rafts for entry into target cells by binding to the receptor ganglioside GM1, which acts specifically in the CT signal transduction pathway by coupling CT with lipid raft microdomains (Badizadegan et al., 2000). GM1

ganglioside allows for the endocytosis and transport of CT into Golgi cisternae and endoplasmic reticulum (Badizadegan et al., 2000). Diseases suggested to be associated with lipid rafts include prion diseases (Taraboulos et al., 1995; Vey et al., 1996; Naslavsky et al., 1997; Klein et al., 1998; Naslavsky et al., 1999) and Alzheimer's disease (Golde and Eckman, 2001; Kakio et al., 2001; Riddell et al., 2001; Kakio et al., 2002).

1.3.3 Lipid Rafts and HIV

Like several other pathogens which involve lipid rafts during their replication cycles, an increasing amount of evidence suggests that HIV-1 also utilizes lipid rafts in both entry into and budding from host cells.

1.3.3.1 Budding of HIV

The budding of HIV-1 out of infected T cells through lipid rafts has been described in detail. Nguyen *et al* were the first to demonstrate that HIV-1 incorporates the raft-specific ganglioside, GM1, as well as GPI-linked proteins Thy-1 and CD59 (Nguyen and Hildreth, 2000). These observations were made using confocal microscopy, which demonstrated that viral proteins co-localized with GM1, Thy-1 and CD59. It was further shown that the HIV-1 matrix (MA) protein and gp41 were found in detergent-resistant, GPI-linked protein-rich fractions, upon membrane fractionation by centrifugation. These results confirmed the association of HIV-1 proteins with lipid rafts and it was proposed that budding occurs through the cholesterol- and sphingolipid-rich domains of the host cell membrane (Nguyen and Hildreth, 2000). These findings were confirmed by Ono *et al*, who demonstrated that

cholesterol depletion significantly impairs virus infectivity by interfering with the budding process (Ono and Freed, 2001). Furthermore, studies have shown that another important function of rafts is to provide a platform for stable binding of Gag to the host cell membrane and for efficient Gag multimerization (Bhattacharya et al., 2004; Bhattacharya et al., 2006; Ono et al., 2007). Lipid rafts are therefore an important cellular component in supporting the assembly and budding process of HIV-1 [reviewed in (Campbell et al., 2001; Suomalainen, 2002; Chazal and Gerlier, 2003)].

1.3.3.2 Entry of HIV

While the role of rafts in the HIV-1 budding process is well documented and in agreement, the involvement of lipid rafts in HIV-1 entry is poorly understood due to contrasting results obtained from different research groups.

Nguyen *et al* have demonstrated that CXCR4 localizes to lipid rafts by disrupting one of the main raft components, cholesterol, using β-cyclodextrin (BCD), which is a chemical known to deplete cholesterol by cleavage of the hydrophobic bonds (Nguyen and Taub, 2002). Depletion of cholesterol in various T cell lines prevented binding of the chemokine ligand, SDF-1, to its natural receptor, CXCR4. This suggests that cholesterol and lipid raft integrity are important for correct CXCR4 functioning. These findings are consistent with those of Viard *et al*, who showed that cholesterol is required for HIV-1 Env-mediated fusion (Viard et al., 2002). Del Real *et al* also claim that a non-raft CD4 mutant prevents X4 and R5 HIV-1 infection of $CD4^+$ T cells (Del Real et al., 2002). Yet further evidence for lipid raft involvement in HIV-1 entry was suggested by Shu *et al*, who suggest that gp41 interacts preferentially with lipid rafts (Shu et al., 2000). This group found that six-helix bundle

formation occurs in the presence of lipid rafts rather than in the GPL-rich membrane environment (Shu et al., 2000).

In contrast, Popik *et al* have published slightly conflicting results in that it was initially shown that productive entry of X4 and R5 HIV-1 into $CD4^+$ T cells does require the presence of intact lipid rafts (Popik et al., 2002). Moreover, it has recently been shown that CD4 receptor localized to non-raft membrane microdomains also supports HIV-1 entry (Popik and Alce, 2004). A novel raft-localizing marker in the membrane-proximal cytoplasmic domain of CD4, namely the RHRRR motif, was identified by this group. When this motif was substituted with alanine residues, CD4 was redirected to non-raft membranes and was still capable of efficiently supporting HIV-1 entry (Popik and Alce, 2004). In addition, Percherancier *et al* suggest that CD4 and CCR5 do not need to associate with lipid rafts in order for HIV-1 entry into target cells to occur (Percherancier et al., 2003). These studies reiterate the importance of identifying and understanding the exact function/s that lipid rafts play in HIV-1 entry into target cells.

1.3.3.3 Therapeutic Applications

The recent insights into the role of rafts in HIV-1 infection have sparked interest into the use of rafts as a potential drug target. The entry stage of the HIV-1 lifecycle has proven to be a potentially successful area for HIV-1 drug development, and more recently lipid rafts have been explored as a possible target for the prevention of HIV-1 entry into target cells. The first well characterised agent to be developed in the new class of fusion inhibitors (FI) is the C-peptide inhibitor, T20 (Wild et al., 1994). There are also a number of co-receptor inhibitors and gp120-attachment inhibitors currently undergoing clinical trials. A promising lipid raft

inhibitor, SP-01A, has recently completed Phase III clinical trials[3]. This inhibitor acts by reducing intracellular cholesterol and biosynthesis of corticosteroid, which inhibits the organisation of lipid rafts in the cellular membrane. This ultimately prevents binding of gp120 with CCR5/CXCR4 and inhibits fusion, as well as having effects on HIV-1 budding.

1.4 Project Perspective

1. Use of primary subtype C viral isolates to study membrane receptor dynamics in real time

This study aims to gain further insights into the roles played by raft and non-raft membrane microdomains in HIV-1 membrane fusion by examining the distribution and re-organisation of the primary HIV-1 and host-cell receptors (gp41, CD4, CXCR4 and CCR5) between these domains during real-time viral infection. So far, studies of the HIV-1 membrane fusion mechanism have utilized cell-cell fusion protocols (Dimitrov et al., 1991; Weiss et al., 1996; Munoz-Barroso et al., 1998; Kliger et al., 2001; Lineberger et al., 2002). Here we aim to quantify the dynamic localization of primary HIV-1 and host cell receptors during real-time infection with primary viral isolates.

[3] Samaritan Pharmaceuticals. "SPA-01A HIV Drug." 2009. <http://www.samaritanpharma.com> [Accessed June-October 2009].

2. Establishment of TAS and an assessment of the effect of this on raft involvement in HIV-1 entry

In order to achieve these outcomes, we describe fusion experiments conducted by arresting the viral fusion process at the temperature-arrested state (TAS), by preincubating U87 host cells with HIV-1 subtype C primary viral isolates at 23 ºC (Mkrtchyan et al., 2005). We assess the localization of CD4, CCR5, CXCR4 and gp41 at TAS and 3 hours post-TAS and observe any changes in the distribution of the receptors and gp41 at these time points. To assess any possible changes, lipid raft and total membrane isolations were performed on infected cells at the two time points. Specific antibody detection methods have been implemented to detect the various receptors and gp41. In addition, we describe the cloning, expression and purification of gp41, to act as a positive control for immunochemical detection of membrane-bound gp41, as well as the cloning and mammalian expression of gp160 to confirm the insertion of gp41 into the host cell membrane.

These studies provide novel qualitative insights into the redistribution of host cell and virus receptors during the early phases of membrane fusion, and the functional significance of lipid rafts during HIV-1 entry that may be relevant to novel therapy and vaccine design.

CHAPTER 2: MATERIALS AND METHODS

2.1 Cell Culture

U87.CD4.CCR5 (U87 R5) and U87.CD4.CXCR4 (U87 X4) cell lines were obtained through the AIDS Research and Reference Reagent Program, Division of AIDS, NIAID, NIH. These cell lines are derived from the U87MG (Human Glioblastoma) cell line, and stably express CD4 and CXCR4 or CCR5. The cells were maintained in Dulbecco's Modified Eagle Medium (DMEM) (Sigma-Aldrich; Steinheim, Germany) supplemented with 15% heat-inactivated fetal calf serum (FCS) (Gibco; Grand Island, USA), L-Glutamine (2 mM) (Gibco; Grand Island, USA), Penicillin (50 U/ml) and Streptomycin (50 U/ml) (Gibco; Grand Island, USA), G418 (500 μg/ml) (Calbiochem; Darmstadt, Germany), and Puromycin (1 μg/ml) (Sigma-Aldrich; Steinheim, Germany). Human Embryonic Kidney (HEK) 293T cells (Invitrogen; Carlsbad, CA) were maintained in DMEM supplemented with 10% FCS and L-Glutamine (2 mM).

2.2 Cloning of gp41- and gp160-Expression Plasmids

gp41-encoding DNA was amplified by PCR and gp160-encoding DNA was excised from a synthetic plasmid template (pGA4-gp160), and both fragments were subcloned into the protein expression vector, pTriEx-3 (Novagen; Darmstadt, Germany) , which is capable of mediating the expression of protein from sequences inserted into the pTriEx multiple cloning site in mammalian, insect and bacterial cells. The resulting recombinant expression plasmids (pTriEx-gp41 and pTriEx-gp160) were used to produce and purify gp41 recombinant protein (expressed in *E. coli*) and transfect mammalian cells, respectively.

2.2.1 PCR Amplification of gp41-Encoding DNA

Amplification of full length gp41 DNA was performed using a synthetic plasmid template, pGA4-gp160, containing a gp160 codon optimized sequence derived from the HIV-1 subtype C isolate, FV3 (accession number DQ382362) (GENEART; Regensburg, Germany). The FV3 viral isolate was isolated from an HIV-positive AIDS patient admitted to the Johannesburg AIDS Clinic, and propagated, sequenced and characterised phenotypically by others in our laboratory (Connell et al., 2008).

Primers for this reaction were designed and synthesized according to the codon optimized gp160 sequence (Inqaba Biotech, Pretoria, Gauteng, South Africa). The gp41 forward primer ($^{5'}$ ATATCCATGGCCGTGGGCATCGGAG $^{3'}$) and the gp41 reverse primer ($^{5'}$ ATATCTCGAGCAGCAGGGCGGCCTCAAAG $^{3'}$) both included 5'-terminal restriction endonuclease recognition sequences (*Xho* I and *Nco* I respectively) to facilitate subsequent cloning procedures into the pTriEx-3 vector (Appendix B).

Direct PCR of the gp41-encoding region was performed using a High Fidelity Expand ^{PLUS} PCR System (Roche; Mannheim, Germany). pGA4-gp160 DNA (approximately 50 ρg/µl) was added to a 100 µl PCR reaction mix, containing 1 x Expand HiFi^{PLUS} Reaction Buffer with 1.5 mM $MgCl_2$, 200 µM dNTPs, 0.4 µM of each gp41 forward and reverse primers and 2.5 U of Expand HiFi^{PLUS} Enzyme Blend. All PCR reactions were carried out using an Applied Biosystems GeneAmp PCR System 9700 (Applied Biosystems; Foster City, CA). An initial hot start at 94 ºC for 3 minutes was followed by a set of 40 cycles with each cycle comprising a denaturation step of 94 ºC for 30 seconds, an annealing step of 60 ºC for 45 seconds and an elongation step of 72 ºC for 3 minutes. Upon completion of the final cycle, a single 10

minute elongation step followed at 72 ºC. Thereafter reactions were cooled to 4 ºC and maintained at this temperature until analysed by gel electrophoresis, or stored at -20 ºC. After analysis of the PCR products on a 0.8% agarose gel (Appendix A2), successful PCR reactions were purified using a HighPure PCR Product Purification Kit (Roche; Mannheim, Germany), according to the manufacturer's instructions.

2.2.2 Preparation of gp160-Encoding DNA for Cloning

A double restriction digest reaction was set up with the restriction endonucleases *Xho* I and *Bsp* HI (*Pag* I) (Fermentas; Ontario, Canada) in order to excise the gp160-encoding DNA from the pGA4-gp160 plasmid. Restriction reactions contained *Xho* I (20 U), *Bsp* HI (20 U), 1 X Fermentas Buffer O, and pGA4-gp160 DNA (1 µg) and were incubated at 37 ºC for 3 hours. The resulting pGA4-gp160 fragments resolved on a 0.8% agarose gel and the gp160-encoding DNA was excised and purified using a MinElute Gel Extraction Kit (Qiagen; Hilden, Germany), according to the manufacturer's instructions. The concentration of the purified gp160 DNA was measured spectrophotometrically (Nanodrop Technologies Inc; Wilmington, DE) and stored at -20 ºC until used in ligation reactions.

2.2.3 Generation of Recombinant gp41- and gp160-Expression Vectors

The amplified gp41 fragment/excised gp160 fragment were sub-cloned into the protein expression vector pTriEx-3 (Novagen; Darmstadt, Germany) (Appendix B). This vector incorporates three different promoters controlling the expression of protein from sequences

inserted into the pTriEx-3 multiple cloning site. This arrangement allows the expression of recombinant proteins in bacterial, insect or mammalian cells.

2.2.3.1 Digestion and Ligation of pTriEx and gp41/gp160 Fragments

The pTriEx-3 vector was prepared for cloning procedures as per methods outlined in Appendix A1.4. Both the pTriEx-3 vector DNA and the amplified gp41 were digested with the restriction endonucleases *Xho* I and *Nco* I (Fermentas; Ontario, Canada). Restriction reactions contained *Xho* I (20 U), *Nco* I (20 U), 1 X Fermentas Tango Buffer, and pTriEx-3 DNA (2 µg) or gp41 DNA (2 µg) and were incubated at 37 ºC for 3 hours. The digested pTriEx-3 vector and gp41 inserts were then resolved on a 0.8% agarose gel, excised and purified using a MinElute Gel Extraction Kit (Qiagen; Hilden, Germany) according to the manufacturer's instructions. gp160-encoding DNA fragments were prepared as per section 2.2.2. Purified vector and insert DNA concentrations were measured spectrophotometrically and stored at -20 ºC until used in ligation reactions.

Ligation reactions were carried out using a Fermentas T4 DNA Ligase Kit (Fermentas; Ontario, Canada) and contained T4 DNA Ligase (1 U), 1 X T4 DNA Ligase Buffer, pTriEx-3 vector DNA (50 ng) and either gp41 insert DNA (50 ng) for pTriEx-gp41 or gp160 insert DNA (125 ng) for pTriEx-gp160 and were set up and incubated overnight at 16 ºC. 5 µl of the ligation mix was then used to transform competent *E. coli* (DH5α) bacterial cells.

2.2.3.2 Colony Screening Procedures

Colonies on positive ligation plates were selected under sterile conditions and cultured in LB Broth containing ampicillin (100 µg/ml). Cultures were incubated overnight at 37 ºC in a shaking incubator.

Initial screening was performed by PCR using a Promega PCR Master Mix (Promega; Madison, WI). Overnight cultures were diluted 1:10 and used in a 20 µl PCR reaction containing 1 X Promega PCR Master Mix and the gp41 forward and gp41 reverse primers described in section 2.2.1. PCR conditions described in section 2.2.1 were used for the amplification of gp41-encoding DNA and PCR products were resolved on a 0.8% agarose gel and visualised under UV light.

The integrity of the clones positive for gp41-/gp160-insertion by PCR was then checked by performing restriction digestion analysis (Appendix B). Recombinant plasmids were isolated from overnight cultures using a Sigma GenElute^{TM} Plasmid Miniprep Kit (Sigma-Aldrich; Steinheim, Germany), according to the manufacturer's instructions. pTriEx-gp41 and pTriEx-gp160 were linearised with *Xho* I and *Bam* HI, respectively (Fermentas; Ontario, Canada), in order to get an accurate estimation of the size of the plasmid containing the insert. A double digestion with restriction endonucleases *Xho* I and *Nco* I or *Xho* I and *Xba* I (Fermentas; Ontario, Canada) was performed on pTriEx-gp41 or pTriEx-gp160, respectively, in order to excise the gp41-/gp160-encoding DNA fragment from the pTriEx-3 vector. All digestion reactions were incubated at 37 ºC for 3 hours. Digested products, undigested plasmid and empty plasmid were then resolved on a 0.8% agarose gel (see section 2.4) and visualised under UV light.

2.2.3.3 Sequencing of pTriEx-gp41 and pTriEx-gp160

From the panel of recombinant pTriEx-gp41 and pTriEx-gp160 clones, one clone for each was selected for sequence analysis. Replica plates of the positive ligation plates were made by streaking 5 µl of the overnight cultures onto agar plates containing ampicillin (100 µg/ml) under sterile conditions. These colonies were used for sequence analysis. PTF ($^{5'}$GTTATTGTGCTGTCTCATC$^{3'}$) and PTR ($^{5'}$TCGATCTCAGTGGTATTTGTG^{3}) primers corresponding to sequences immediately flanking the pTriEx-3 multiple cloning site were used to sequence the gp41 and gp160 clones. In addition to the PTF and PTR primers, primers corresponding to internal regions of the gp160-encoding fragments, gp160CO FV3 F1 ($^{5'}$GCTGATCAACTGCAACAC^{3}), $^{'}$gp160CO FV3 F2 ($^{5'}$CTGCAGTGTCGGATCAAG$^{3'}$), gp160CO FV3 R1 ($^{5'}$GATCTTGATGTACCACAG$^{3'}$) and gp160CO FV3 R2 ($^{5'}$AGATCTCGGTCTTGTTCTC$^{3'}$) were also used to sequence the gp160 clone due to its larger size. All primers were synthesized by Inqaba Biotech (Pretoria, Gauteng, South Africa). Sequencing reactions were set up by Dr Maria Papathanosopoulos and thereafter sequencing was conducted by The HIV Genotyping Laboratory (University of the Witwatersrand Medical School, Johannesburg, South Africa). Sequences were assembled, edited and analysed using Sequencher v4.6 (GeneCodes, Ann Arbor, MI).

2.3 Expression of gp41 in Bacterial Cell Culture

BL21 (DE3) pLysS Singles Competent Cells (Novagen; Darmstadt, Germany) were transformed under sterile conditions with recombinant pTriEx-gp41. After overnight incubation at 37 ºC on agar plates containing ampicillin (100 µg/ml) and chloramphenicol (35

μg/ml) (Calbiochem; Darmstadt, Germany) (Appendix A1), a single colony was selected under sterile conditions and used to inoculate 5 ml of LB Broth containing ampicillin (100 μg/ml) and chloramphenicol (35 μg/ml). These cultures were incubated overnight at 37 ºC in a shaking incubator.

The following morning, the cultures were split between two tubes and diluted 1:10 with LB Broth containing the appropriate antibiotics. The cultures were further incubated at 37 ºC in a shaking incubator to stimulate log phase growth for approximately 1 hour. Once the A_{600} measurement reached approximately 0.3, Isopropyl-β-D-thiogalactopyranoside (IPTG) (Roche; Mannheim, Germany) was added to a final concentration of 2.5 mM in order to induce protein expression. IPTG was omitted from negative control cultures. Cultures were incubated for a further 4 hours at 37 ºC in a shaking incubator and 500 μl samples were collected from each culture at 1 hour intervals. The 500 μl samples were centrifuged at 2000 x g for 20 minutes. The pellets were resuspended in 50 μl of Phosphate Buffered Saline (PBS) (Sigma-Aldrich; Steinheim, Germany) and 50 μl of 2 X Treatment Buffer (Appendix A8), incubated at 80 ºC for 3 minutes and stored at -20 ºC until analysed for the presence of gp41 by SDS-PAGE and Western Blotting (Appendices A6 and A8).

2.4 Protein Purification and Concentration of gp41

2.4.1 Analysis of Protein Solubility

Before final purification of recombinant gp41, the solubility of the expressed protein was assessed. Expression of gp41 in BL21 cells was confirmed as described in section 2.5 and

thereafter the gp41-induced culture was centrifuged at 2000 x g for 20 minutes. The supernatant was collected and designated S1. The pellet was resuspended in lysis buffer (20 mM Na-Phosphate Buffer pH 7.8, 100 mM KCl, 1mM EDTA, 2mM β-mercaptoethanol, 1% Nonidet P-40) containing 1 X Complete protease inhibitor (Roche; Mannheim, Germany) (Appendix A4), snap-frozen in liquid nitrogen and then thawed at 37 ºC. Thereafter, the sample was sonicated on ice for three rounds of 15 second pulses and centrifuged at 10000 x g for 5 minutes. The supernatant, containing soluble protein was collected and designated S2. The insoluble pellet was resuspended in lysis buffer containing 8 M urea (Appendix A4) and designated S3. Samples were stored at -20 ºC until analysed via SDS-PAGE and Western Blotting.

2.4.2 Preparation of Protein Samples to be Purified

Two tubes containing 200 ml of gp41-induced BL21 cell culture each were centrifuged at 2000 x g for 20 minutes and the pellet resuspended in 10 ml lysis buffer containing 1 X Complete protease inhibitor. The samples were then snap-frozen in liquid nitrogen, thawed at 37 ºC and sonicated on ice as described. Sonicated samples were centrifuged at 2000 x g for 20 minutes, the supernatants were collected and imidazole was added to the supernatants to a final concentration of 10 mM (lysate).

2.4.3 Preparation of Columns

Nickel-charged iminodiacetate-sepharose 6B resin (kindly prepared and donated by Dr Wolfgang Prinz) was used to purify the recombinant gp41 protein. This is made possible by

the presence of a His-Tag on the recombinant gp41 protein, which binds to the nickel-charged sepharose. Two tubes containing 2 ml of the above mentioned bead solution each were washed with 30 ml of dH_2O and centrifuged at 3220 x g for 5 minutes. 10 ml of a 0.1 M $NiSO_4$ solution was added to each tube, which were incubated at room temperature on a shaker for 10 minutes. The tubes were centrifuged at 3220 x g for 5 minutes and the supernatant removed. Beads were washed and centrifuged twice at 3220 x g for 5 minutes and thereafter equilibrated with 10 ml of equilibration buffer (20 mM Na-Phosphate Buffer, 100 mM NaCl, 2 mM β-mercaptoethanol, 0.1 mM EDTA) containing 10 mM imidazole (Appendix A4). They were centrifuged again and the supernatant was removed.

2.4.4 Purification Procedure

Purification of recombinant gp41 protein was performed using a batch procedure. The lysates (10 ml) were added to the beads (2 ml) and incubated overnight at 4 ºC on a shaker. After the overnight incubation, the beads were centrifuged at 3220 x g for 5 minutes and the supernatant was collected (flow-through). The beads were then washed three times with 10 ml of wash buffer (20 mM Na-Phosphate Buffer ph 7.8, 100 mM NaCl, 2 mM β-mercaptoethanol, 0.1 mM EDTA) containing 10 mM imidazole and thereafter a further three times with 10 ml of wash buffer containing 50 mM imidazole. The protein was eluted in 1 ml of equilibration buffer containing 500 mM imidazole, by centrifuging at 3220 x g for 5 minutes at 4 ºC and collecting the supernatants. 100 µl samples were taken from the lysate, the flow-through, all the washing steps and the elution for analysis by SDS-PAGE and Western Blotting.

2.4.5 Concentration of Recombinant gp41

The purified gp41 samples were pooled and dialysed in 1 L of PBS overnight at 4 ºC, using SnakeSkin® Pleated Dialysis Tubing (Pierce; Rockford, IL). The following day the protein was further dialysed for 2 hours at 4 ºC in 1 L of fresh PBS. The dialysed protein was then concentrated using Amicon® Ultra-15 Centrifugal Filter devices (Molecular Weight cut off 10 kDA) (Millipore; Billerica, MA), according to the manufacturer's instructions and stored at -80 ºC until analysed via SDS-PAGE and Western Blot. Western Blot analysis was achieved using the F-240 antibody (NIH AIDS Research and Reference Reagent Program, Division of AIDS, NIAID, NIH), which recognizes the LGIWGCSGKLICTT epitope located in the membrane-proximal region (MPER) of the gp41 protein. The purity of the recombinant gp41 was assessed via Coomassie and Silver Staining (Appendix A7).

2.5 Expression of gp160 in Mammalian Cell Culture

HEK 293T cells were transfected with recombinant pTriEx-gp160 using $CaCl_2$ (Appendix A3). The concentration of pTriEx-gp160 DNA was measured spectrophotometrically and diluted to 20 µg in dH_20 to a final volume of 450 µl (143 µl of pTriEx-gp160 DNA + 307 µl of dH_20). 50 µl of $CaCl_2$ solution (2.5 M) and 500 µl of HEPES solution (Appendix A3) were then added to the DNA solution and the complexes were incubated at room temperature for 20 minutes before being added to the cells. Transfection complexes containing no DNA were also used as negative controls. Cells were incubated with the transfection complexes overnight at 37 ºC with CO_2 levels strictly set at 5%. After the overnight incubation, the medium was

removed and 10 ml of fresh medium was added. Total membrane and lipid raft isolations were performed 72 hours after transfections (see sections 2.6 and 2.7).

2.6 Total Membrane Isolation

Membrane isolation was performed by sucrose gradient centrifugation according to methods described by Alexander *et al*, with minor adjustments (Alexander et al., 2004). Approximately 6 X 10^6 U87 X4 and U87 R5 cells or transfected HEK 293T cells were centrifuged for 5 minutes at 200 x g and resuspended in 400 µl of flotation buffer (25 mM Tris-HCl pH 7.4, 150 mM NaCl, 5 mM EDTA, 10 mM β-Glycerol phosphate Disodium salt Pentahydrate, 30 mM $NaPO_4$). Thereafter the cells were lysed by three cycles of freeze-thawing in liquid nitrogen and a 37 °C water bath. Nuclei and unbroken cells were centrifuged at 2000 x g for 5 minutes and the supernatant was collected (S1). The pellet was washed with 100 µl of flotation buffer, centrifuged again at 2000 x g for 5 minutes and the resulting supernatant (S2) was added to S1. Combined supernatants were adjusted to 80% sucrose in a volume of 2 ml, which was layered at the bottom of an SW41 Beckman centrifuge tube (Beckman Coulter Inc; Fullerton, CA). Layers of 65% (5.5 ml) and 10% (4.5 ml) sucrose solutions (in flotation buffer) were added gently to the top of the 80% sucrose sample and the tubes were centrifuged using a Beckman Coulter Optima™ L-80 XP Ultracentrifuge (Beckman Coulter Inc; Fullerton, CA) at 35000 rpm for 18 hours at 4 °C. 1 ml fractions were gently removed from the top of the gradient and stored at –20 °C until analysed by SDS-PAGE, Western Blotting and Immuno-Slot Blotting (see section 2.9).

2.7 Lipid Raft Isolation

Lipid rafts were isolated by sucrose gradient centrifugation according to the methods described by Triantafilou *et al*, with minor modifications (Triantafilou et al., 2004). Approximately 6 X 10^6 U87 X4 and U87 R5 cells or transfected HEK 293T cells were centrifuged for 5 minutes at 200 x g and resuspended in 400 µl of flotation buffer containing 1% Triton X-100 and incubated on ice for 1 hour. Nuclei and unbroken cells were centrifuged at 2000 x g for 5 minutes and the supernatant was collected (S1). The pellet was washed with 100 µl of flotation buffer containing 1% Triton X-100, centrifuged at 2000 x g for 5 minutes and the resulting supernatant (S2) was added to S1. This was then adjusted to 45% sucrose in a final volume of 2 ml, which was layered at the bottom of an SW41 Beckman centrifuge tube (Beckman Coulter Inc; Fullerton, CA). Layers of 30% (5.5 ml) and 5% (4.5 ml) sucrose solutions (in flotation buffer) were then gently added on top of the 45% sucrose sample and the tubes were centrifuged using a Beckman Coulter Optima™ L-80 XP Ultracentrifuge at 35000 rpm for 18 hours at 4 °C. 1 ml fractions were gently removed from the top of the gradient and stored at –20 °C until analysed by SDS-PAGE, Western Blotting and Immuno-Slot Blotting.

2.8 Western Blot Analysis

Proteins were transferred from SDS-PAGE gels onto Hybond-C nitrocellulose membrane (Amersham Biosciences UK Limited; Little Chatfont, Buckinghamshire, England) using a Trans-Blot SD Semi-Dry Transfer Cell System (Bio-Rad; Hercules, CA). Following protein transfer, the membrane was blocked in 5% fat free milk powder solution in Tris-buffered

saline (TBS) containing 0.1% Tween-20 (T-TBS). The membrane was then probed with either anti-transferrin (250 ng/ml or 300 ng/ml), anti-tubulin (200 ng/ml or 250 ng/ml), anti-CD4 (70 ng/ml or 100 ng/ml), anti-CXCR4 (200 ng/ml), anti-CCR5 (200 ng/ml) or anti-F-240 (2 µg/ml or 4 µg/ml) primary antibodies and thereafter with either anti-mouse, anti-human or anti-goat secondary antibodies conjugated with horseradish peroxidase (HRP) (details outlined in Appendix A8). Detection of protein was performed by standard chemiluminescence methods (Appendix A9).

2.9 Immuno-Slot Blot Analysis

100 µl of each sample was diluted in 200 µl of flotation buffer. Membrane and lipid raft fractions were slotted onto nitrocellulose membrane using a slot blot apparatus (Schleicher and Schuell; Dassel, Germany) and blocked with 5% fat free milk powder solution in T-TBS. The membrane was then washed three times with T-TBS and incubated for 1 hour with a cholera toxin subunit B (recombinant) horseradish peroxidase (HRP) conjugate (CT-B) solution (1 µg/ml) (Molecular Probes, Oregon, USA) at room temperature on the bench top. The membrane was washed three times with T-TBS and analysed by standard chemiluminescence methods.

2.10 Fluorescence Microscopy Analysis of Co-receptor Localization

2.10.1 Cell Preparation on Chamber Slides

Fluorescence experiments were carried out using a Lab-Tek® II Chamber Slide System (Nunc; Naperville, IL). Approximately 1 X 10^5 U87 R5 or U87 X4 cells were seeded onto the chamber slides 24 hours prior to antibody staining. The following day, the growth medium was removed and the chambers were gently washed three times with PBS at room temperature. The cells were fixed onto the chamber slides using 3% formaldehyde solution (Appendix A10) for 15 minutes at room temperature. The fixative was then removed and the chambers were gently washed three times with PBS at room temperature. Thereafter, the chamber slides were blocked for 10 minutes at room temperature, using PBS containing 0.5% BSA (Appendix A10). The blocking buffer was removed and the chamber slides were probed with either a FITC-labelled anti-transferrin, Alexa Fluor 488 conjugated CT-B, PE-labelled anti-CXCR4 or PE-labelled anti-CCR5 antibody overnight at 4 ºC (details outlined in Appendix A10). After the overnight incubation, the antibodies were removed and the slides were gently washed three times with PBS containing 0.5% BSA at room temperature. The nuclei were then stained using 4', 6 diamidino-2-phenylindole (DAPI) solution (100 ηg/ml) (Sigma-Aldrich; Steinheim, Germany), for 10 minutes at 4 ºC in the dark, and the chambers were once again gently washed three times with PBS at room temperature. The chambers were removed and cover slips were mounted onto the slides using FluorSave Reagent (Calbiochem; Darmstadt, Germany). The slides were stored at 4 ºC in the dark for a minimum of 1 hour before visualisation.

2.10.2 Visualisation of Slides under Fluorescence Microscope

Slides were visualised using an Olympus IX71 Fluorescence Microscope System (Olympus; Center Valley, PA) and images were captured using the analySIS LS Research Olympus Imaging Software System (Olympus; Center, PA). The PE-labelled antibodies were excited at 590 nm and the emitted light collected at 617 nm. The red fluorescence was detected with the standard Alexa Fluor 546 filter set. The FITC-labelled antibody and the Alexa Fluor 488-conjugated antibody were excited at 494 nm and the emitted light collected at 518 nm. DAPI was excited at 345 nm and the emitted light collected at 455 nm. All slides were viewed and images captured using the 60 X objective.

2.11 Infections and Fusion Studies

In order to conduct the fusion experiments, viruses were needed to be amplified in order to saturate U87 X4/R5 cells with enough virus to ensure successful fusion events occurred and to ensure successful detection of gp41 with the monoclonal antibody, F-240. Two representative HIV-1 subtype C viral isolates, FV3 and FV5, which have previously been isolated and propagated in our laboratory, were used to infect U87 X4 and U87 R5 cells respectively.

2.11.1 Infections

2.11.1.1 Amplification of Virus

Viral stocks were amplified by successive infections of cells in 25 cm^2, 75 cm^2 and 175 cm^2 cell culture flasks (Nunc; Naperville, IL). Briefly, U87 X4 and U87 R5 cells were seeded into the cell culture flasks and once cells reached approximately 60% confluency, they were infected with the FV3 ($TCID_{50}$= 5 x 10^8) and FV5 ($TCID_{50}$ = 5 x 10^9) viral stocks, respectively. Infections were allowed to proceed for 5 days, following removal of the original inoculum after 24 hours and replacement with fresh medium. 200 µl samples were collected every second day for analysis (by p24 antigen ELISA). Supernatants were harvested and stored at -80 ºC on day 5. These samples were used for p24, viral load as well as SDS-PAGE and Western Blot analysis.

2.11.1.2 Post-Infection Analyses

Viral replication was confirmed by the presence of p24 antigen in the harvested supernatants. This was ascertained using a Beckman Coulter™ HIV-1 p24 Antigen EIA kit (Beckman Coulter Inc; Fullerton, CA) according to the manufacturer's instructions. In addition, to corroborate p24 measurements and enable MOI estimations for fusion experiments, viral titres (expressed as particles/ml) were calculated by viral load testing at the PCR laboratory (University of the Witwatersrand Medical School, Johannesburg, South Africa). To confirm the presence and relative quantity of FV3/FV5 gp41, SDS-PAGE and

Western Blot analysis was performed on samples of the virus-containing supernatants using the monoclonal antibody, F-240.

2.11.2 Fusion Studies

Fusion experiments were performed according to methods described by Mkrtchyan *et al*, with adjustments (Mkrtchyan et al., 2005). U87 R5 cells were seeded either into 25 cm^2 cell culture flasks, each containing 5 ml of growth medium, or onto Lab-Tek® II Chamber Slides, each containing 2 ml of growth medium. Once cells reached approximately 70% confluency, the growth medium was removed and 5 ml/2 ml fresh medium was added to each flask/chamber. Cells were incubated with the fresh medium for a minimum of 30 minutes. Thereafter, cells were pre-incubated at 23 ºC for a further 30 minutes in order for cell cultures to adjust to the lowered temperature to be used for the fusion experiments. This temperature has been found to permit gp120-CD4 receptor engagement, but is non-permissive for fusion of the viral and host cell membranes (Mkrtchyan et al., 2005). Once U87 R5 cells were equilibrated at 23 ºC, they were infected with approximately 250 viral particles/cell of amplified FV5 virus (Appendix C) and incubated at 23 ºC for 2 hours to synchronize infecting virions at the temperature-arrested stage (TAS). Thereafter, flasks/chamber slides were transferred back to 37 ºC and incubated for a further 3 hours, to allow for completion of the fusion process. Uninfected cells were used throughout these experiments as negative controls. Total membrane and lipid raft isolations (described in sections 2.6 and 2.7) were performed on all cells grown in cell culture flasks, from both the TAS and the 3 hours post-TAS stages, and thereafter samples were subjected to SDS-PAGE and Western Blot

analysis. Fluorescence microscopy analysis (described in section 2.10) was performed on all cells grown on the chamber slides, from both the TAS and the 3 hours post-TAS stages.

CHAPTER 3: RESULTS

3.1 Generation of Recombinant gp41- and gp160-Expression Vectors

The generation of a gp41-expression vector (pTriEx-gp41) was performed in order to produce and purify a recombinant subtype C gp41 protein as an immunoblotting control. Further, a vector (pTriEx-gp160) expressing the gp160 envelope in transfected mammalian cells, was used to pilot the extraction and immunodetection of the corresponding, membrane-embedded gp41 protein. Full length gp41-encoding DNA was amplified from a plasmid template containing a codon optimized gp160 sequence derived from the HIV-1 subtype C isolate, FV3 (pGA4-160). PCR primers were designed in order for the gp41 gene to be amplified and cloned in the pTriEx-3 plasmid. A 1 kb band, resolved on a 0.8% agarose gel (Figure 3.1 A), confirmed that PCR amplification was successful.

Double-digested gp41 PCR product and gp160-encoding DNA were inserted into the multiple cloning site of the double-digested pTriEx-3 plasmid at a 1:5 molar ratio of vector: insert. In order to confirm that the inserts and the vector were successfully ligated, PCR was performed on colonies from the ligation plates that were incubated overnight in LB Broth. For both gp41 and gp160, the gp41 primers were used and positive PCR reactions were shown by the presence of a 1 kb DNA product on a 0.8% agarose gel (Figure 3.1 B).

After PCR confirmation, recombinant plasmids were isolated from LB Broth and their integrity was confirmed by restriction digestion analysis. gp41-pTriEx plasmids were linearised with *Xho* I, which yielded a DNA product of approximately 6 kb (Figure 3.1 C, Lane 3) , and the insert was excised from the plasmid using *Xho* I and *Nco* I, which yielded two DNA products

of approximately 1 kb and 5 kb (Figure 3.1 C, Lane 4). Likewise, gp160-pTriEx plasmids were linearised with a *Bam* HI, which yielded a DNA product of approximately 7.5 kb (Figure 3.1 D, Lane 2). The insert was excised from the plasmid using *Xho* I and *Xba* I, yielding two DNA products of approximately 2.9 kb and 4.6 kb (Figure 3.1 D, Lane 3). *Xba* I was used in the excision of the gp160 insert as *Nco* I and *Bsp* HI do not reconstitute a recognizable restriction site even though they do form compatible sticky ends. The *Xba* I restriction site is situated outside the 3' extremity of the insert and this, therefore, yielded a slightly larger DNA product compared to the expected 2.5 kb size of the insert and a slightly smaller pTriEx-3 product compared to the normal size of 5 kb (Restriction Maps in Appendix B).

Plasmids containing the correct size of gp41 and gp160 inserts were sequenced, which confirmed that the inserts were in the correct orientation, in the correct reading frame and that no mutations had been generated during amplification. DNA sequences of the gp41 and gp160 clones were aligned against the FV3 codon optimized gp160 sequence (Appendix C). Amino acid sequences were also aligned and key domains, as well as important gp41 monoclonal antibody epitopes, were identified and highlighted (Figure 3.2).

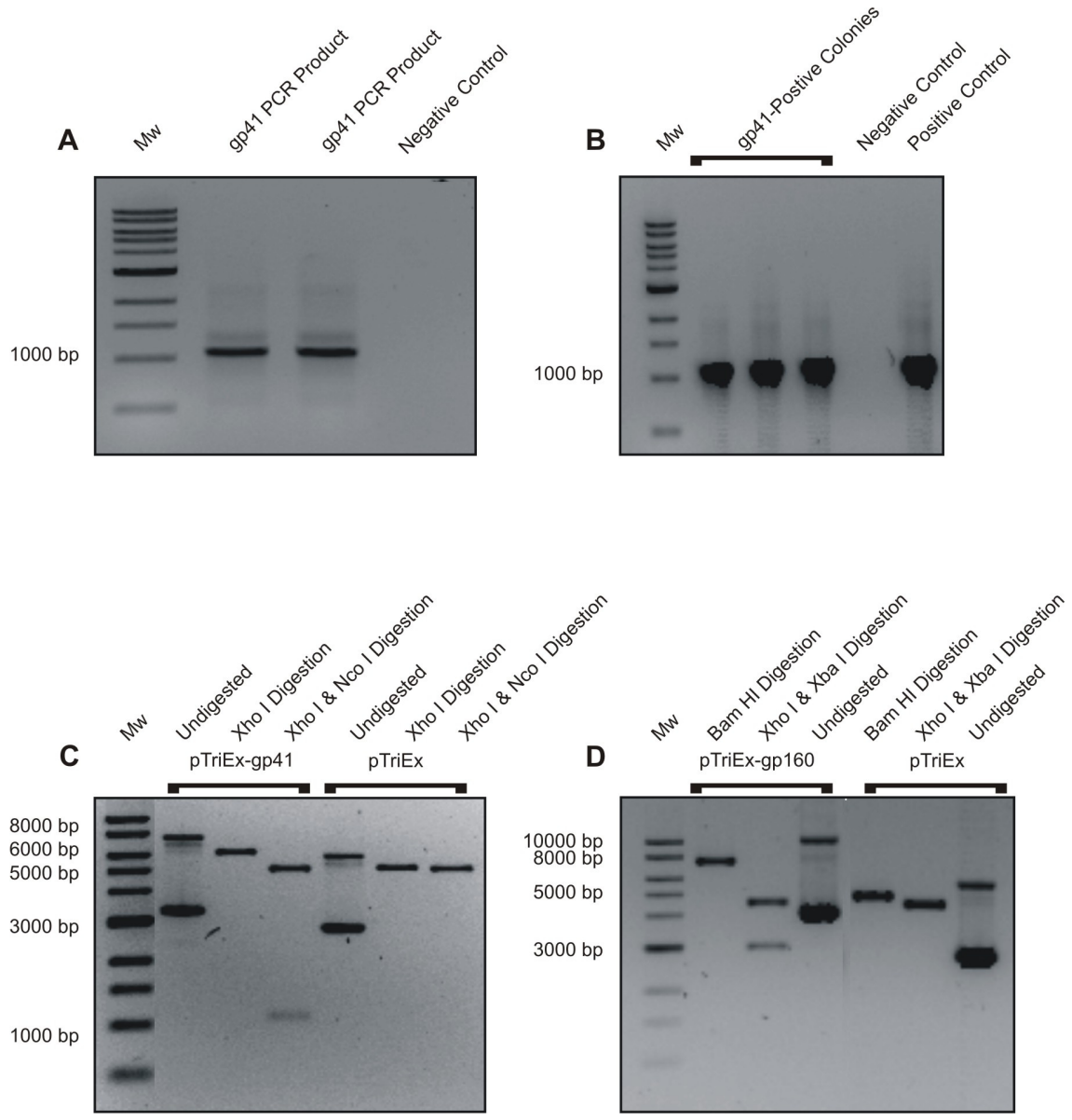

Figure 3.1: Agarose gel electrophoresis of PCR products and restriction digestion analysis. All DNA samples were resolved on a 0.8% agarose gel, and visualised under UV light. **(A) Purified gp41 PCR products. (B) Representative agarose gel of PCR screening.** Colonies selected from plates containing *E. coli* cells transformed with ligation mixes were grown overnight and subjected to PCR using gp41-specific primers. Generation of a 1 kb DNA fragment implied positive recombination between pTriEx-3 vector and gp41 or gp160 insert DNA. Representative digestion restriction analysis of **(C) recombinant pTriEx-gp41 and (D) recombinant pTriEx-gp160 vectors.**

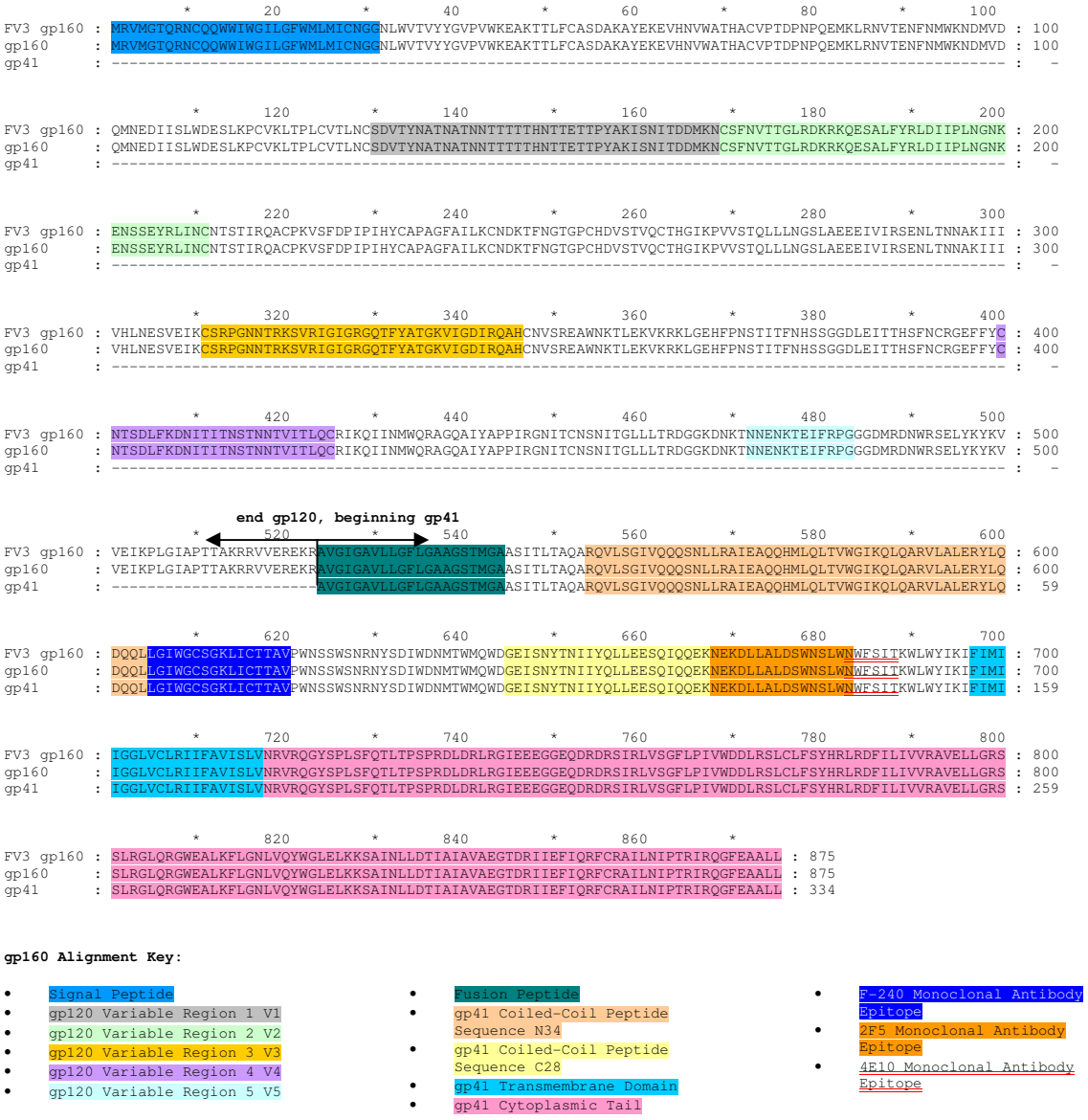

Figure 3.2: Amino acid sequence alignment of gp41 and gp160 clones. Sequences of gp41 and gp160 clones were aligned and compared to the FV3 codon optimized gp160 sequence. Amino acid sequences of gp160 and gp41 showed 100% similarity to the codon optimized sequence. Highlighted sections show the different domains of the gp160 protein; also shown are the epitopes of several important monoclonal antibodies that bind gp41, two of which have broadly neutralising activities (2F5, 4E10).

3.2 Expression and Purification of gp41

Recombinant gp41 was expressed in BL21 pLysS *E. coli* cells and purified by affinity chromatography procedures, whereby the His-Tag included in the cloned gp41 sequence was able to bind to nickel-charged beads. This protein (designated gp41-6xHis) was utilized as a positive control for gp41 recognition by the monoclonal antibody, F-240, during viral fusion experiments. Expression of the gp41-6xHis protein was assessed over a 4 hour period, following induction with IPTG. Expressed gp41 was detected by Western Blot analysis using the F-240 antibody (Figure 3.3 A), which recognizes the gp41 epitope, LGIWGCSGKLICTT.

The solubility of the expressed gp41-6xHis was then assessed and it was found that a significant amount of the protein was present in the soluble form (Figure 3.3 B, Lane 5). This was unexpected as other studies have shown that most recombinant gp41 proteins are expressed as forms that need to be solubilized with agents such as urea and guanidine-HCL (Wingfield et al., 1997; Krell et al., 2004; Penn-Nicholson et al., 2008). The reasons for this are unclear, but this observed atypical solubility could be due to different folding patterns of the recombinant protein, which may or may not be sequence-specific. Solubility could possibly arise from the masking or shielding of the insoluble domains of gp41-6xHis by the soluble domains during folding, therefore making the protein more hydrophilic. Such shielding could be influenced by intramolecular associations, whereby the hydrophobic domains are masked by the hydrophilic domains during oligomerisation and six-helix bundle formation. Intermolecular associations could also play a role in producing a soluble form of gp41 due to the proteins aggregating in such a manner as to shield the hydrophobic regions.

The purification of the soluble protein was performed by affinity chromatography using a nickel-charged iminodiacetate-sepharose 6B resin, to bind a C-terminal poly-histidine tag on the recombinant gp41-6xHis. The efficiency of gp41-6xHis binding and elution was shown by Western Blot analysis using the F-240 antibody (Figure 3.3 C), and Coomassie and Silver Stain analysis confirmed the purity of concentrated recombinant gp41-6xHis (Figures 3.3 D and E).

gp41-6xHis appeared to exist in three different forms (probably monomers, dimers and trimers) which were seen through Western Blot analysis. The monomer was seen as a 26 kDa protein band, which is smaller than the predicted size of 41 kDa. The 'dimer' was observed as a 75 kDa protein band and the 'trimer' as a 127 kDa protein band. While unexpected, these observations are consistent with previously published data, which has shown that recombinant gp41 readily olgimerises into highly stable dimeric and trimeric forms that are resistant to denaturation during denaturing PAGE (Frey et al., 2008). The sizes we obtained, however, are slightly different to those found in the previously published literature. This has been suggested to be due to the complex folding and strong hydrophobic bonds formed during gp41 oligomerisation. The positive control utilized throughout these experiments is an *E. coli* derived recombinant gp41 protein containing the immunodominant regions of gp41, which resolves at the predicted 41 kDa on SDS-PAGE gels (obtained from RPC Diagnostic Systems Ltd., Russia). This is most likely due to the fact the protein was purified and stored in urea, a chaotropic agent used to disrupt strong inter- and intramolecular hydrophobic protein interactions.

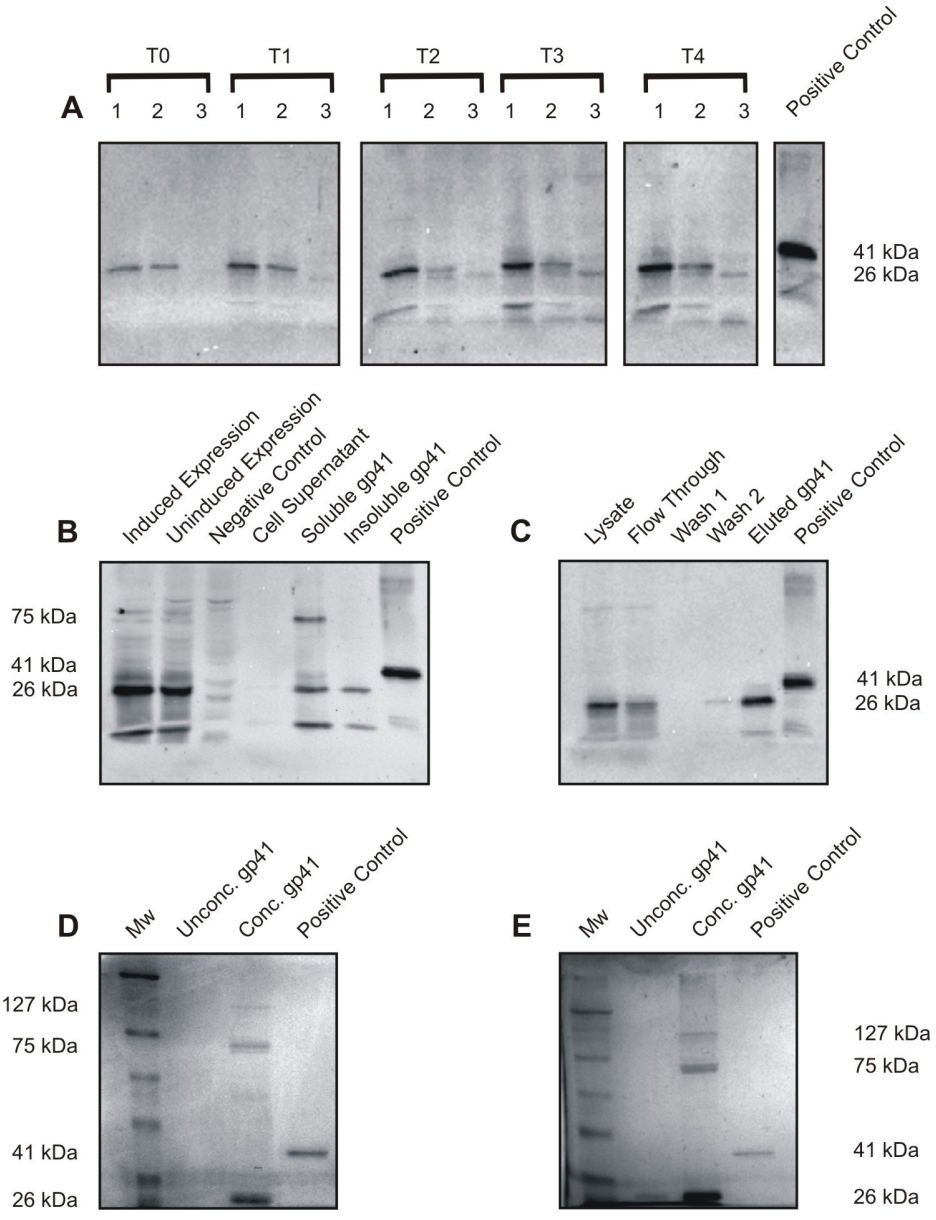

Figure 3.3: Analysis of gp41 expression, solubility and purification. gp41 expression studies were carried out in BL21 pLysS *E. coli* cells induced with 2.5 mM IPTG. The solubility of expressed gp41 was assessed and the protein was purified by batch preparation using nickel-charged iminodiacetate-sepharose 6B resin. **(A) Western Blot analysis of gp41 expression.** T0: Point at which IPTG was added. T1: 1 hr-post induction. T2: 2 hrs-post induction. T3: 3 hrs-post induction. T4: 4 hrs-post induction; 1: Induced samples. 2: Uninduced samples. 3: Negative control. **(B) Western Blot analysis of gp41 solubility. (C) Western Blot analysis of batch purification of gp41.** Wash 1: 10 mM imidazole. Wash 2: 50 mM imidazole. gp41 eluted in 150 mM imidazole. **(D) Coomassie Staining and (E) Silver Staining.** Samples were resolved on 10% SDS-PAGE gels to assess the purity of concentrated gp41.

3.3 Expression of gp160

HEK 293T cells were transfected with recombinant pTriEx-gp160 in order to assess the efficiency of the extraction and detection of gp41 in isolated total membrane/raft fractions using monoclonal antibody F-240. The isolated total membrane and lipid raft fractions were pooled for this experiment (See Figure 3.4 for diagram showing the flotation procedure). Pool 1 corresponds to fractions 1-3, pool 2 to fractions 4-6, pool 3 to fractions 7-9 and pool 4 to fractions 10-12. This was done as it had already been ascertained that these pooled fractions consistently showed the same results, therefore allowing for more rapid optimization. Pooled samples were resolved on 10% SDS-PAGE gels and Western Blot analysis was performed using the monoclonal antibody F-240 (Figure 3.5). Results showed that two bands of approximately 43 kDa and 160 kDa, ostensibly representing the gp41 and gp160 proteins respectively, localized to membrane fraction 2. The corresponding bands were seen in fraction 4 of the lipid raft samples. This further confirmed membrane localization of gp160, as membrane-bound proteins would be located in the bottom sucrose fraction when treated with detergent, since they would no longer possess the buoyancy of the membrane to allow for flotation in the sucrose gradient. No bands of similar sizes were seen in the untransfected raft and membrane samples. These results indicated that the isolation and detection of gp41 expressed on the surface of cells by density-gradient centrifugation and Western Blot techniques respectively, was successful.

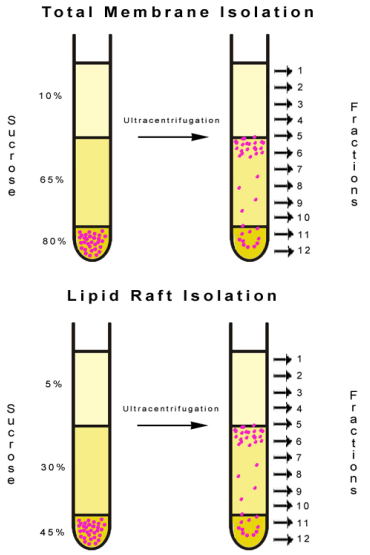

Figure 3.4: Diagram showing the principle of membrane flotation by sucrose density gradient centrifugation. Lysed cell samples (snap-frozen and thawed for total membrane isolations and treated with Triton X-100 for lipid raft isolations) are layered at the bottom of a centrifuge tube and upon centrifugation, the buoyancy of the membranes causes migration through the density gradient. Proteins associated with membrane or lipid raft domains co-migrate in this manner and proteins not bound to these domains remain at the bottom of the sucrose gradient.

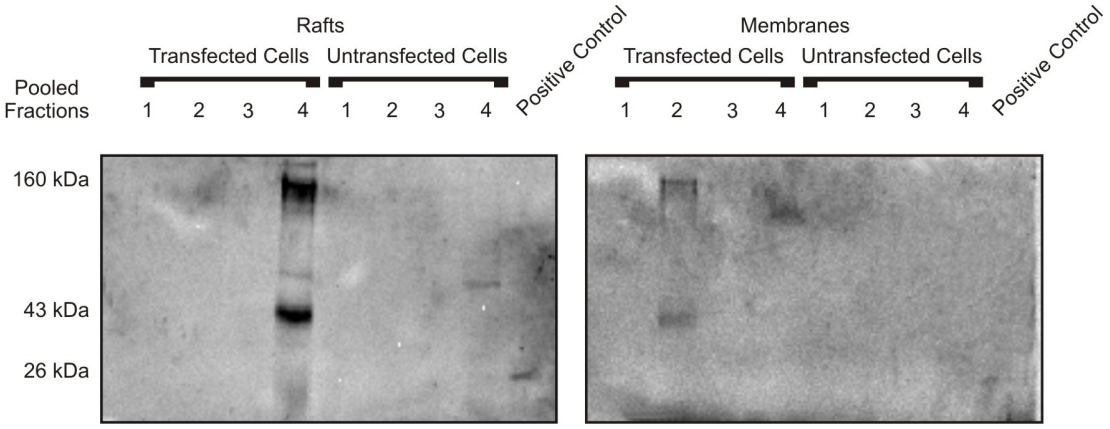

Figure 3.5: Western Blots showing gp160 expression in HEK 293T cells. HEK 293T cells were transfected with pTriEx-gp160. Lipid raft and membrane domains of transfected and untransfected cells were extracted and pooled samples were resolved on 10% SDS-PAGE gels. Western blot analysis was then performed using the F-240 antibody.

3.4 Analysis of Membrane Domain Localization of HIV-1 Receptor Proteins CD4, CCR5 and CXCR4 in Uninfected Cells

3.4.1 Western Blot Analysis of CD4, CCR5 and CXCR4 Receptors

U87 X4 and U87 R5 cells were used for the analysis of receptor protein localization in membrane and lipid raft domains. Lipid raft and total membrane fractions were isolated by density-gradient centrifugation and the collected fractions were resolved on 10% SDS-PAGE gels. Western Blot analysis was then performed on the fractions using a transferrin (TFR) antibody to detect the TFR non-raft marker, a tubulin (TUB) antibody to detect the TUB cytoplasmic marker, a CD4 antibody to detect CD4 (Figure 3.6), the CXCR4 antibody to detect X4 and the CCR5 antibody to detect R5 (Appendix F). Slot Blot analysis was also performed on the 12 raft and 12 membrane fractions using the cholera toxin sub-unit B HRP conjugate antibody to detect the GM1 ganglioside lipid raft marker, as this lipid is too small, and perhaps too hydrophobic, to be resolved on a SDS-PAGE gel (Figure 3.6). Cholera toxin was used, as it is well known that this bacterial toxin naturally binds to GM1 ganglioside in order for entry into its host cell and therefore it acts as a good detection method when conjugated to HRP for Western Blot analysis.

GM 1 ganglioside was detected mostly in raft fractions 3, 4 and 5 (Figure 3.6 A and B, Lanes 3, 4 and 5), which is consistent with its role as a fundamental structural component of raft microdomains. As expected, smaller amounts were also seen in the total membrane fractions, illustrating the constituent contribution of rafts to the membrane bilayer (Figure 3.6 A and B, Lanes 4 and 5). TFR was detected predominantly in total membrane fraction 5 and

in fractions 10-12 of the raft gradients, consistent with it being a non-raft, membrane-bound protein (Figure 3.6 A and B, Lanes 5, 10, 11 and 12). TUB was detected in fractions 10, 11 and 12 of the raft and total membrane extractions, confirming a cytoplasmic localization (Figure 3.6 A and B, Lanes 10, 11 and 12). A small amount of TUB was seen in total membrane fractions 5 and 6, which probably results from partial association and flotation with the inner portion of the cell membrane (Figure 3.6 A and B, Lanes 5 and 6). The CD4 receptor was detected in both the raft and total membrane fractions 4 and 5, showing an equal distribution between the two domains (Figure 3.6 A and B, Lanes 4 and 5), which is consistent with previously published literature (Del Real et al., 2002; Kozak et al., 2002; Popik et al., 2002; Percherancier et al., 2003; Popik and Alce, 2004). The U87 X4 cells and U87 R5 cells showed similar patterns of distribution for all the above mentioned proteins, although expression levels appeared to be higher in the U87 R5 cells as compared to the U87 X4 cells (Figure 3.6 B and A, respectively). The reasons for this are unclear, but could be due to a difference in cell line and the different co-receptors influencing the expression of CD4 on the cell surface, as the number of cells used for the lipid raft and total membrane extractions were the same in both cell lines.

The lipid raft and total membrane fractions were pooled as described in section 3.3 for the Western Blot analysis of co-receptor localization (Appendix F). Despite several reports in the literature describing successful detection of CXCR4 and CCR5 in U87 cells by Western Blot, overall, the results of our experiments were disappointing. Our Western Blot analysis showed variable results as there was a high degree of non-specificity and cross-reactivity of the antibodies to the proteins. The reasons for such variation could be due to these seven-transmembrane-domain proteins being too hydrophobic for Western Blot analysis, making it difficult to obtain consistent results. Also, the available antibodies for this type of detection are possibly of poor quality. These experiments were repeated numerous times in order to

optimize co-receptor detection by Western Blot, however these attempts were unsuccessful. A decision was therefore taken to analyse CXCR4 and CCR5 membrane domain localization by fluorescence microscopy. While our original objective was to obtain a quantitative assessment of receptor localization within membrane microdomains, and fluorescence microscopy is a more qualitative method of analysis, the latter has been widely utilized in detecting CXCR4 and CCR5 in cell membranes (Manes et al., 2000; Kozak et al., 2002; Popik et al., 2002; Viard et al., 2002; Percherancier et al., 2003; Nguyen et al., 2005).

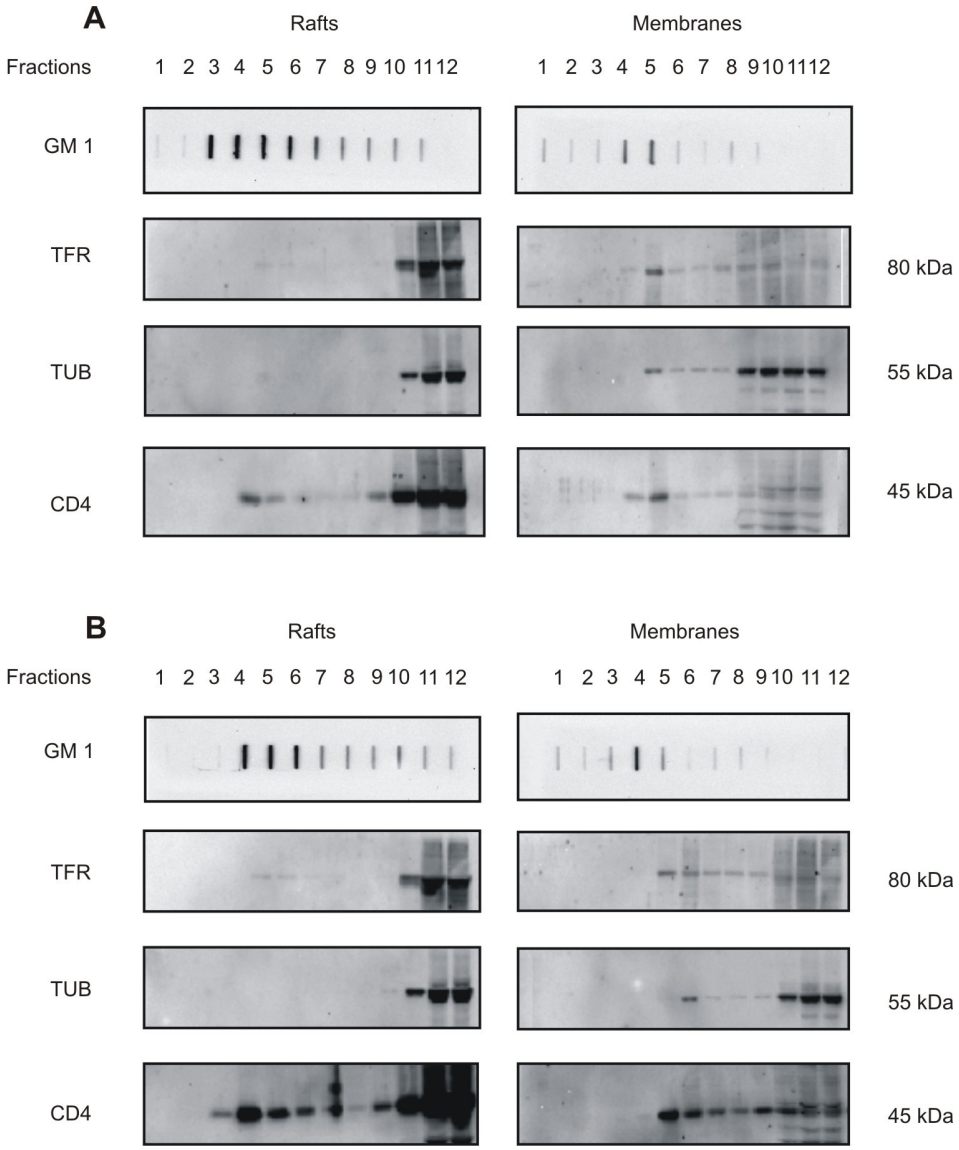

Figure 3.6: Slot- and Western Blots of U87 X4 and U87 R5 raft and membrane extractions. 12 Fractions collected from raft and membrane extractions, performed on 7 x 10^6 U87 X4/R5 cells, were analysed via Slot Blot procedures to detect the raft marker, GM 1 ganglioside, and via Western Blot procedures to detect the membrane marker, TFR, the cytoplasmic marker, TUB, and the membrane receptor, CD4. **(A) Raft and membrane extractions of U87 X4 cells and (B) Raft and membrane extractions of U87 R5 cells.** The same volume of each fraction was resolved on 10% SDS-PAGE gels/loaded onto the Slot Blot apparatus and extractions were all done on the same amount of U87 X4/R5 cells, 7 x 10^6 cells.

3.4.2 Fluorescence Microscopy Analysis of CXCR4 and CCR5 Receptors

U87 X4 and U87 R5 cells were fixed onto microscope slides and stained with various antibodies in order to assess whether these receptors naturally co-localized with membrane or lipid raft domains (Figures 3.7 and 3.8). Cells were stained with DAPI in order to visualise cell nuclei in blue. The co-receptors were probed with Phycoerythrin-conjugated antibodies (X4-PE or R5-PE) in order to visualise X4 and R5 in red. The membrane and lipid rafts were stained green with anti-TFR-FITC and CT-B-Alexa Fluor 488 conjugates, respectively. Images were then merged and yellow areas showed co-localization of the co-receptors with the membrane and/or raft markers. Controls included cells stained with DAPI only and cells stained with DAPI and X4-PE for U87 R5 cells or R5-PE for U87 X4 cells, which controlled for the specificity of antibody recognition. Cells were also stained with DAPI, the membrane or lipid raft marker and X4-PE for U87 R5 cells or R5-PE for U87 X4 cells, which controlled for the interference between the different antibodies. This method of qualitative assessment of co-localization has been widely used in many studies (Manes et al., 2000; Kozak et al., 2002; Popik et al., 2002; Viard et al., 2002; Percherancier et al., 2003; Nguyen et al., 2005). As in the case of our co-localization studies, frequently, images of green and red fluorophores labelling different proteins are overlapped and assessed for the predominance of yellow pixels in the combined image. This then indicated whether or not there was an interaction between the proteins.

Images of cells stained with anti-TFR-FITC merged with the corresponding anti-CXCR4/CCR5-PE-stain revealed diffuse and extensive yellow colouration of the cell surface (Figures 3.7 and 3.8, Row B I, Panel 4). The same results were seen for images of cells stained with anti-CT-Alexa Fluor 488 merged with the corresponding co-receptor stain

(Figures 3.7 and 3.8, Row B II, Panel 4). Insofar as the resolution of the channel-merging methodology of fluorescence microscopy is concerned, it appears that CXCR4 and CCR5 are, under normal conditions, found in close association with both raft and non-raft membrane domains in U87 cells. However, CCR5 seems to associate with rafts to a lesser extent than that of CXCR4 (See arrows in Figures 3.7 and 3.8, Row B II, Panel 4). Our results are in agreement with Viard *et al* and Popik *et al*, who show that these receptors are distributed in a diffuse manner throughout the cellular membrane, under normal, unstimulated conditions (Popik et al., 2002; Viard et al., 2002). In contrast, others have shown exclusive localization of the co-receptors to lipid raft microdomains (Manes et al., 2000; Nguyen et al., 2005), while some studies suggest non-raft localization of CXCR4 and CCR5 (Kozak et al., 2002; Percherancier et al., 2003). The reasons for this are unclear, but could be due to differences in experimental procedures or different cell lines and antibodies used.

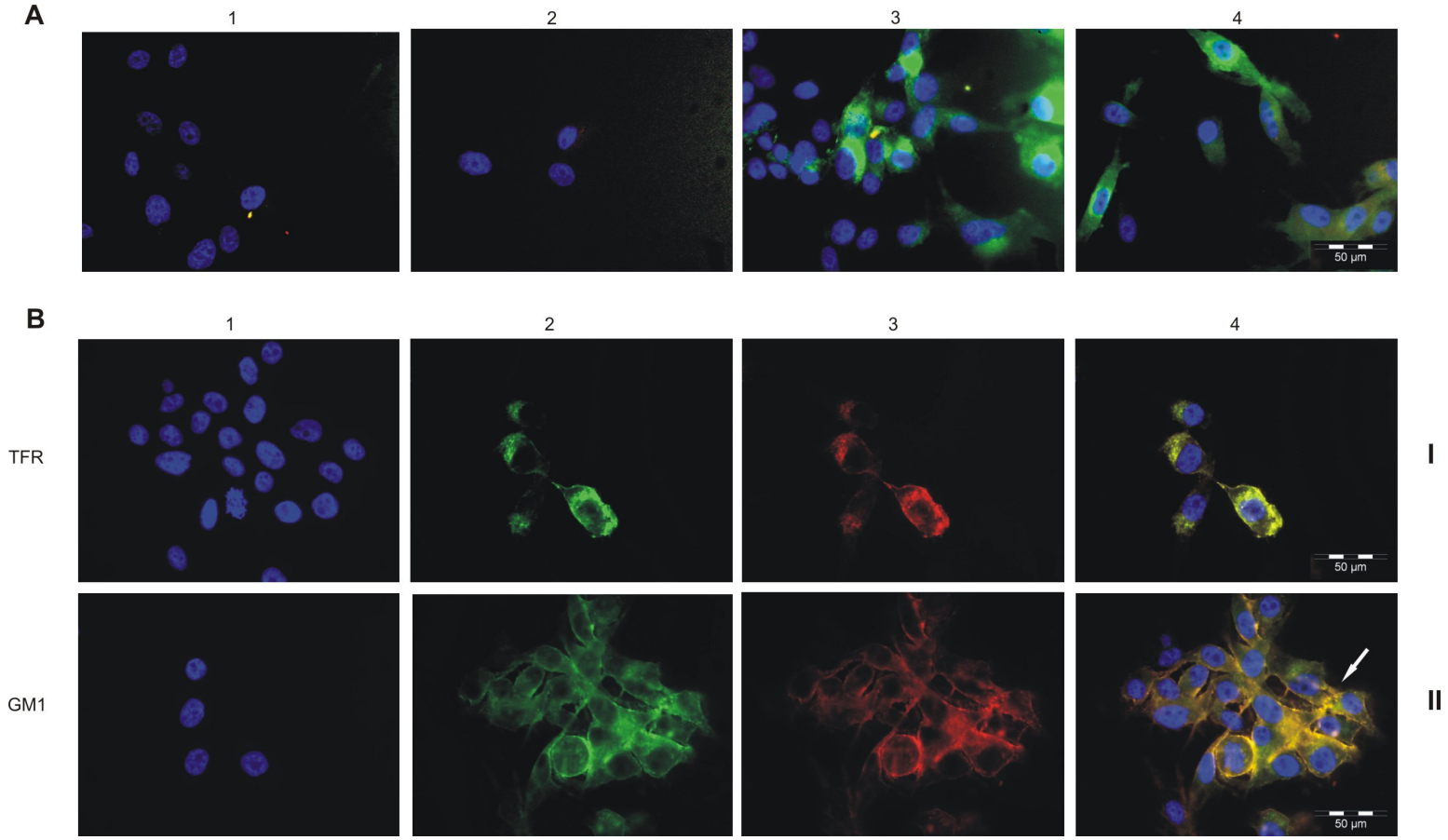

Figure 3.7: Localization of CXCR4 receptor in U87 membrane and lipid raft domains. U87 X4 cells were fixed onto slides and probed with fluorophore-conjugated antibodies to assess representative localization of the X4 receptor using fluorescence microscopy. Scale bars represent 50 microns (600X). **(A) Control slides.** Panel 1: Cells stained with DAPI only, no antibody. Panel 2: Cells probed with R5-PE antibody only. Panel 3: Cells probed with R5-PE and TFR-FITC (TFR green fluorescence=membrane domain marker) antibodies. Panel 4: Cells probed with R5-PE and CT-Alexa Fluor 488 (GM 1 ganglioside green fluorescence=lipid raft marker) antibodies. **(B) Slides showing CXC4 localization.** Panel 1: DAPI. Panel 2: TFR-FITC (Top) or CT-Alexa Fluor 488 (Bottom). Panel 3: X4-PE. Panel 4: Merged images show co-localization in yellow.

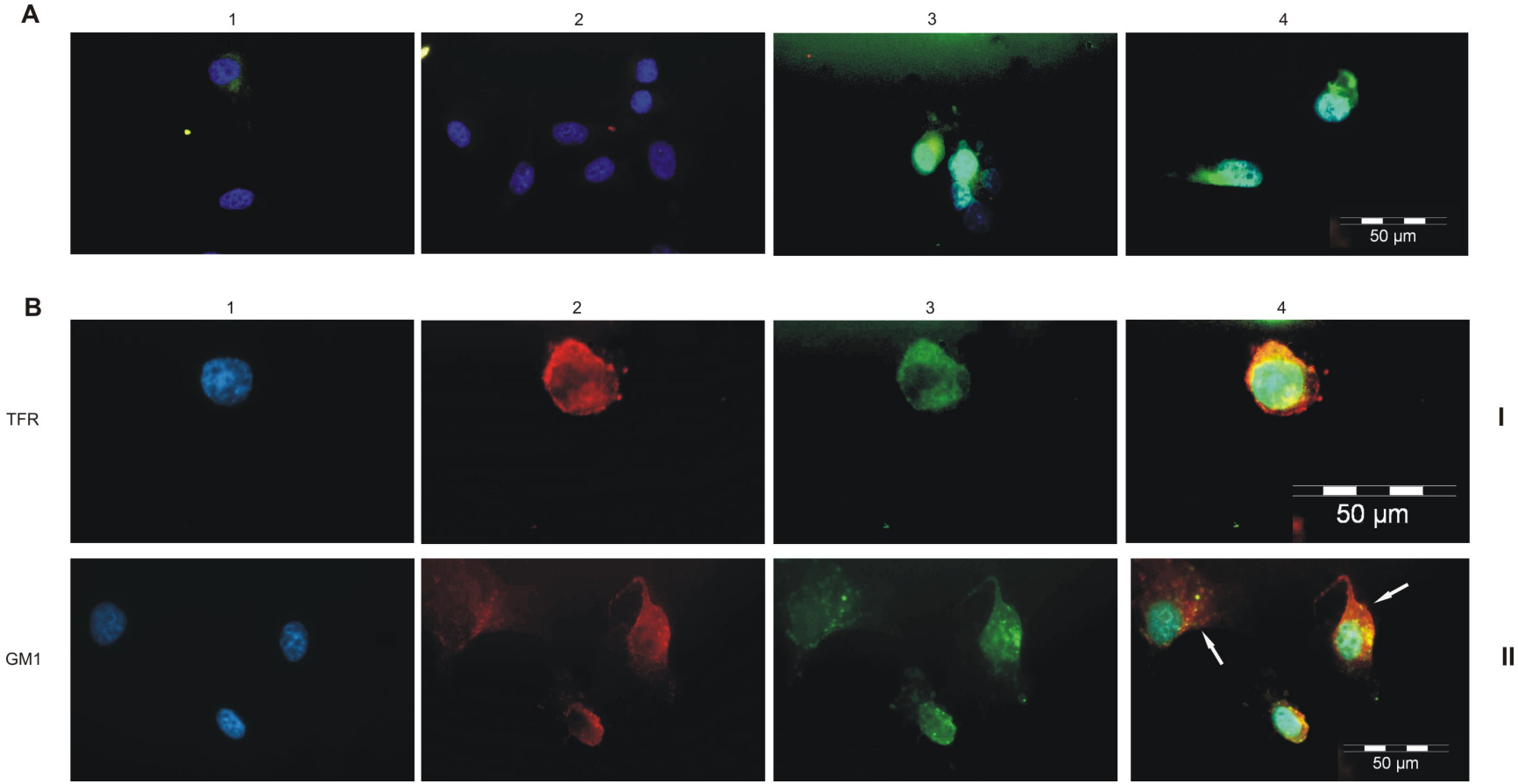

Figure 3.8: Localization of CCR5 receptor in U87 membrane and lipid raft domains. U87 R5 cells were fixed onto slides and probed with fluorophore-conjugated antibodies to assess representative localization of the R5 receptor using fluorescence microscopy. Scale bars represent 50 microns (600X). **(A) Control slides.** Panel 1: Cells stained with DAPI only, no antibody. Panel 2: Cells probed with X4-PE antibody only. Panel 3: Cells probed with X4-PE and TFR-FITC (TFR green fluorescence=membrane domain marker) antibodies. Panel 4: Cells probed with X4-PE and CT-Alexa Fluor 488 (GM 1 ganglioside green fluorescence=lipid raft marker) antibodies. **(B) Slides showing CCR5 localization.** Panel 1: DAPI. Panel 2: TFR-FITC (Top) or CT-Alexa Fluor 488 (Bottom). Panel 3: R5-PE. Panel 4: Merged images show co-localization in yellow.

3.5 HIV-1 and Fusion Studies

We infected U87 X4 and U87 R5 cell lines with two primary subtype C viral isolates in order to assess the localization of host cell receptors CD4, CXCR4 and CCR5, as well as the HIV-1 envelope protein gp41, during the early stages of viral and host membrane fusion. Specifically, we were interested in the redistribution of viral and host cell membrane receptors during the fusion process that might shed light on the importance of lipid rafts in HIV-1 entry.

3.5.1 Amplification of FV3 and FV5 Viral Isolates

In order to conduct the fusion studies, cells needed to be infected with extremely high viral titres. This was in order for cells to be saturated with virus to ensure successful fusion events would occur, as well as for allowing successful detection of the gp41 protein with the F-240 monoclonal antibody. After viruses were cultured, Western Blot, viral load, and p24 results all confirmed successful amplification of the FV5 virus (Figure 3.9, Appendix D and Appendix E). FV5 gp41 was successfully detected by the monoclonal antibody F-240 and its levels increased significantly from the time of viral input to the time of supernatant harvest (day 5), showing that amplification of the FV5 had taken place (Figure 3.9, Lanes 6 and 7). Furthermore, viral load quantification (Appendix E) and p24 results (Appendix D) confirmed an increase in FV5 particle production.

In contrast, the FV3 virus was not successfully amplified as active infection was not observed for this viral isolate by p24 analysis, which showed no productive infection by this virus in the

cell cultures over the 5-day incubation period (Appendix D). This was consistent with the viral load assay, which failed to detect increased viral RNA in the cell culture (Appendix E), and Western Blot analysis, which showed no detectable particle-associated FV3 gp41 in these samples (Figure 3.9, Lanes 3 and 4). Collectively, these data show that the amplification of FV3 was unsuccessful, and repeated attempts to amplify FV3 failed. The reasons for this are unclear, but could be due to the loss of viability of FV3, or possibly that the inoculum viral titres were high, causing cell death. Storage conditions of the FV3 viral stocks could have also played a role in not maintaining viability. It was therefore decided to carry out fusion experiments with FV5 infections in the U87 R5 cells only.

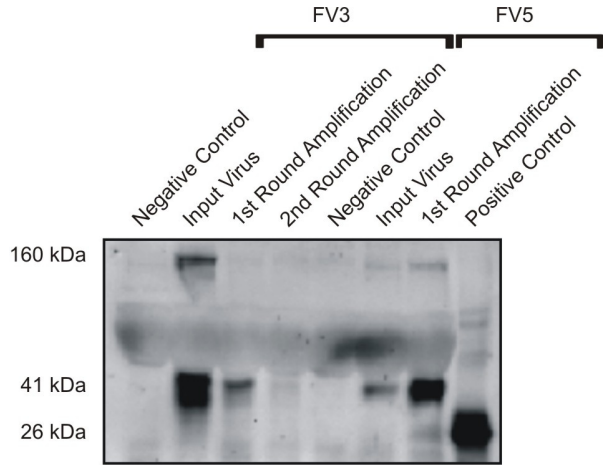

Figure 3.9: gp41 Western Blot analysis of FV3 and FV5 virus-containing supernatants following amplification in U87 X4 and U87 R5 cell, respectively. Viral amplification was performed in order to obtain high titres of virus for fusion experiments. U87 X4 cells were infected with CXCR4-utilising FV3 viral isolate and U87 R5 cells were infected with CCR5-utilising FV5 viral isolate. Supernatant samples were taken 5 days post-infection and analysed by SDS-PAGE and Western Blotting using the anti-gp41 antibody, F-240. Negative Control: U87 X4/R5 cell growth medium.

3.5.2 Fusion Studies

U87 R5 cells were infected with an MOI of approximately 250 FV5 viral particles/cell. TAS was established in order to synchronize gp120-CD4 attachment, and to assess the distribution of CD4, CCR5 and gp41 at TAS and 3 hours post-TAS. Lipid raft and total membrane isolations were then performed on cells at each time point (if in cell culture flasks) or the cells on the microscope slides were fixed with 3% formaldehyde. In order to confirm successful infection under the conditions employed, one cell culture flask and one microscope slide of cells infected with the virus, were incubated for a further 4 days and samples were analysed by p24 ELISA (Appendix D).

Western Blot analysis was performed on the fractionated U87 R5 raft and total membrane samples to assess CD4 (Figure 3.10) and gp41 (Figures 3.10 and Appendix G) localization in these cells at TAS and 3 hours post-TAS. In parallel, control samples that were not infected were also assessed (designated NVC). The TFR membrane marker and TUB cytoplasmic marker showed the expected distribution within the non-raft and cytoplasmic domains. However there was a slight shift in the relative abundance of these proteins within the different fractions between TAS and 3 hours post-TAS, which could be temperature-dependent. In addition, there was an interesting redistribution of the GM1 ganglioside from the expected raft microdomain in the NVC samples to the majority of the lipid being detected in the total membrane microdomain upon the addition of the FV5 virus at 3 hours post TAS. The reason for this redistribution is unclear, but possibly reflects a disruption of the membrane lipid structure by gp41 upon insertion of the fusion peptide and maturation of the fusion pore.

CD4 and gp41, in the FV5-infected samples at TAS and 3 hours post-TAS, appear to localize with the total membrane fractions, with little or no detectable levels evident in the raft fractions, respectively. These results are in agreement with previous findings that CD4 localization within the raft microdomains is not needed for successful HIV-1 entry in host cells (Percherancier et al., 2003; Popik and Alce, 2004). Others suggest, however, that CD4 and gp41 localize to raft microdomains upon fusion (Kozak et al., 2002; Viard et al., 2002; Chan et al., 2005; Chen et al., 2009). CD4 shows localization with both lipid rafts and total membrane domains at TAS and 3 hours post TAS in the NVC samples, which is consistent with the initial studies performed on the natural localization of CD4 (Figure 3.6). However, the intensity of the bands is significantly less than those seen in the initial localization studies. The reason for this is probably due to the fact that the number of cells used for the fusion experiments was approximately 50 % less than that used for the initial localization studies. Infections took place on the cells at 70 % confluency and thereafter, approximately 10-20 % of those cells experienced cell death, possibly due to the changes in temperature or the large amount of virus added. Intriguingly, the addition of the FV5 virus appeared to induce a conformational or structural change in CD4, suggested by the detection of two species of the protein by CD4 Western Blotting (Figure 3.10, Row 4, FV5 Membrane Fractions 4 and 5). One of these species could represent a particular cleavage product involved in gp120-induced signalling through CD4, or a metastable conformational intermediate involved in membrane fusion. Similar CD4 signalling pathways have been documented, for example Zap-70 (Chan et al., 1991) or Lck signalling (Holdorf et al., 2002) during T cell receptor (TCR) signal transduction, yet structural rearrangements of the receptor have not been shown. This pattern of migration was also seen for TUB, however, and suggests that the virus specifically changes the structure of these two proteins. To our knowledge, this is the first report of such a change induced by the addition of a primary viral isolate to cells in culture to assess the HIV-1 fusion process.

Fluorescence microscopy analysis of the CCR5 co-receptor during the fusion studies showed diffuse distribution of receptor in both the membrane and lipid raft domains at TAS and 3 hours post TAS (Figures 3.11 and 3.12). In the presence of virus, CCR5 did appear to cluster to a greater extent with the non-raft microdomains compared to the raft microdomains (Figures 3.11 and 3.12, Rows III and IV, Panel 4). Although, more localized patches of CCR5 were noted within the lipid raft domains, compared to the more diffuse pattern found in the non-raft domains (see arrows in Figures 3.11 and 3.12, Row III, Panel 4 to compare). This would suggest that upon gp120-CD4 engagement, although there is still a diffuse distribution of CCR5 on the cell surface, there is slight redistribution of the receptor into localized lipid raft patches. In addition, at 3 hours post-TAS the association of CCR5 with the non-raft microdomains in the FV5-infected cells seemed to increase as compared to that seen at TAS. Published reports on CCR5 membrane localization during the fusion process are minimal and in disagreement. Percherancier *et al* suggest that CCR5 localization within lipid raft microdomains is not essential for HIV-1 entry, whereas Popik *et al* state that the association of CCR5 with rafts is necessary for successful fusion and entry of HIV-1 into target cells (Popik et al., 2002; Percherancier et al., 2003).

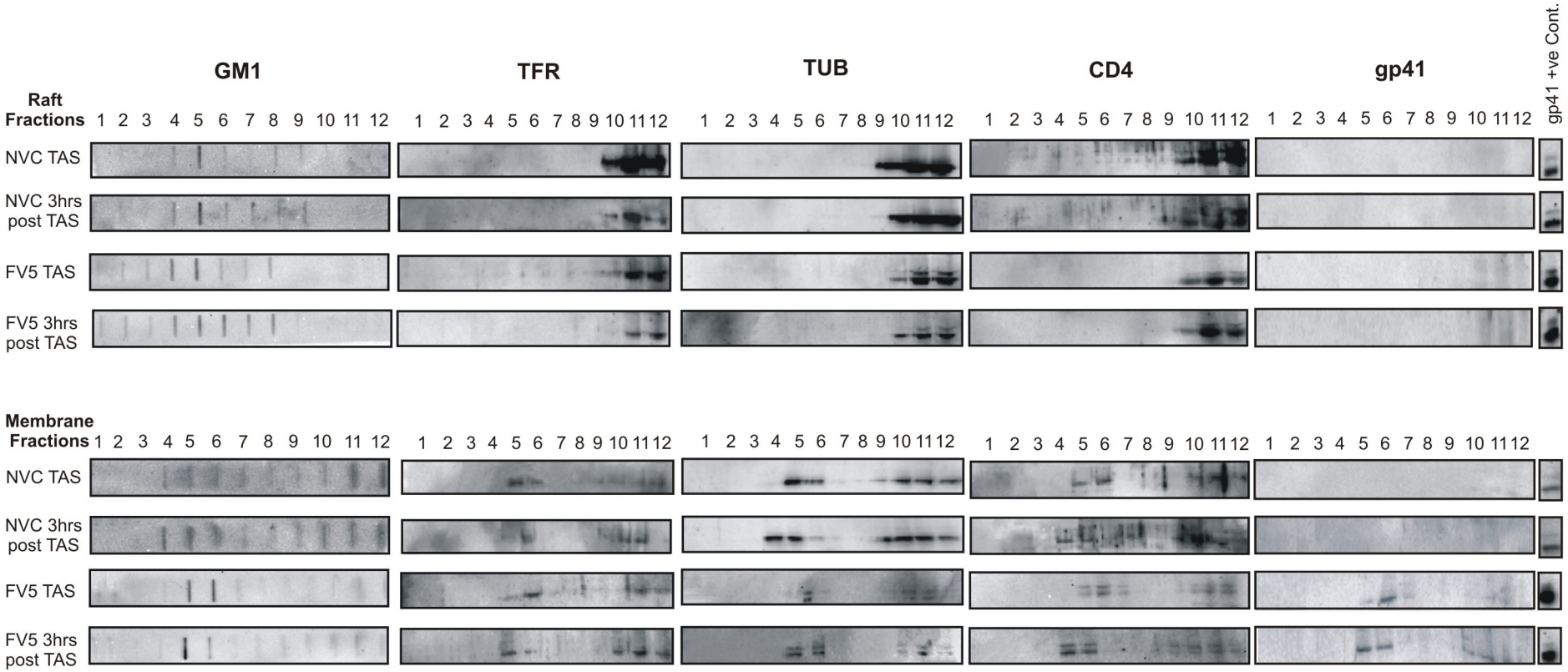

Figure 3.10: Slot Blot and Western Blot analysis of FV5 fusion studies. U87 R5 cells were infected with the FV5 viral isolate (FV5) or left uninfected, as a non-virus control (NVC). Infections were then left to incubate at 23 ° C for 2 hours (TAS), to allow for gp120-CD4 engagement, and then for a further 3 hours at 37 ° C (3 hrs post TAS) to allow for fusion to occur. TAS and 3 hrs post TAS infections were subjected to lipid raft and membrane extractions, and collected fractions were resolved on 10% SDS-PAGE gels. Western Blots were performed using the appropriate antibodies to detect localization of the CD4 receptor and gp41.

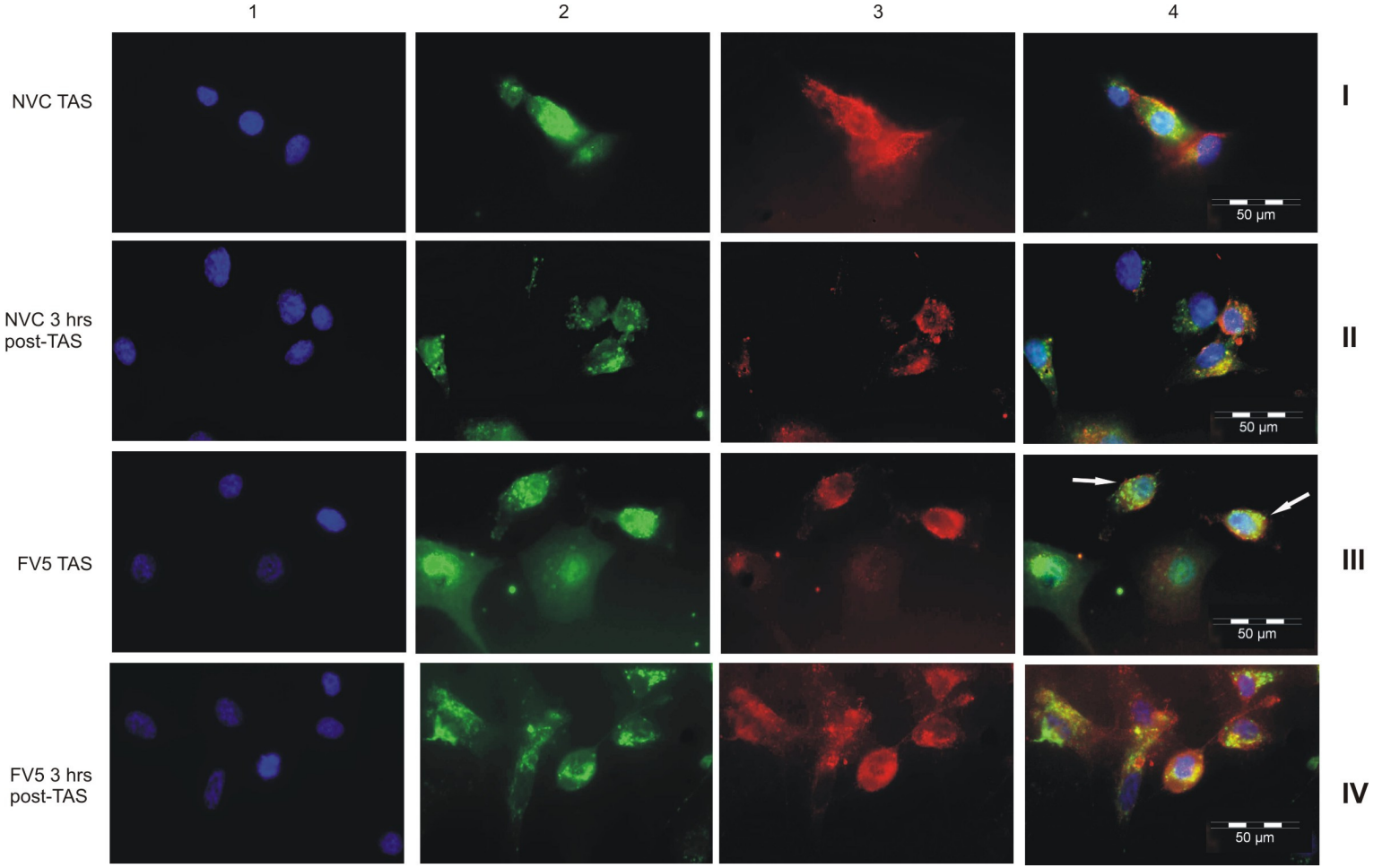

Figure 3.11: Localization of CCR5 receptor in lipid raft domains. U87 R5 cells were seeded onto microscope slides and infected with the FV5 viral isolate. Uninfected cells served as a negative control (NVC). Slides were incubated at 23 ℃ for 2 hours (TAS), to allow for gp120-CD4 engagement, and thereafter for 3 hours at 37 ℃ (3 hours post-TAS), to allow for fusion to occur. At the end of each incubation point, cells were fixed onto the slides, stained and representative images are shown in this figure. 1: DAPI. 2: CT-B-Alexa Fluor 488. 3: R5-PE. 4: Merged images showed co-localization in yellow. Arrows indicate co-localized CCR5 and lipid raft patches.

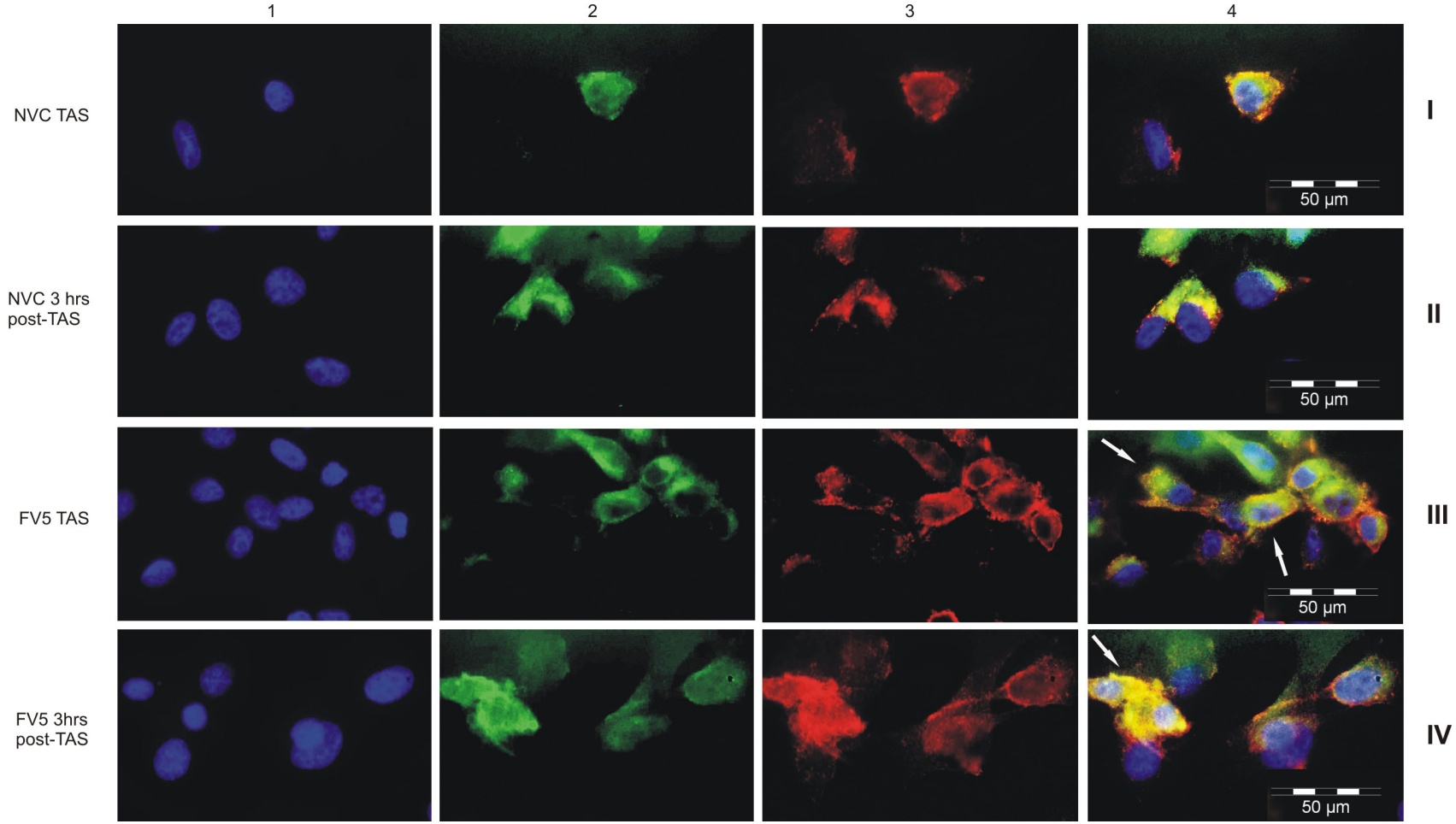

Figure 3.12: Localization of CCR5 receptor in membrane domains. U87 R5 cells were seeded onto microscope slides and infected with the FV5 viral isolate. Uninfected cells served as a negative control (NVC). Slides were incubated at 23 ℃ for 2 hours (TAS), to allow for gp120-CD4 engagement, and thereafter for 3 hours at 37 ℃ (3 hours post-TAS), to allow for fusion to occur. At the end of each incubation point, cells were fixed onto the slides, stained and representative images are shown in this figure. 1: DAPI. 2: TFR-FITC. 3: R5-PE. 4: Merged images showed co-localization in yellow. Arrows indicate diffuse interactions between CCR5 and non-raft domains.

CHAPTER 4: DISCUSSION

4.1 Cloning of gp41- and gp160-encoding DNA

A recombinant gp41-expression vector (pTriEx-gp41) was generated in order to express and purify a recombinant subtype C gp41 protein (derived from viral isolate FV3). This was used to control for the detection of gp41 extracted in membrane fractions isolated from FV3- and FV5-infected cell cultures, using the monoclonal antibody F-240. In parallel, a recombinant gp160-expression vector (pTriEx-gp160) was generated in order to assess the efficient recovery and detection of membrane-bound gp41, when expressed in mammalian cell culture. The generation of both gp41- and gp160-recombinant expression vectors, utilizing a plasmid template containing a codon optimized gp160 sequence derived from the FV3 viral isolate (pGA4-gp160) was successful (Figure 3.1), and sequence analysis confirmed the integrity of the FV3 gp41- and gp160-encoding sequences (Figure 3.2).

4.2 gp41 Recombinant Protein

The expression of gp41-6xHis from pTriEx-gp41 expression vector was induced in transformed BL21 pLysS *E. coli* cells and culture lysates from these cells tested positive for the presence of gp41 in time course induction experiments by Western Blot analysis (Figure 3.3). These experiments confirmed efficient expression of, and immunochemical detection of this protein using the monoclonal antibody, F-240. The positive control used in all the Western Blot analyses of gp41 expression and purification is an *E. coli* derived recombinant gp41 protein (from a subtype B viral isolate) containing the immunodominant regions of gp41, which resolves at 41 kDa on SDS-PAGE gels.

The solubility of the expressed gp41-6xHis protein was then assessed and it was noted that the majority of the protein was recoverable in a soluble form (Figure 3.3, Lane 5). This observation was unexpected and surprising, as other literature describes recombinant gp41 as a predominantly insoluble protein at neutral pH (Lu et al., 1995), which is thought to be due to highly hydrophobic residues located within the transmembrane domain and cytoplasmic tail regions of the protein (Gallaher et al., 1989; Scholz et al., 2005). Soluble Env protein has been documented, but with modifications. These modifications include the routine deletion of hydrophobic residues (Weissenhorn et al., 1996; Wingfield et al., 1997; Qiao et al., 2005; Frey et al., 2008; Noah et al., 2008), refolding of the purified protein at an acidic pH (<3.5) (Wingfield et al., 1997; Krell et al., 2004) and adding various 'solubility tags' to gp41 constructs to increase the solubility of purified recombinant protein (Scholz et al., 2005; Noah et al., 2008; Penn-Nicholson et al., 2008).

The reasons for our findings are unclear; however it is possible that complex folding patterns and oligomerisation of gp41 produces species with unexposed hydrophobic regions. In support of this, the purified recombinant gp41 appeared to exist in monomeric, dimeric and trimeric forms, suggested by the presence of three separate bands of molecular weights 26 kDa, 75 kDa and 127 kDa detected by Coomassie, Silver Stain and Western Blot analyses (Figure 3.3). This is consistent with published data showing that, even under denaturing conditions, gp41 migrates as three separate bands on SDS-PAGE gels (Weissenhorn et al., 1996; Frey et al., 2008). Differences in sequence could possibly affect the folding patterns of gp41, and thereby influence the solubility of the protein. Alternatively, inconsistencies between published literature and our work could be due to differences in expression systems, none of which mimic the true environment of expressed gp41 protein. Western Blot analysis of purified gp41 also confirmed the detectability of the recombinant protein with monoclonal antibody, F-240,

demonstrating the feasibility of viral particle-associated gp41 detection using the same methods.

4.3 gp160 Expression in HEK 293T Cells

To confirm the ability to recover membrane-associated gp41 from cells using density-gradient centrifugation and to detect the protein using the immunochemical methods described, expression of gp160 in HEK 293T cells was assessed by transfecting cells with the pTriEx-gp160 expression vector and isolating lipid raft and membrane fractions from the transfected cells. gp160 expression was successfully detected in the isolated membrane fractions using Western Blot procedures with the F-240 antibody (Figure 3.5). Similar gp160 expression studies have been performed by others, where various Env constructs have been used to transfect HEK 293T cells and lipid raft isolations and Western Blot analyses have been performed (Chan et al., 2005; Chen et al., 2009). These pilot expression studies establish that the use of the Western Blot detection methods described, using the monoclonal antibody F-240, was successful and suggest that such methods were feasible for the detection of membrane-bound gp41 in the virus-cell fusion experiments.

4.4 Receptor Localization in Membrane Domains

In order to determine the natural localization of CD4, CCXR4 and CCR5 receptors in cell membrane domains, U87 X4 and U87 R5 cells were subjected to total membrane and lipid raft extractions by sucrose density centrifugation. Cell membranes are naturally buoyant when the cells are lysed and subjected to sucrose density-gradient centrifugation

and therefore migrate to a density equal to that represented by between 10-65% sucrose in aqueous solution (Figure 3.4). Lipid rafts migrate to between 5-30% sucrose concentrations in aqueous solution (Figure 3.4). Western Blot analysis was performed on the fractions collected from the extractions (Figure 3.6). To determine that the raft and total membrane extractions were successful and that we correctly isolated the respective membrane components, we checked the localization of markers with well-established membrane domain distribution. Antibodies against transferrin (TFR) and tubulin (TUB) were used to confirm correct fractionation of membrane and cytoplasmic components, respectively. The GM1 ganglioside lipid raft marker was detected most efficiently using Slot Blot analysis, and this detected GM1 ganglioside was mostly in raft fractions 3, 4 and 5, consistent with its role as a structural component of raft microdomains. TFR was detected predominantly in membrane fraction 5 and in fractions 10-12 of the raft gradients, consistent with it being a membrane-bound protein. TUB was detected in the bottom fractions of the raft and membrane extractions, confirming a predominant cytoplasmic localization. Collectively, these data confirm that lipid raft and membrane extractions were successful, and we efficiently isolated the correct membrane domain components.

4.4.1 CD4 Localization

CD4 was shown to be naturally located in both lipid raft and non-raft microdomains on the surface of uninfected U87 X4 and U87 R5 cells (Figure 3.6). Similar Western Blot analyses have been performed by others to determine the localization of CD4 in cell membranes. When compared to our results, these show the same pattern of CD4 distribution in detergent-resistant and detergent-soluble fractions following lipid raft extractions (Del Real et al., 2002; Kozak et al., 2002; Popik et al., 2002; Percherancier et

al., 2003; Popik and Alce, 2004). The experimental procedures, however, differ from those utilized in our experiments and the published literature only focuses on discussing CD4 localization within lipid raft domains. It is clear from our results, however, that a substantial amount of CD4 also exists in non-raft microdomains in the cell line tested (U87), under natural conditions.

4.4.2 CXCR4 and CCR5 Localization

After several attempts, using different approaches, we were unable to detect CXCR4 and CCR5 receptors isolated by membrane flotation using immunochemical procedures. These findings were surprising and disappointing, as there are several published reports describing the successful detection of CXCR4 and CCR5 using Western Blot analysis (Manes et al., 2000; Kozak et al., 2002; Popik et al., 2002; Viard et al., 2002; Percherancier et al., 2003; Nguyen et al., 2005). Despite following the methodologies articulated in these reports closely, in general, variable results were obtained each time the experiments were repeated with a high degree of non-specificity and cross-reactivity noted for the antibodies that were used (Appendix E). The reasons for this are still unclear, and our assumption is that our inability to detect CXCR4 and CCR5 by immunoblotting procedures is related the hydrophobic properties of these seven-transmembrane domain chemokine receptors, making it difficult to obtain consistent results via Western Blot detection. Another possibility could be that the quality of the antibodies used was poor, most likely due to poor epitope specificity.

Because of the difficulties experienced in detecting these two proteins by immunoblotting procedures, a decision was made to characterise CXCR4 and CCR5 localization using fluorescence microscopy (Figures 3.7 and 3.8). While using microscopic methods of detection deviated from our original purpose of obtaining a quantitative assessment of co-

receptor localization during real-time virus fusion, it was anticipated that they would nonetheless be able to give valuable insights in this context. Moreover, fluorescence microscopy is a well-documented and well-accepted detection method for cell surface receptors and provides a platform for localization analysis of these receptors in the different membrane microdomains without manipulating the cells as intrusively as is needed in the case of Western Blot analysis. Co-localization studies of CXCR4 and CCR5 with the TFR membrane marker and the GM1 ganglioside lipid raft marker revealed that, under normal conditions, CXCR4 and CCR5 were found in close association with both raft and non-raft membrane domains in U87 cells. While expression on the cell surface appeared to be diffuse for both receptors, in our hands CCR5 seemed to associate with lipid rafts to a lesser extent than that seen for CXCR4, as suggested by more red colouration seen in the merged panel of U87 R5 cells probed with R5-PE and CT-Alexa Fluor 488 (see arrows in Figure 3.8, Row B II, Panel 4), as compared to more yellow colouration seen in the merged panel of U87 X4 cells probed with X4-PE and CT-Alexa Fluor 488 (see arrow in Figure 3.7, Row B II, Panel 4).

Fluorescence microscopy studies performed by others on the localization of CXCR4 and CCR5 within the raft/non-raft microdomains have generated contrasting results. Manes *et al* show that, under normal conditions, CXCR4 is located in lipid raft microdomains on the cell surface of 293-CD4 cells (Manes et al., 2000), while Nguyen *et al* show that the localization of this protein in lipid rafts only occurs in the presence of CD4 on the surface of Jurkat cells (Nguyen et al., 2005). Kozak *et al*, however, show that CXCR4 does not co-localize with lipid rafts using immunoblotting procedures on H9 and U87 X4 cells (Kozak et al., 2002). When assessing CCR5 distribution, under normal conditions, by both Western Blot and fluorescence microscopy analysis, Popik *et al* show some co-localization with lipid rafts on the surface of PM1 T cells (Popik et al., 2002), whereas Percherancier *et al* state that CCR5 is not located in lipid raft microdomains on A3.01 T cells (Percherancier et al., 2003). The fluorescence microscopy studies on the

localization of the G-protein coupled receptors have generally made use of a technique called 'patching'. Patching involves the artificial aggregation of the lipid raft microdomains with various proteins or raft-specific antibodies before carrying out the co-localization studies using fluorescence microscopy in order to concentrate proteins associated with lipid rafts into distinct areas or patches. This artificial aggregation or 'patching' technique probably compromises the aim of trying to assess the natural distribution of this receptor on the cell surface (Popik et al., 2002).

Consistent with our results, Viard *et al* show that CXCR4 is distributed in a diffuse manner using Western Blot analysis on human peripheral blood T lymphocytes and state that fluorescence microscopy found CXCR4 to be randomly distributed on the surface of unstimulated CEM cells (Viard et al., 2002). Popik *et al* do suggest, however, that both CXCR4 and CCR5 are constitutively, yet not exclusively associated with lipid raft microdomains (Popik et al., 2002). Percherancier *et al* also show an even distribution of CCR5 over the plasma membrane prior to raft 'patching' and upon induced aggregation it seems that CCR5 is excluded from the lipid raft microdomains during fluorescence microscopy analysis (Percherancier et al., 2003). Collectively, our data are in agreement with Viard *et al*, Popik *et al* and Percherancier *et al* and suggest that under normal, unstimulated conditions, CXCR4 and CCR5 are randomly and diffusely distributed within both lipid raft and non-raft microdomains.

4.5 HIV-1 and Fusion Studies

To our knowledge, this is the first study to document the use of infectious HIV-1 subtype C primary viral isolates in viral-cell fusion assays to assess the redistribution of viral and host cell receptors during the fusion process, in real time. Our aim was to shed light on the importance of lipid rafts for HIV-1 by examining the dynamics of virus and host cell

receptor localization during the membrane fusion process. Our results augment those generated by other studies which have made use of pseudotyped viruses, recombinant gp120 or gp41 proteins, or cell-cell fusion assays to study receptor localization (Manes et al., 2000; Del Real et al., 2002; Kozak et al., 2002; Popik et al., 2002; Viard et al., 2002; Nguyen and Taub, 2003; Percherancier et al., 2003; Popik and Alce, 2004) and provide new insights into the dynamic distribution of gp41, CD4 and CCR5 upon viral entry into target cells.

The use of the 'temperature-arrested state' (TAS) (incubation of cells at 23 ºC at inoculation) during fusion studies was a critical component of our analyses. TAS allows for the synchronization of the viral entry process, by stalling the fusion process immediately after CD4- and co-receptor-engagement (Melikyan et al., 2000). Increasing the temperature to 37 ºC then enables initiation of active membrane fusion, maturation of the fusion pore and entry of HIV-1 into the target cell (Melikyan et al., 2000). TAS has been utilized as a technique to study the kinetics of viral fusion (Melikyan et al., 2000; Golding et al., 2002; Buzon et al., 2005; Mkrtchyan et al., 2005), as well as analysing the various gp41 conformations associated with viral fusion with the host cell membrane (Melikyan et al., 2000; Gallo et al., 2001; Melikyan et al., 2006) It has also been useful in studying the localization of host cell receptors upon fusion (Manes et al., 2000; Del Real et al., 2002; Popik et al., 2002; Nguyen and Taub, 2003).

4.5.1 Amplification of FV3 and FV5

We amplified HIV-1 subtype C primary viral stocks that had been previously propagated, maintained and characterised in our laboratory, to high viral titres. This enabled us to perform infections using an MOI of 250, such that detectable amounts of fusion events would take place and allow for the successful detection of gp41. The X4-tropic FV3 viral

isolate and R5-tropic FV5 viral isolate were amplified in the U87 X4 and U87 R5 cell lines, respectively. Amplification was detected by p24 ELISA (Appendix D), viral load measurements (Appendix E) and Western Blot analysis with the F-240 antibody (Figure 3.9).

The FV5 virus was shown to amplify successfully under the cell culture conditions employed, as seen by p24, viral load and Western Blot analyses. In contrast, the FV3 virus was not successfully amplified. Active infection was not noted with p24 ELISA detection and a decrease in the viral load measurements were observed, as compared to the original amount of input virus. Western Blot analysis showed a marked decrease in the amount of gp41 detected over time and repeated attempts at amplify FV3 were unsuccessful. The reasons for the unsuccessful amplification of FV3 are unclear, but could possibly be due to the death of U87 X4 cells, as original input virus titre was too high, therefore compromising productive infection in these cells. Another possibility is that the FV3 virus was unable to infect the U87 X4 cells due to a loss of viability of the viral stocks used, perhaps through inactivation during long-term storage. Our fusion experiments were thus limited to those performed on the FV5 viral isolate and ongoing work by others in our laboratory aims to optimize the FV3 viral amplification procedure, in order to obtain a more comprehensive insight into CD4 and CCR5 as well as CXCR4 redistribution on the cell surface during fusion.

4.5.2 gp41, CD4 and CCR5 Receptor Localization During HIV-1 Fusion

Our fusion experiments involved infection of U87 R5 cells using the primary HIV-1 isolate FV5. We focussed on the dynamic localization of viral gp41, CD4 and CCR5 in raft and non-raft membrane domains during the early phases of virus attachment and membrane fusion. FV5 virus was added to U87 cells and incubated at 23 ºC for 2 hours to

synchronize all infectious viral particles on the surface of host cells at TAS. Thereafter, the temperature was increased to 37 ºC for a further 3 hours to allow for fusion to proceed. Localization of gp41, CD4 (by Western Blotting following membrane fractionation) (Figure 3.10) and CCR5 (by fluorescence microscopy) (Figures 3.11 and 3.12) was assessed at both TAS and 3 hours post-TAS, and changes in the distribution of these proteins were evaluated.

4.5.2.1 gp41 Localization at TAS and 3 Hours Post-TAS

Western Blot analysis showed gp41 associated with non-raft microdomains on the target cell membrane, at both TAS and 3 hours post-TAS, using the monoclonal antibody F-240 (Figure 3.10, gp41 Panel 4, Membrane Fractions Lanes 5 and 6). Published data utilizing various synthetic peptides derived from the N-terminal fusion peptide of gp41 consistently show that gp41 readily associates with phospholipid bilayers such as those which occur on the plasma membrane (Kliger et al., 1997; Korazim et al., 2006; Moreno et al., 2007). The finding that gp41 is already associated with the target cell membrane at TAS is interesting, as it is thought that membrane insertion of gp41 occurs only at 37 ºC (Melikyan et al., 2000; Mkrtchyan et al., 2005). It has, however, been noted that at TAS, gp41 is likely to be exposed (Melikyan et al., 2000; Gallo et al., 2001), as gp120 has already undergone extreme conformational changes that accompany CD4 and CXCR4/CCR5 engagement. In contrast, our results indicate that gp41 is already inserted into the membrane at TAS, and possibly already engaged in the process of six-helix bundle formation. This is suggested by the protein resolving at a different size to that seen for the gp160 expression studies and the FV5 viral amplification Western Blot analysis. It appears to resolve at a size of approximately 75 kDa, a size similar to that of one of the oligomeric forms of gp41 seen during the purification stages of our

recombinant gp41-6xHis protein (Discussed in section 4.2). At 3 hours post-TAS, there is a noticeable increase in gp41 in fraction 5 of the total membrane samples, compared with the amount at TAS, where the majority of gp41 is found in fraction 6. Moreover, while the amount of membrane-associated gp41 at 3 hours post-TAS appears to be greater than that at TAS, which is likely to result from maturation of the gp41 folding process at the thermodynamically permissive 37 ºC, the conditions for membrane insertion of gp41 appear to be satisfied at TAS. These findings provide significant insight into the process by which gp41 inserts into the host cell membrane, forms the six-helix bundle and drives membrane fusion. The fact that gp41 is associated with the target cell membrane at TAS, could have possible implications for vaccine developments. In particular, epitopes previously thought to be inaccessible at this stage, may be targetable earlier in the fusion process than previously believed. Moreover, these results, taken together with kinetic studies on the fusion process, could yield useful information in further understanding the pathogenesis of HIV-1 entry and help to further the development of potential HIV-1 entry/fusion inhibitors.

4.5.2.2 CD4 Localization at TAS and 3 Hours Post-TAS

Upon the addition of virus, and eventual fusion of viral and host cell membranes, there appears to be no evidence for significant CD4 redistribution to lipid raft microdomains. Western Blot analysis of the raft fractions collected after lipid raft isolations show CD4 located entirely in the detergent soluble fractions (seen in raft fractions 10, 11 and 12, Figure 3.10). This confirmed the localization of CD4 to the non-raft fractions, as seen by the bands detected on the Western Blots for the total membrane isolations (Figure 3.10). Our findings are consistent with Percherancier *et al* and Popik *et al*, who showed that CD4 localization in non-raft membrane microdomains supported HIV-1 entry

(Percherancier et al., 2003; Popik and Alce, 2004). However, other studies show that CD4 segregated to lipid raft microdomains on the cell surface is required for HIV-1 fusion and entry into the host cell (Kozak et al., 2002; Viard et al., 2002). However, all of the above mentioned studies used pseudotyped HIV-1 virus and HIV-1 envelope glycoprotein-mediated cell-cell fusion assays to assess the localization of CD4 upon viral-host cell membrane fusion, whereas we performed virus-host cell membrane fusion experiments to obtain our results. The majority of these papers also confirm localization results by depleting the cholesterol on the cell surface using, for example, methyl-β-cyclodextrin, which is a chemical agent known to deplete cholesterol (Percherancier et al., 2003; Popik and Alce, 2004). We did not employ this technique, and so it should be noted that any further investigations would benefit from cholesterol depletion assays, as it provides for an important control when assessing the importance of lipid rafts in HIV-1 infection.

Interestingly, CD4 extracted from infected cells at both TAS and 3 hours post-TAS, resolved on the SDS-PAGE gels as two bands of slightly different sizes (Figure 3.10, Panel 4, FV5 Membrane Fractions). This was unexpected and none of the published literature has reported such a result. The significance of this intriguing observation is unclear, but could possibly be due to protein cleavage induced by fusion, perhaps in the down regulation pathway of CD4 in HIV-1 infected cells. Another possibility could be that the virus influences the host cell membrane in such a way that causes the CD4 receptor to exist as a metastable conformational intermediate involved in membrane fusion and, under the denaturing conditions implemented, resolves as two separate domains. CD4 signalling events, similar to the pathway utilized by HIV-1, have been reported and involve Zap-70 (Chan et al., 1991) or Lck signalling (Holdorf et al., 2002) during TCR signal transduction. It has been shown that CD4 acts as a co-receptor during the regulation of T cell signalling (Konig et al., 1992; Konig et al., 1995), however, structural changes of this receptor during these signalling events has not been documented. TUB,

however, also existed as two separate species upon the addition of FV5. None of the published reports utilize direct primary virus and host cell fusion assays and so any effects that the virus may have on the host cell, and particularly on the receptors, were not seen in the results of these reports (Percherancier et al., 2003; Popik and Alce, 2004). Further work would be required in order to pinpoint the specific reason for this interesting result.

During Western Blot analysis of the fusion studies, it was noted that the GM1 ganglioside lipid raft marker also appeared to undergo redistribution upon the addition of FV5 to the U87 R5 cell cultures (Figure 3.10). The reasons for this surprising observation are unclear. However, we surmise that this could reflect lipid redistributions caused by the virus and consequent destabilization of the host cell membrane upon insertion of gp41 into the cell membrane. A relative increase in the amount of GM1 ganglioside in membrane fraction 5 was apparent at 3 hours post-TAS in samples from the FV5-infected total membrane isolation fractions (Figure 3.10, Panel 1, FV5 Membrane Fractions, Lane 5). Various groups have explored the mechanisms by which gp41 destabilizes the host cell membrane during fusion (Kliger et al., 1997; Pereira et al., 1997; Korazim et al., 2006; Moreno et al., 2007). These groups utilize synthetic gp41 N-terminal fusion peptides to conduct functional and structural characterisations on the interactions of the gp41 fusion peptide with the target plasma membrane. The documented results suggest that gp41 is able to permeabilize or destabilize the host cell membrane by rupturing the permeability barrier and allowing for fusion to occur by the formation of a fusion pore (Kliger et al., 1997; Pereira et al., 1997; Korazim et al., 2006; Moreno et al., 2007). These results could possibly explain why we observed redistribution of the GM1 ganglioside within the cell membrane microdomains upon FV5-induced fusion. Moreover, these results possibly support the idea that gp41 insertion into the target cell membrane causes changes in the migration patterns of the CD4 and TUB domains during SDS-PAGE and Western Blot

analysis, again suggesting interference of the virus with the host cell membrane and its receptors.

4.5.2.3 CCR5 Localization at TAS and 3 Hours Post-TAS

When assessing CCR5 localization via fluorescence microscopy, it was discovered that this receptor seemed to cluster to a greater extent with non-raft microdomains as compared to lipid raft microdomains, upon FV5-cell membrane fusion (Figures 3.11 and 3.12). While there was evidence of localized patches of CCR5 within the lipid raft microdomains (see arrows on Figure 3.11, Row III, Panel 4) the association with non-raft microdomains generally appeared more extensive (see arrows on Figure 3.12, Rows III and IV, Panel 4). Taking into account the qualitative and subjective nature of this type of data analysis, it is difficult to state whether there appears to be any significant redistribution of CCR5 during HIV-1 fusion. It can, however, be said that CCR5 does not exclusively localize with either raft or non-raft microdomains, but rather is diffusely distributed within non-raft microdomains and more localized patches of the receptor are seen in the lipid raft microdomains, during the HIV-1 fusion process.

Published data describing CCR5 localization to raft or non-raft microdomains during the fusion process is inconsistent (Popik et al., 2002; Percherancier et al., 2003). For example, Percherancier *et al* state that HIV-1 entry into T cells is not dependent on CCR5 localization in lipid raft microdomains (Percherancier et al., 2003), whereas Popik *et al* suggest that CCR5 association with lipid rafts is needed for successful fusion and entry of HIV-1 into target cells (Popik et al., 2002). Both groups utilized pseudotyped viruses to carry out the fusion experiments, and performed both Western Blot and fluorescence microscopy analysis to obtain the results described above. It is clear, when taking our results together with the published data into account, that further, and more standardized,

analysis is needed to obtain a comprehensive description of the dynamics of CCR5 localization during HIV-1 membrane fusion.

4.5.2.4 Additional Comments on Fusion Studies

Firstly, the number of cells used for the lipid raft and total membrane isolations was markedly lower than the number of cells used in the initial experiments to determine the natural distribution of the host cell receptors and membrane domain markers. This was due to the requirement, for optimal viral infection, of a cell confluency of approximately 60%. In addition, there is significant cytotoxicity associated with infecting cell cultures with high viral titres, such as those used in this study. This is likely to have compromised the efficiency of receptor recovery from the infected cell cultures, as was suggested by the decrease in intensity of the protein bands seen on the Western Blot figures of samples isolated during fusion studies (Compare Figures 3.6 and 3.10). Secondly, co-receptor localization studies could have benefited from the possible use of cell lines stably expressing tagged CXCR4 and CCR5, or by immunoprecipitation studies and possibly ELISA or flow cytometry analyses. In addition, Z-sectioning using confocal microscopy could have been applied to better resolve the areas of co-localization within the lipid raft domains. Such experiments could contribute to a more quantitative and comprehensive assessment of the dynamic localization of the co-receptors during HIV-1 membrane fusion.

Another limitation to these fusion studies is that only receptor-mediated membrane fusion of HIV-1 is accounted for. It has been shown, however, that HIV-1 can also gain entry into the host cell via endocytosis, which was recently detailed by Miyauchi *et al* (Miyauchi et al., 2009). These results suggest that complete HIV-1 fusion occurred in endosomes and that viral fusion directly with the host cell membrane did not progress past the lipid

mixing step. The use of time-resolved imaging of single viruses during the fusion/entry process of HIV-1 allowed for the above mentioned results to be obtained. This method was similar to the one used by ourselves to track the fusion process in real time using single, primary viral isolates. Such findings are controversial, as it has been widely accepted that the receptor-mediated fusion pathway is the preferred process by which HIV-1 enters the cell, and could have interesting consequences for the interpretation of the HIV-1 fusion process in the future. The utilization of this entry pathway by HIV-1 could possibly explain the inconsistent data reported for receptor localization by various authors.

4.6 Concluding Remarks

In conclusion, this study has provided valuable insights into the HIV-1 subtype C entry process and the involvement that lipid rafts play in this stage of the viral lifecycle by analysing virus-host cell membrane fusion, in real time. These fusion studies provide evidence that there is no apparent requirement for CD4 and/or gp41 to associate with lipid raft microdomains. Secondly, CCR5 is diffusely distributed in both lipid raft and non-raft microdomains, whether in uninfected cells or at TAS and 3 hours post-TAS in infected cells. Our findings suggest, however, that lipid rafts are possibly important in the sequestration of CCR5 to the point at which gp120 engages CD4, but more evidence, of a quantitative nature, is needed to confirm this suggestion as our results were only of a qualitative nature. Some interesting observations included the possible cleavage or degradation of CD4 and the possible destabilization of the plasma membrane upon the addition of the FV5 primary viral isolate. The fact that gp41 appears to begin oligomerisation at TAS was also an unexpected, yet fascinating observation. To our knowledge, none of the above mentioned interesting findings have been documented

before, using a single virus-cell fusion assay to assess the real-time rearrangements occurring within the host cell membrane upon fusion. Further work is needed on the analysis of the corresponding distribution of CXCR4, in order to incorporate these findings into insights made for CD4 and CCR5, and to consolidate a theory of the role of lipid rafts during HIV-1 infection.

APPENDICES

Appendix A: Standard Protocols and Recipes

A1 Bacterial Cell Culture

A1.1 Solutions for Bacterial Culture

- *A1.1.1 Luria-Bertani (LB) Broth (1 L)*

  10 g of tryptone powder (Oxoid Inc; Basingstoke, Hampshire, England), 5 g of yeast extract powder (Biolab; Wadeville, Gauteng, South Africa) and 5 g of NaCl were dissolved in dH_2O to a final volume of 1 L. The broth was autoclaved (121 ºC, 1 kg/cm^2, 20 minutes) and stored at room temperature until use.

- *A1.1.2 Agar Plates*

  3 g of agar powder was added to 200 ml of LB Broth prior to autoclaving. After autoclaving, the solution was allowed to cool to approximately 55 ºC before the addition of appropriate antibiotics, poured into 90 mm Petri dishes and allowed to set.

- *A1.1.3 Ampicillin Stock (100 mg/ml)*

  1 g of ampicillin (Sigma-Aldrich; Steinheim, Germany) was dissolved in 70% ethanol to a final volume of 10 ml and stored at -20 ºC until use.

- *A1.1.4 Chloramphenicol Stock (35 mg/ml)*

  350 mg of chloramphenicol (Calbiochem; Darmstadt, Germany) was dissolved in 70% ethanol to a final volume of 10 ml and stored at -20 ºC until use.

- *A1.1.1.5 Transformation Buffer (100 mM $CaCl_2$, 10 mM PIPES-HCl, 15% Glycerol, pH 7.0)*

  1.4702 g of $CaCl_2.2H_2O$, 0.3024 g of PIPES (Boehringer Mannheim; GmbH, Germany) and 15 ml of glycerol were mixed with dH_20 to a final volume of 100 ml. The pH of the solution was adjusted to 7.0 using 10 M NaOH, it was then autoclaved and stored at -20 ºC until use.

A1.2 Preparation of Competent DH5α Cells

100 ml of LB Broth was inoculated with 5 µl of glycerol stock DH5α cells (Novagen; Darmstadt, Germany), under sterile conditions. The culture was incubated overnight at 37 ºC in a shaking incubator. The overnight culture was diluted 1:10 in LB and grown for a further 2-3 hours at 37 ºC in a shaking incubator to stimulate log phase growth. Once the A_{600} measurement reached approximately 0.4, the culture was centrifuged at 300 x g for 10 minutes at 4 ºC in order to pellet the cells. The supernatant was discarded and the pellet was resuspended in 10 ml of ice cold transformation buffer per 50 ml of culture and incubated on ice for 20 minutes. The cells were then pelleted again at 300 x g for 10 minutes at 4 ºC. The supernatant was discarded and the pellet was resuspended in 1 ml of ice cold transformation buffer. 100 µl aliquots were made of the competent cells, which were stored at -80 ºC until use.

A1.3 Transformation of Competent *E. coli* Cells

0.5 µl of plasmid DNA or 5 µl of ligation reaction was added to 50 µl of competent *E. coli*, and the suspension was incubated on ice for 20-25 minutes. A mock transformation was also set up, containing no DNA, and this served as a negative control. Cells were then heat shocked at 42 ºC for 30 seconds and immediately put back on ice for a further 2 minutes. Each transformation reaction was spread onto an agar plate, under sterile conditions, and incubated overnight at 37 ºC. Agar plates seeded with transformed DH5α cells contained 100 µg/ml ampicillin, whereas agar plates inoculated with transformed BL21 pLysS cells contained both 100 µg/ml ampicillin and 35 µg/ml chloramphenicol.

A1.4 Plasmid Preparations of pTriEx-3 and pGA4-gp160

50 µl of competent DH5α bacterial cells (Novagen; Darmstadt, Germany) were transformed with 0.5 µl of pTriEx-3 plasmid (approximately 1 µg/µl) (Appendix A1) or 0.5 µl of pGA4-gp160 plasmid (Appendix B) (approximately 50 ng/µl) (GENEART; Regensburg, Germany) (Appendix A1), plated out onto ampicillin-positive agar plates and incubated overnight at 37 ºC. A single colony was selected and used to inoculate Luria-Bertani Broth (LB Broth) containing ampicillin (100 µg/ml) (Sigma-Aldrich; Steinheim, Germany), under sterile conditions (Appendix A1). The cultures were incubated overnight at 37 ºC in a shaking incubator. The pTriEx-3 plasmid or pGA4-gp160 plasmid was then isolated from the overnight culture using the Sigma GenElute^{TM} Plasmid Maxiprep Kit (Sigma-Aldrich; Steinheim, Germany) according to the manufacturer's instructions. Isolated plasmids were resolved on 0.8% agarose gels and visualised under UV light.

A2 Agarose Electrophoresis

A2.1 Solutions for Agarose Electrophoresis

- *A2.1.1 0.5 M EDTA (pH 8.0)*

  93.05 g of EDTA powder was dissolved in dH_20 to a final volume of 500 ml. The pH of the solution was adjusted to 8.0 using 10 M NaOH. It was then autoclaved and stored at room temperature until use.

- *A2.1.2 50 X TAE Buffer*

  242 g of Tris base, 57.1 ml of glacial acetic acid and 100 ml of 0.5 M EDTA were mixed with dH_20 to a final volume of 1 L and stored at room temperature until use. Immediately before use, the solution was diluted to 1 X TAE by mixing 20 ml of 50 X TAE with 980 ml of dH_20.

- *A2.1.3 6 X DNA Loading Buffer*

  10 mM of Tris-HCl (Merck kGaA; Darmstad, Germany), 0.03% bromophenol blue, 60 % glycerol and 60 mM EDTA were combined and HCl was used to pH the solution to 7.6. This solution was stored at -20 ºC until use.

A2.2 Preparation of Agarose Gels

0.8% agarose gels were prepared by adding 0.8 g of agarose powder to 100 ml of 1 X TAE Buffer (diluted from 50 X stock solution) (Appendix A2.1.2). The mixture was then heated until the agarose powder had dissolved; prior to pouring the gels, 0.5 µg/ml of ethidium bromide (Promega; Madison, WI) was added. Gels were poured into a Bio-Rad Gel Chamber System (Bio-Rad; Hercules, CA) and allowed to set.

A2.3 Electrophoresis Procedure

Gels were run in a Bio-Rad Gel Tank System (Bio-Rad; Hercules, CA) submerged in 1 X TAE buffer (Appendix A2.1.2) to allow for even heat conduction. All DNA samples, controls and the Quick-Load™ 1 kb DNA Ladder (New England Biolabs; Ipswich, MA) were mixed with DNA Loading Buffer (Appendix A2.1.3). Gels were then run at maximum current and at 30 V as samples exited the wells, and thereafter at 60 V until samples had adequately resolved. DNA bands on the gels were visualised and images captured under UV light using the Versadoc™ Imaging System (Bio-Rad; Hercules, CA) and the Quantity One Version 4.6.1 Software Programme (Bio-Rad; Hercules, CA) .

A3 Mammalian Cell Culture

A3.1 Solutions for $CaCl_2$ Transfections

- *A3.1.1 2 X HEPES Solution (280 mM NaCl, 50 mM HEPES, 1.5 mM Na_2HPO_4, pH 7.1)*

  0.817 g of NaCl, 0.6 g of HEPES powder and 0.011 g of Na_2HPO_4 were dissolved in dH_20 to a final volume of 50 ml. The pH of the solution was adjusted using 10 M NaOH, thereafter the solution was filter sterilized using 0.22 µM Acrodisc® 25 mm syringe filters (Pall Corporation; Ann Arbor, MI) and stored at -20 ºC in 5 ml aliquots until use.

- *A3.1.2 2.5 M $CaCl_2$ Solution*

  91.85 g of $CaCl_2.2H_20$ was dissolved in dH_20 to a final volume of 250 ml. The solution was then filter sterilized and stored at -20 ºC in 10 ml aliquots until use.

A3.2 $CaCl_2$ Transfection Protocol

24 hours prior to transfection, 1.5 X 10^6 HEK 293T cells were seeded in 25 cm^2 cell culture flasks. 1 hour prior to transfection, growth medium was removed from flasks and 2 ml of fresh growth medium was added. Transfection complexes were then added to the cells in a drop-wise manner, swirled gently for even distribution, and flasks were placed in a 37 ºC incubator to allow for transfections to proceed.

A4 Protein Purification

A4.1 Solutions for Protein Purification

- *A4.1.1 Na-Phosphate Buffer (200 mM, pH 7.8)*

  500 mM stock solutions of NaH_2PO_4 (A) and Na_2HPO_4 (B) were prepared.
  For solution A: 39.003 g of powder dissolved in dH_20 to a final volume of 500 ml.
  For solution B: 44.498 g of powder dissolved in dH_20 to a final volume of 500 ml.
  Thereafter, 38 ml of solution A and 162 ml of solution B were mixed with dH_20 to a final volume of 1 L.

- *A4.1.2 Lysis Buffer (20 mM Na-Phosphate Buffer pH 7.8, 100 mM KCl, 1mM EDTA, 2 mM β-mercaptoethanol, 1% Nonidet P-40)*

  50 ml of 200 mM stock Na-Phosphate Buffer, 0.7455 g of KCl, 70.5 µl of β-mercaptoethanol, 1 ml of 0.5 M stock EDTA and 5 ml of Nonidet P-40 were mixed with dH_20 to a final volume of 500 ml. This solution was freshly prepared each time before use.

- *A4.1.3 8 M Urea in Lysis Buffer*

  14.4 g of urea (Calbiochem; Darmstadt, Germany) was dissolved in lysis buffer to a final volume of 30 ml. This solution was freshly made up each time before use.

- *A4.1.4 0.1 M $NiSo_4$ Solution*

  2.63 g of $NiSO_4$ was dissolved in 100 ml of dH_20 and stored at 4 ºC until use.

- *A4.1.5 Equilibration Buffer (20 mM Na-Phosphate Buffer ph 7.8, 100 mM NaCl, 2 mM β-mercaptoethanol, 0.1 mM EDTA)*

  50 ml of 200 mM stock Na-Phosphate Buffer, 2.922 g of NaCl, 70.5 µl of β-mercaptoethanol and 100 µl of 0.5 M stock EDTA were mixed with dH_20 to a final volume of 500 ml. This solution was freshly prepared each time before use.

- *A4.1.6 500 mM Imidazole Solution*

  1.702 g of imidazole powder was dissolved in equilibration buffer to a final volume of 50 ml. This solution was stored at 4 ºC until use.

A4.2 Preparation of Columns for Purification Procedure

Nickel-charged iminodiacetate-sepharose 6B resin (kindly prepared and donated by Dr Wolfgang Prinz) was used to purify the recombinant gp41 protein. This was possible by the expression of a C-terminal His-Tag on the recombinant gp41 protein, which binds to the nickel-charged sepharose. Two tubes containing 2 ml of the above mentioned bead solution each were washed with 30 ml of dH_2O and centrifuged at 3220 x g for 5 minutes. 10 ml of 0.1 M $NiSO_4$ solution was added to each tube and incubated at room temperature on a shaker for 10 minutes. The tubes were centrifuged at 3220 x g for 5 minutes and the supernatant removed. The beads were washed and centrifuged twice at 3220 x g for 5 minutes and thereafter equilibrated with 10 ml of equilibration buffer (20

mM Na-Phosphate Buffer, 100 mM NaCl, 2 mM β-mercaptoethanol, 0.1 mM EDTA) containing 10 mM imidazole (diluted 1:50 from 500 mM stock solution) (Appendix A4). They were centrifuged again and the supernatant was removed.

A5 Cell Counting

Cell counts were determined by tryptan blue exclusion using a haemocytometer. The cells were diluted 1:10 with 0.4% Trypan Blue Solution (Sigma-Aldrich; Steinheim, Germany) and an average number of cells counted in each block of the haemocytometer was obtained. This average was then multiplied by the dilution factor (10) and divided by the volume of the haemocytometer (0.1cm X 0.1cm X 0.001cm = 1 X 10^{-4} cm^3) to give the amount of cells/ml. This was then multiplied by the total volume of cells collected to obtain the final amount of cells.

A6 SDS-PAGE

A6.1 Solutions for SDS-PAGE

- *A6.1.1 4 X Running Gel Buffer (1.5 M Tris-HCL, pH 8.8)*

  36.3 g of Tris-HCl was dissolved in dH_20 to a final volume of 200 ml. HCl was used to adjust the pH of the solution and thereafter it was stored at 4 ºC, in the dark, until use.

- *A6.1.2 4 X Stacking Gel Buffer (0.5 M Tris-HCl, pH 6.8)*

  3 g of Tris-HCl was dissolved in dH_20 to a final volume of 50 ml. HCl was used to adjust the pH of the solution and thereafter it was stored at 4 ºC, in the dark, until use.

- *A6.1.3 10% Sodium Dodecyl Sulphate (SDS)*

  10 g of SDS was dissolved in dH_20 to a final volume of 100 ml. This solution was stored at room temperature until use.

- *A6.1.4 10% Ammonium Persulphate (APS)*

  0.1 g of APS was dissolved in dH_20 to a final volume of 1 ml. This solution was made up freshly each time before use.

- *A6.1.5 Running Gels (4 gels)*

  12 ml of Monomer Solution (Sigma-Aldrich; Steinheim, Germany), 11.23 ml of 4 X Running Gel Buffer, 450 µl of 10% SDS and 21.3 ml of dH_20 were combined. Just prior to pouring the gels, 225 µl of 10% APS and 15 µl of Tetramethylethylene-diamine (TEMED) (Sigma-Aldrich; Steinheim, Germany), were added to the solution.

- *A6.1.6 Stacking Gels (4 gels)*

  1.99 ml of Monomer Solution (Sigma-Aldrich; Steinheim, Germany), 3.75 ml of 4 X Stacking Gel Buffer, 150 µl of 10% SDS and 9 ml of dH_20 were combined. Just prior

to pouring the gels, 75 µl of 10% APS and 10 µl of TEMED (Sigma-Aldrich; Steinheim, Germany), were added to the solution.

- *A6.1.7 2 X Treatment Buffer (0.125 M Tris-HCl, 4% SDS, 20% v/v Glycerol, 0.2 M DTT, 0.02% Bromophenol Blue, pH 6.8)*

  2.5 ml of 4 X Stacking Gel Buffer, 4 ml of 10% SDS, 2 ml of glycerol, 2 mg of bromophenol blue (Saarchem; Merck Chemicals, Wadeville, Gauteng, South Africa) and 0.31 g of dithiothreitol (DTT) were mixed with dH_20 to a final volume of 10 ml. This solution was stored at -20 ºC in 500 µl aliquots until use.

- *A6.1.8 5 X Treatment Buffer (pH 6.8)*

  0.305 g of Tris-HCl, 1 g of SDS, 5 ml of glycerol, 0.2% bromophenol blue and 10% β-mercaptoethanol were mixed with dH_20 to a final volume of 10 ml. HCl was used to adjust the pH of this solution and thereafter it was stored in 1 ml aliquots at -20 ºC until use.

- *A6.1.9 10 X Tank Buffer*

  30.28 g of Tris-HCl, 144.13 g of glycine and 10 g of SDS were mixed with dH_20 to a final volume of 1 L. This solution was stored at room temperature until use.

A6.2 Preparation of SDS-PAGE Gels

SDS-PAGE gels were assembled using the Hoefer Gel Casting System (Hoefer Scientific Instruments; San Francisco, CA). Briefly, the casting chamber was assembled and sealed, the running gel solution was added to the chambers and a layer of isopropanol was added to seal and level out the gels. Once set, the isopropanol was rinsed off and the stacking gel solution was added and allowed to set.

A6.3 Electrophoresis Procedure

Gels were run under denaturing conditions using the Hoefer Gel System (Hoefer Scientific Instruments; San Francisco, CA) submerged in 1 X Tank Buffer to allow for even heat conduction. All protein samples and controls were mixed with either 2 X Treatment Buffer or 5 X Treatment Buffer, incubated at 80 ºC for 3 minutes to allow for protein denaturation and loaded into the wells of the gels. Prestained Protein Marker, Broad Range (6-175 kDa) (New England Biolabs; Ipswich, MA) was used for molecular weight calculation. Gels were run at 10 mA per gel through the stacking gel and at 25 mA per gel to resolve the samples.

A7 Staining Procedures

A7.1 Solutions for Staining Procedures

- *A7.1.1 Coomassie Staining Solution*

  0.25 g of Coomassie® Brilliant Blue R250 (Sigma-Aldrich; Steinheim, Germany) was dissolved in 500 ml of methanol, 100 ml of acetic acid and 400 ml of dH_20. This solution was stored at room temperature until use.

- *A7.1.2 Destaining Solution 1 (40% Methanol, 7% Acetic Acid)*

  400 ml of methanol, 70 ml of acetic acid and 530 ml of dH_20 were mixed and stored at room temperature until use.

- *A7.1.3 Destaining Solution 2 (5% Methanol, 7% Acetic Acid)*

  50 ml of methanol, 70 ml of acetic acid and 880 ml of dH_20 were mixed and stored at room temperature until use.

A7.2 Protocols for Staining Procedures

- *A7.2.1 Coomassie Staining*

SDS-PAGE gels were stained with Coomassie® Brilliant Blue R-250 (Sigma-Aldrich; Steinheim, Germany) overnight at room temperature with gentle shaking. The gels were

destained for 3 hours with Destaining Solution 1 and then for a further 30 minutes with Destaining Solution 2, both at room temperature with shaking. Protein bands were then visualised and images captured under white light using the Versadoc™ Imaging System (Bio-Rad; Hercules, CA) and the Quantity One Version 4.6.1 Software Programme (Bio-Rad; Hercules, CA).

- *A7.2.2 Silver Staining*

SDS-PAGE gels were fixed in a 40% Methanol and 10 % Acetic Acid solution for 1 hour at room temperature with shaking. Thereafter gels were silver stained using the Bio-Rad Silver Stain Kit (Bio-Rad; Hercules, CA), according to the manufacturer's instructions. Protein bands on the gels were then visualised and images captured as described.

A8 Western- and Immuno-Slot Blotting

A8.1 Solutions for Western Blotting

- *A8.1.1 Transfer Buffer*

  200 ml of methanol, 100 ml of 10 X Tank Buffer and 700 ml of dH_20 were mixed and stored at room temperature until use.

A8.2 Solutions for both Western Blotting and Immuno-Slot Blotting

- *A8.2.1 10 X Tris-Buffered Saline (TBS) (pH 7.4)*

  160 g of NaCl, 4 g of KCl and 60 g of Tris-HCl were dissolved in dH_20 to a final volume of 2 L. HCl was used to adjust the pH of the solution and thereafter it was autoclaved. This solution was stored at room temperature until use.

- *A8.2.2 T-TBS*

  Just before use, 10 X TBS was diluted 1:10 with dH_20 and Tween 20 added to a final concentration of 0.1% (v/v).

A8.3 Western Blotting Procedures

SDS-PAGE gels and nitrocellulose membrane were equilibrated in Transfer Buffer and placed on the Trans-Blot apparatus. Transfer conditions were set at maximum voltage and between 40-180 mA (depending of number of gels being transferred) for 1 hour and 15 minutes. Following protein transfer, nitrocellulose membrane was blocked in 5% fat free milk powder solution in T-TBS (made from a 10 X TBS stock) for 1 hour or 3 hours at room temperature with shaking. The milk powder solution was then rinsed off with T-TBS and the nitrocellulose membrane was probed with a primary antibody (See Table A1). Incubation was either for 1 hour at room temperature on the bench top, or for 2 hours at room temperature or overnight at 4 ºC with shaking. The nitrocellulose membrane was then washed 3 times, for 5 minutes or 10 minutes each, with T-TBS on a shaker in order to remove any unbound antibody. Secondary antibody probing was then performed for 1 hour at room temperature on the bench top (See Table A1). The nitrocellulose

membrane was washed, as described above, in order to remove any unbound secondary antibody before protein detection.

Protein detection was performed by standard chemiluminescence methods. Bands were visualised and images captured using the Versadoc^{TM} Imaging System (Bio-Rad; Hercules, CA) and the Quantity One Version 4.6.1 Software Programme (Bio-Rad; Hercules, CA) as described by the manufacturer.

Table A1: Table of Antibodies used in Western Blotting

ANTIBODY	STARTING CONCENTRATION	SECONDARY ANTIBODY USED	SUPPLIER
PURIFIED MOUSE ANTI-TRANSFERRIN RECEPTOR MONOCLONAL ANTIBODY (TFR)	250 MG/ML	ANTI-MOUSE	BD BIOSCIENCES PHARMINGEN; BELGIUM
ANTI-α-TUBULIN (BOVINE), MOUSE IGG_1, MONOCLONAL 236-10501 (TUB)	200 MG/ML	ANTI-MOUSE	MOLECULAR PROBES; OREGON, USA
MONOCLONAL MOUSE ANTI-HUMAN CD4, CLONE MT310 (CD4)	100 MG/ML	ANTI-MOUSE	DAKOCYTOMATION; DENMARK
CKR-5 (D-6): SC-17833 (CCR5)	200 MG/ML	ANTI-GOAT	SANTA CRUZ BIOTECHNOLOGY INC; SANTA CRUZ, CA
FUSIN (C-20): SC-6190 (CXCR4)	200 MG/ML	ANTI-GOAT	SANTA CRUZ BIOTECHNOLOGY INC; SANTA CRUZ, CA

HIV-1 GP41 MONOCLONAL ANTIBODY F240	2 MG/ML	ANTI-HUMAN	NIH AIDS RESEARCH AND REFERENCE REAGENT PROGRAM, DIVISION OF AIDS, NIAID, NIH
ECL™ ANTI-MOUSE IGG, HRP LINKED WHOLE ANTIBODY (FROM SHEEP) SECONDARY ANTIBODY	UNKNOWN	N/A	AMERSHAM BIOSCIENCES UK LIMITED; LITTLE CHATFONT, BUCKINGHAMSHIRE, ENGLAND
ECL™ ANTI-HUMAN IGG, HRP LINKED WHOLE ANTIBODY (FROM SHEEP) SECONDARY ANTIBODY	UNKNOWN	N/A	AMERSHAM BIOSCIENCES UK LIMITED; LITTLE CHATFONT, BUCKINGHAMSHIRE, ENGLAND
PEROXIDASE-CONJUGATED AFFINIPURE DONKEY ANTI-GOAT IGG	0.8 MG/ML	N/A	JACKSON IMMUNORESEARCH LABORATORIES; WEST GROVE, PA

A9 Standard Chemiluminescence Methods

Equal volumes of Stable Peroxide Solution and Luminol/Enhancer Solution from the SuperSignal® West Pico Chemiluminescent Substrate Kit (Pierce; Rockford, IL, USA) were mixed and added to nitrocellulose membrane for 5 minutes at room temperature on the bench top.

A10 Fluorescence Microscopy Analysis

A10.1 Solutions for Fluorescence Microscopy Analysis

- *A10.1.1 3% Formaldehyde Solution*

  1 ml of 37% stock formaldehyde solution was mixed with PBS (Sigma-Aldrich; Steinheim, Germany), in a glass beaker, to a final volume of 12.33 ml (1:12.33 dilution). This solution was freshly made up each time before use.

- *A10.1.2 PBS Containing 0.5% BSA*

  0.25 g of Bovine Serum Albumin (BSA) was dissolved in PBS (Sigma-Aldrich; Steinheim, Germany) to a final volume of 50 ml. This solution was stored at 4 ºC until use.

A10.2 Antibodies used for Fluorescence Microscopy Analysis

Table A2: Table of Antibodies used for Fluorescence Detection

ANTIBODY	COLOUR OF FLUORESCENCE	SUPPLIER
FITC-LABELLED MOUSE ANTI-HUMAN CD71 (TFR)	GREEN	BD BIOSCIENCES PHARMINGEN; BELGIUM
CHOLERA TOXIN SUBUNIT B (RECOMBINANT ALEXA FLUOR® 488 CONJUGATE, 100 UG)	GREEN	INVITROGEN; CARLSBAD, CA

PE-LABELLED ANTI-HUMAN CD184 (CXCR4)	RED	BD BIOSCIENCES PHARMINGEN; BELGIUM
PE-LABELLED ANTI-HUMAN CD195 (CCR5)	RED	BD BIOSCIENCES PHARMINGEN; BELGIUM

Appendix B: Restriction Map Diagrams

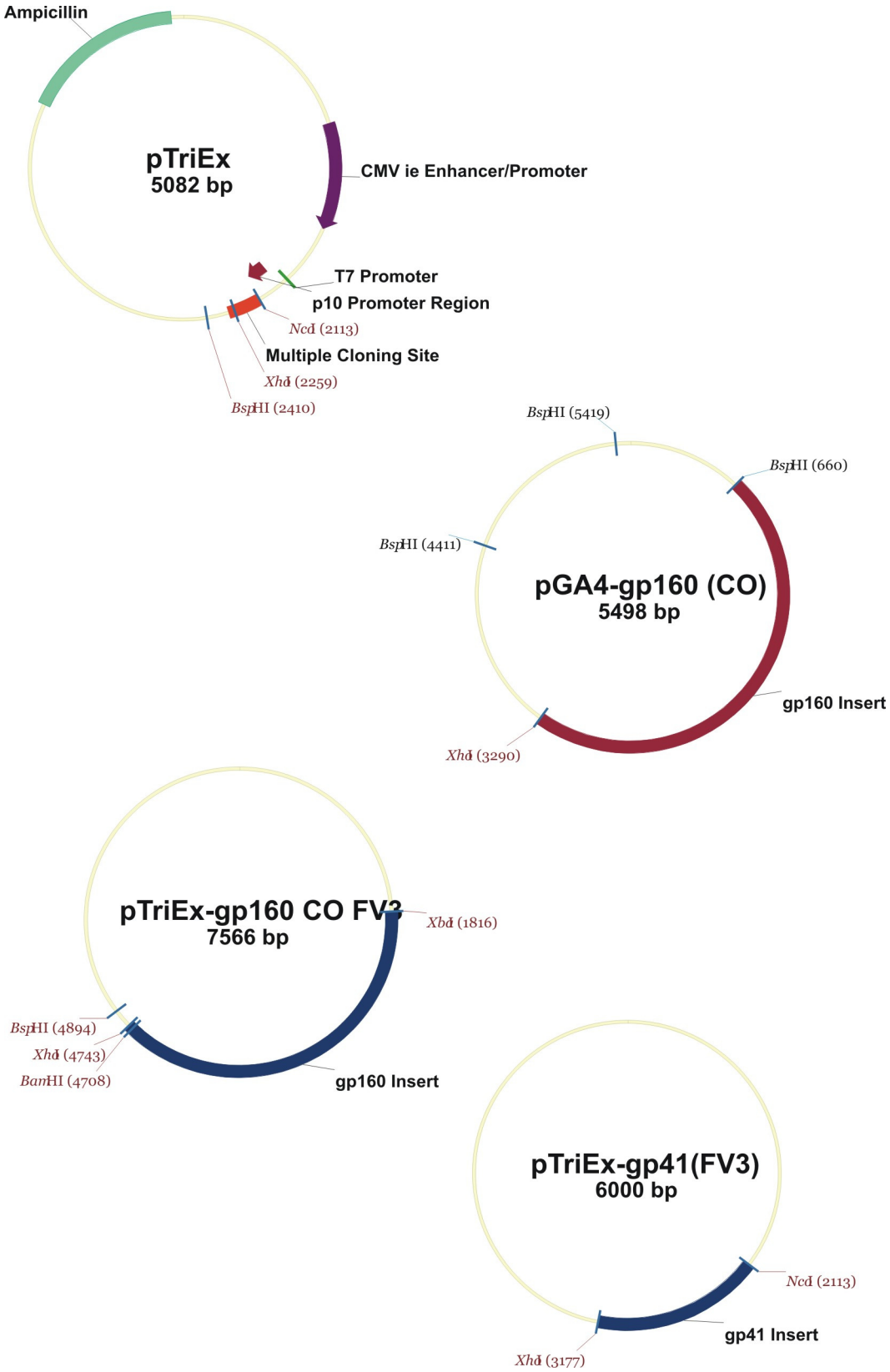

Appendix C: Nucleotide Sequence Alignment of gp160 and gp41 Clones

There appeared to be one silent mutation, at position 2094, in both the gp160 and gp141 clones (highlighted in green).

```
                    *       20          *       40          *       60          *       80          *      100
CONSENSUS : ATGAGGGTGATGGGCACCCAGCGGAACTGCCAGCAGTGGTGGATCTGGGGCATCCTGGGCTTTTGGATGCTGATGATCTGCAACGGCGGCAACCTGTGGG :  100
GP160     : ATGAGGGTGATGGGCACCCAGCGGAACTGCCAGCAGTGGTGGATCTGGGGCATCCTGGGCTTTTGGATGCTGATGATCTGCAACGGCGGCAACCTGTGGG :  100
GP41      : ------------------------------------------------------------------------------------------------- :    -

                    *      120          *      140          *      160          *      180          *      200
CONSENSUS : TGACCGTGTACTACGGCGTGCCCGTGTGGAAAGAGGCCAAGACCACCCTGTTCTGCGCCAGCGACGCCAAGGCCTACGAGAAAGAGGTGCACAACGTCTG :  200
GP160     : TGACCGTGTACTACGGCGTGCCCGTGTGGAAAGAGGCCAAGACCACCCTGTTCTGCGCCAGCGACGCCAAGGCCTACGAGAAAGAGGTGCACAACGTCTG :  200
GP41      : ------------------------------------------------------------------------------------------------- :    -

                    *      220          *      240          *      260          *      280          *      300
CONSENSUS : GGCCACCCACGCCTGCGTGCCCACCGACCCCAACCCCCAGGAAATGAAGCTGCGGAACGTGACCGAGAACTTCAACATGTGGAAGAACGACATGGTGGAC :  300
GP160     : GGCCACCCACGCCTGCGTGCCCACCGACCCCAACCCCCAGGAAATGAAGCTGCGGAACGTGACCGAGAACTTCAACATGTGGAAGAACGACATGGTGGAC :  300
GP41      : ------------------------------------------------------------------------------------------------- :    -

                    *      320          *      340          *      360          *      380          *      400
CONSENSUS : CAGATGAACGAGGACATCATCAGCCTGTGGGACGAGAGCCTGAAGCCCTGCGTGAAGCTGACCCCCCTGTGCGTGACCCTGAACTGCAGCGACGTGACCT :  400
GP160     : CAGATGAACGAGGACATCATCAGCCTGTGGGACGAGAGCCTGAAGCCCTGCGTGAAGCTGACCCCCCTGTGCGTGACCCTGAACTGCAGCGACGTGACCT :  400
GP41      : ------------------------------------------------------------------------------------------------- :    -

                    *      420          *      440          *      460          *      480          *      500
CONSENSUS : ACAACGCCACCAATGCCACCAACAATACCACCACCACAACCCACAACACCACCGAGACCACCCCCTACGCCAAGATCAGCAACATCACCGACGACATGAA :  500
GP160     : ACAACGCCACCAATGCCACCAACAATACCACCACCACAACCCACAACACCACCGAGACCACCCCCTACGCCAAGATCAGCAACATCACCGACGACATGAA :  500
GP41      : ------------------------------------------------------------------------------------------------- :    -

                    *      520          *      540          *      560          *      580          *      600
CONSENSUS : GAACTGCAGCTTCAACGTGACCACCGGCCTGCGGGACAAGCGGAAGCAGGAAAGCGCCCTGTTCTACCGGCTGGACATCATCCCCCTGAACGGCAACAAA :  600
GP160     : GAACTGCAGCTTCAACGTGACCACCGGCCTGCGGGACAAGCGGAAGCAGGAAAGCGCCCTGTTCTACCGGCTGGACATCATCCCCCTGAACGGCAACAAA :  600
GP41      : ------------------------------------------------------------------------------------------------- :    -

                    *      620          *      640          *      660          *      680          *      700
CONSENSUS : GAGAACAGCAGCGAGTACCGGCTGATCAACTGCAACACCAGCACCATCAGACAGGCTTGCCCCAAGGTGTCCTTCGACCCCATCCCCATCCACTACTGCG :  700
GP160     : GAGAACAGCAGCGAGTACCGGCTGATCAACTGCAACACCAGCACCATCAGACAGGCTTGCCCCAAGGTGTCCTTCGACCCCATCCCCATCCACTACTGCG :  700
GP41      : ------------------------------------------------------------------------------------------------- :    -

                    *      720          *      740          *      760          *      780          *      800
CONSENSUS : CCCCTGCCGGCTTCGCCATCCTGAAGTGCAACGACAAGACCTTCAACGGCACCGGCCCCTGCCACGACGTGAGCACCGTGCAGTGCACCCACGGCATCAA :  800
GP160     : CCCCTGCCGGCTTCGCCATCCTGAAGTGCAACGACAAGACCTTCAACGGCACCGGCCCCTGCCACGACGTGAGCACCGTGCAGTGCACCCACGGCATCAA :  800
GP41      : ------------------------------------------------------------------------------------------------- :    -

                    *      820          *      840          *      860          *      880          *      900
CONSENSUS : GCCCGTGGTGTCCACCCAGCTGCTGCTGAACGGCAGCCTGGCCGAGGAAGAGATCGTGATCAGAAGCGAGAACCTGACCAACAATGCCAAGATCATCATC :  900
GP160     : GCCCGTGGTGTCCACCCAGCTGCTGCTGAACGGCAGCCTGGCCGAGGAAGAGATCGTGATCAGAAGCGAGAACCTGACCAACAATGCCAAGATCATCATC :  900
GP41      : ------------------------------------------------------------------------------------------------- :    -

                    *      920          *      940          *      960          *      980          *     1000
CONSENSUS : GTGCACCTGAACGAGAGCGTGGAGATCAAGTGCAGCAGGCCCGGCAACAACACCCGGAAGAGCGTGCGGATCGGCATCGGCAGGGGCCAGACCTTTTACG : 1000
GP160     : GTGCACCTGAACGAGAGCGTGGAGATCAAGTGCAGCAGGCCCGGCAACAACACCCGGAAGAGCGTGCGGATCGGCATCGGCAGGGGCCAGACCTTTTACG : 1000
GP41      : ------------------------------------------------------------------------------------------------- :    -

                    *     1020          *     1040          *     1060          *     1080          *     1100
CONSENSUS : CCACCGGCAAGGTGATCGGCGACATCAGGCAGGCCCACTGCAACGTGAGCCGGGAGGCCTGGAACAAGACCCTGGAAAAGGTGAAACGGAAGCTGGGCGA : 1100
GP160     : CCACCGGCAAGGTGATCGGCGACATCAGGCAGGCCCACTGCAACGTGAGCCGGGAGGCCTGGAACAAGACCCTGGAAAAGGTGAAACGGAAGCTGGGCGA : 1100
GP41      : ------------------------------------------------------------------------------------------------- :    -

                    *     1120          *     1140          *     1160          *     1180          *     1200
CONSENSUS : GCACTTCCCCAACAGCACCATCACCTTCAACCACAGCAGCGGCGGAGACCTGGAAATCACCACCCACAGCTTCAACTGCAGGGGCGAGTTCTTCTACTGC : 1200
GP160     : GCACTTCCCCAACAGCACCATCACCTTCAACCACAGCAGCGGCGGAGACCTGGAAATCACCACCCACAGCTTCAACTGCAGGGGCGAGTTCTTCTACTGC : 1200
GP41      : ------------------------------------------------------------------------------------------------- :    -

                    *     1220          *     1240          *     1260          *     1280          *     1300
CONSENSUS : AATACCAGCGACCTGTTCAAGGACAATATCACCATCACCAACAGCACAAACAACACCGTGATCACCCTGCAGTGTCGGATCAAGCAGATTATCAATATGT : 1300
GP160     : AATACCAGCGACCTGTTCAAGGACAATATCACCATCACCAACAGCACAAACAACACCGTGATCACCCTGCAGTGTCGGATCAAGCAGATTATCAATATGT : 1300
GP41      : ------------------------------------------------------------------------------------------------- :    -

                    *     1320          *     1340          *     1360          *     1380          *     1400
CONSENSUS : GGCAGAGAGCCGGCCAGGCCATCTACGCCCCTCCCATCCGGGGCAATATCACCTGCAACTCCAATATCACAGGCCTGCTGCTGACCCGGGACGGCGGCAA : 1400
GP160     : GGCAGAGAGCCGGCCAGGCCATCTACGCCCCTCCCATCCGGGGCAATATCACCTGCAACTCCAATATCACAGGCCTGCTGCTGACCCGGGACGGCGGCAA : 1400
GP41      : ------------------------------------------------------------------------------------------------- :    -

                    *     1420          *     1440          *     1460          *     1480          *     1500
```

```
CONSENSUS : GGACAACAAGACCAACAACGAGAACAAGACCGAGATCTTCCGGCCTGGCGGCGGAGATATGCGGGACAACTGGCGGAGCGAGCTGTACAAGTACAAGGTG : 1500
GP160     : GGACAACAAGACCAACAACGAGAACAAGACCGAGATCTTCCGGCCTGGCGGCGGAGATATGCGGGACAACTGGCGGAGCGAGCTGTACAAGTACAAGGTG : 1500
GP41      : ------------------------------------------------------------------------------------------------- :    -

                    *      1520         *      1540         *      1560         *      1580         *      1600
CONSENSUS : GTGGAGATTAAGCCCCTGGGCATCGCTCCCACCACCGCCAAGCGGCGGGTGGTGGAGCGGGAGAAGCGGGCCGTGGGCATCGGAGCCGTGCTGCTGGGCT : 1600
GP160     : GTGGAGATTAAGCCCCTGGGCATCGCTCCCACCACCGCCAAGCGGCGGGTGGTGGAGCGGGAGAAGCGGGCCGTGGGCATCGGAGCCGTGCTGCTGGGCT : 1600
GP41      : ----------------------------------------------------------------GCCGTGGGCATCGGAGCCGTGCTGCTGGGCT :   31

                    *      1620         *      1640         *      1660         *      1680         *      1700
CONSENSUS : TCCTGGGAGCCGCCCGGAAGCACAATGGGGGCCGCCAGCATCACCCTGACCGCCCAGGCCAGGCAGGTGCTGTCCGGCATCGTGCAGCAGCAGAGCAACCT : 1700
GP160     : TCCTGGGAGCCGCCGGAAGCACAATGGGGGCCGCCAGCATCACCCTGACCGCCCAGGCCAGGCAGGTGCTGTCCGGCATCGTGCAGCAGCAGAGCAACCT : 1700
GP41      : TCCTGGGAGCCGCCGGAAGCACAATGGGGGCCGCCAGCATCACCCTGACCGCCCAGGCCAGGCAGGTGCTGTCCGGCATCGTGCAGCAGCAGAGCAACCT :  131

                    *      1720         *      1740         *      1760         *      1780         *      1800
CONSENSUS : GCTGCGGGCTATCGAGGCCCAGCAGCATATGCTCCAGCTGACCGTGTGGGGCATCAAGCAGCTGCAGGCCCGGGTGCTGGCCCTGGAAAGATACCTGCAG : 1800
GP160     : GCTGCGGGCTATCGAGGCCCAGCAGCATATGCTCCAGCTGACCGTGTGGGGCATCAAGCAGCTGCAGGCCCGGGTGCTGGCCCTGGAAAGATACCTGCAG : 1800
GP41      : GCTGCGGGCTATCGAGGCCCAGCAGCATATGCTCCAGCTGACCGTGTGGGGCATCAAGCAGCTGCAGGCCCGGGTGCTGGCCCTGGAAAGATACCTGCAG :  231

                    *      1820         *      1840         *      1860         *      1880         *      1900
CONSENSUS : GACCAGCAGCTCCTGGGCATCTGGGGCTGCAGCGGCAAGCTGATCTGCACCACCGCCGTGCCCTGGAACAGCAGCTGGTCCAACCGGAACTACAGCGACA : 1900
GP160     : GACCAGCAGCTCCTGGGCATCTGGGGCTGCAGCGGCAAGCTGATCTGCACCACCGCCGTGCCCTGGAACAGCAGCTGGTCCAACCGGAACTACAGCGACA : 1900
GP41      : GACCAGCAGCTCCTGGGCATCTGGGGCTGCAGCGGCAAGCTGATCTGCACCACCGCCGTGCCCTGGAACAGCAGCTGGTCCAACCGGAACTACAGCGACA :  331

                    *      1920         *      1940         *      1960         *      1980         *      2000
CONSENSUS : TCTGGGACAACATGACCTGGATGCAGTGGGACGGCGAGATCTCCAACTACACCAACATTATCTACCAGCTCCTCGAAGAGAGCCAGATCCAGCAGGAAAA : 2000
GP160     : TCTGGGACAACATGACCTGGATGCAGTGGGACGGCGAGATCTCCAACTACACCAACATTATCTACCAGCTCCTCGAAGAGAGCCAGATCCAGCAGGAAAA : 2000
GP41      : TCTGGGACAACATGACCTGGATGCAGTGGGACGGCGAGATCTCCAACTACACCAACATTATCTACCAGCTCCTCGAAGAGAGCCAGATCCAGCAGGAAAA :  431

                    *      2020         *      2040         *      2060         *      2080         *      2100
CONSENSUS : GAACGAGAAGGACCTGCTCGCTCTGGACAGCTGGAACAGCCTGTGGAACTGGTTCAGCATCACCAAGTGGCTGTGGTACATCAAGATCTTCATTTATGATC : 2100
GP160     : GAACGAGAAGGACCTGCTCGCTCTGGACAGCTGGAACAGCCTGTGGAACTGGTTCAGCATCACCAAGTGGCTGTGGTACATCAAGATCTTCATTTATGATC : 2100
GP41      : GAACGAGAAGGACCTGCTCGCTCTGGACAGCTGGAACAGCCTGTGGAACTGGTTCAGCATCACCAAGTGGCTGTGGTACATCAAGATCTTCATTTATGATC :  531

                    *      2120         *      2140         *      2160         *      2180         *      2200
CONSENSUS : ATCGGCGGCCTGGTCTGCCTGCGGATCATCTTCGCCGTGATCAGCCTGGTGAACAGAGTGCGGCAGGGCTACAGCCCCCTGAGCTTCCAGACCCTGACCC : 2200
GP160     : ATCGGCGGCCTGGTCTGCCTGCGGATCATCTTCGCCGTGATCAGCCTGGTGAACAGAGTGCGGCAGGGCTACAGCCCCCTGAGCTTCCAGACCCTGACCC : 2200
GP41      : ATCGGCGGCCTGGTCTGCCTGCGGATCATCTTCGCCGTGATCAGCCTGGTGAACAGAGTGCGGCAGGGCTACAGCCCCCTGAGCTTCCAGACCCTGACCC :  631

                    *      2220         *      2240         *      2260         *      2280         *      2300
CONSENSUS : CCTCCCCCAGGGACCTGGACCGGCTGAGGGGCATCGAGGAAGAGGGCGGCGAGCAGGACCGGGACAGATCCATCCGGCTGGTGTCCGGCTTCCTGCCCAT : 2300
GP160     : CCTCCCCCAGGGACCTGGACCGGCTGAGGGGCATCGAGGAAGAGGGCGGCGAGCAGGACCGGGACAGATCCATCCGGCTGGTGTCCGGCTTCCTGCCCAT : 2300
GP41      : CCTCCCCCAGGGACCTGGACCGGCTGAGGGGCATCGAGGAAGAGGGCGGCGAGCAGGACCGGGACAGATCCATCCGGCTGGTGTCCGGCTTCCTGCCCAT :  731

                    *      2320         *      2340         *      2360         *      2380         *      2400
CONSENSUS : CGTGTGGGACGACCTGCGGAGCCTGTGCCTGTTCAGCTACCACCGGCTGAGAGACTTCATCCTGATCGTGGTGCGCGCCGTGGAGCTGCTGGGGCGGAGC : 2400
GP160     : CGTGTGGGACGACCTGCGGAGCCTGTGCCTGTTCAGCTACCACCGGCTGAGAGACTTCATCCTGATCGTGGTGCGCGCCGTGGAGCTGCTGGGGCGGAGC : 2400
GP41      : CGTGTGGGACGACCTGCGGAGCCTGTGCCTGTTCAGCTACCACCGGCTGAGAGACTTCATCCTGATCGTGGTGCGCGCCGTGGAGCTGCTGGGGCGGAGC :  831

                    *      2420         *      2440         *      2460         *      2480         *      2500
CONSENSUS : AGCCTGCGGGGCCTGCAGAGAGGCTGGGAGGCCCTGAAGTTCCTGGGCAACCTGGTGCAGTACTGGGGCCTGGAACTGAAGAAGAGCGCCATCAACCTGC : 2500
GP160     : AGCCTGCGGGGCCTGCAGAGAGGCTGGGAGGCCCTGAAGTTCCTGGGCAACCTGGTGCAGTACTGGGGCCTGGAACTGAAGAAGAGCGCCATCAACCTGC : 2500
GP41      : AGCCTGCGGGGCCTGCAGAGAGGCTGGGAGGCCCTGAAGTTCCTGGGCAACCTGGTGCAGTACTGGGGCCTGGAACTGAAGAAGAGCGCCATCAACCTGC :  931

                    *      2520         *      2540         *      2560         *      2580         *      2600
CONSENSUS : TGGACACCATCGCCATCGCCGTGGCCGAGGGCACCGACCGGATCATCGAGTTCATCCAGCGGTTCTGCCGGGCCATTCTGAACATCCCCACCCGGATCCG : 2600
GP160     : TGGACACCATCGCCATCGCCGTGGCCGAGGGCACCGACCGGATCATCGAGTTCATCCAGCGGTTCTGCCGGGCCATTCTGAACATCCCCACCCGGATCCG : 2600
GP41      : TGGACACCATCGCCATCGCCGTGGCCGAGGGCACCGACCGGATCATCGAGTTCATCCAGCGGTTCTGCCGGGCCATTCTGAACATCCCCACCCGGATCCG : 1031

                    *      2620
CONSENSUS : GCAGGGCTTTGAGGCCGCCCTGCTG : 2625
GP160     : GCAGGGCTTTGAGGCCGCCCTGCTG : 2625
GP41      : GCAGGGCTTTGAGGCCGCCCTGCTG : 1056
```

Appendix D: p24 Results for Infections and Fusion Experiments

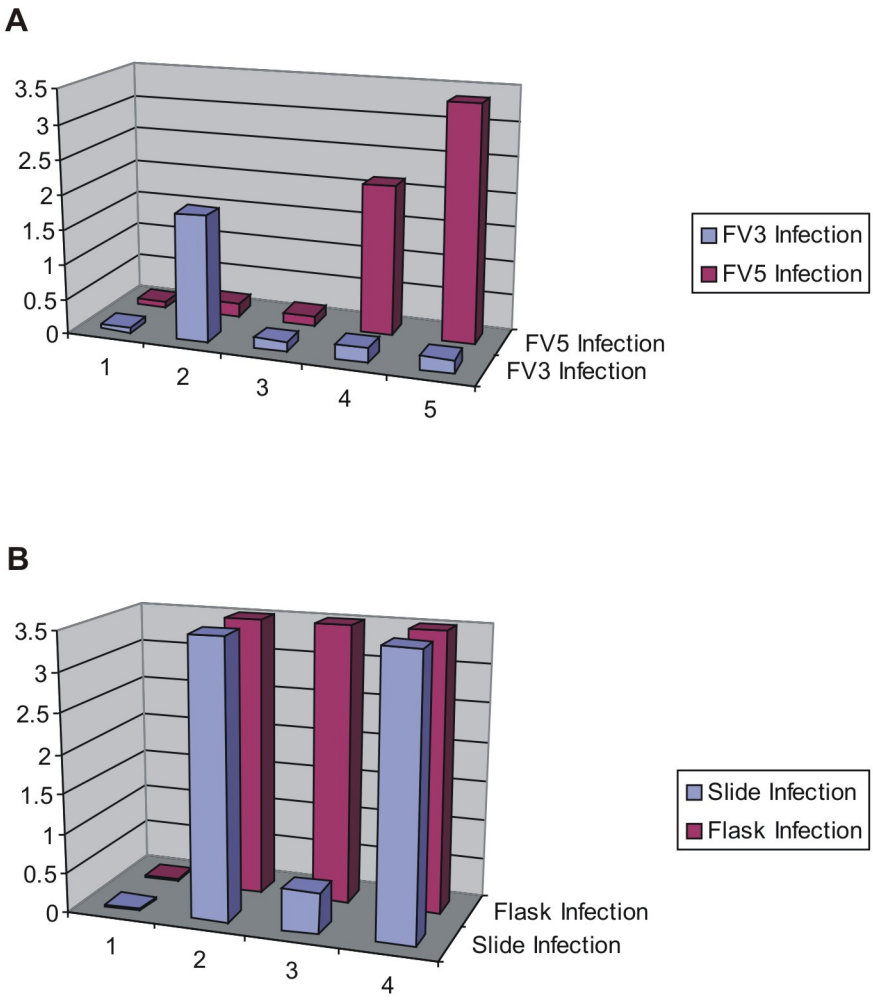

Figure D1: p24 analysis of (A) FV3 and FV5 infections for amplification of virus for fusion experiments, and (B) FV5 infections in flasks and on slides for confirmation of infection during fusion experiments. 1: Cell growth medium before the addition of virus. 2: T0 (Immediately after virus was added to cells). 3: T1 (24 hours post-infection). 4: T3 (72 hours post-infection). 5: T5 (120 hours post-infection).

Appendix E: Viral Load Calculations

Virus-containing cell culture supernatants were diluted 1:4000 with cell growth medium. The determined viral load for this FV5 amplified isolate was 3.2 X 10^5 viral particles/ml. This was then multiplied by the dilution factor (4000) and a final viral load of 1.28 X 10^9 viral particles/ml was achieved. Approximately 5 X 10^6 U87 R5 cells were infected with the FV5 viral isolate. The cells were infected with 1 ml of the FV5 viral supernatant, which amounts to 256 viral particles/cell.

Appendix F: Western Blot Analysis of CXCR4 and CCR5 Membrane Domain Localization

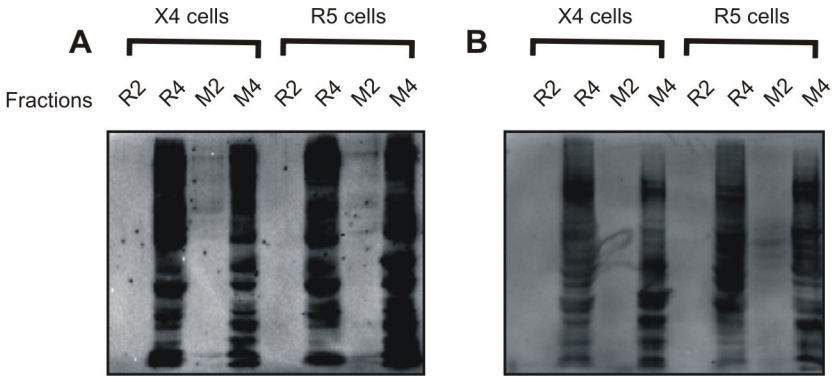

Figure F1: Western Blot analysis of CXCR4 and CCR5 receptor localization. Lipid raft and membrane extractions were performed on U87 X4 and U87 R5 cells and samples were pooled. Pooled samples were resolved on 10% SDS-PAGE gels and subjected to Western Blotting using (A) X4 and (B) R5 antibodies. R2: Raft fraction 2. R4: Raft fraction 4. M2: Membrane fraction 2. M4: Membrane fraction 4.

Appendix G: Western Blot Analysis of gp41 During Fusion Experiments

Full Western Blot images of gp41 detection during fusion experiments to show oligomerisation of the membrane-inserted HIV-1 protein.

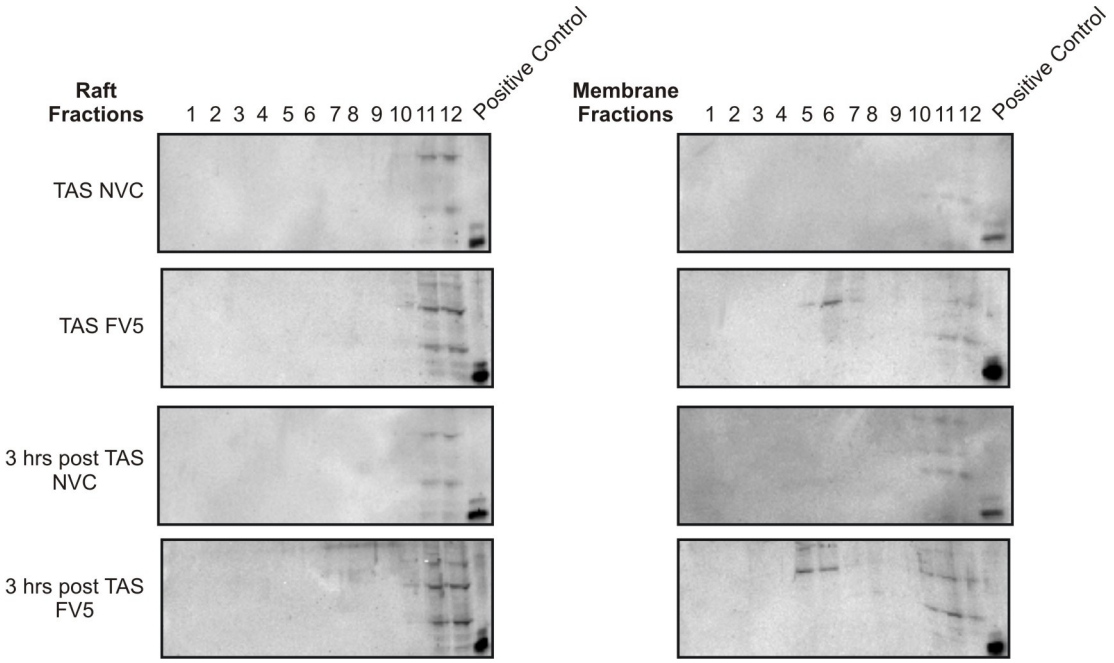

Figure G1: Western Blot analysis of gp41 localization from FV5 fusion studies. U87 R5 cells were infected with the FV5 viral isolate (FV5) or left uninfected, as a non-virus control (NVC). Infections were then left to incubate at 23 ° C for 2 hours (TAS), to allow for gp120-CD4 engagement, and then for a further 3 hours at 37 ° C (3 hrs post TAS) to allow for fusion to occur. TAS and 3 hrs post TAS infections were subjected to lipid raft and membrane extractions, and collected fractions were resolved on 10% SDS-PAGE gels. Western Blots were performed using the F-240 antibody to detect any shift in localization of the gp41.

Appendix H: Ethics Waiver and Biosafety Clearance

An ethics waiver was issued for this study, reference number W-CJ-091211-1-Revised 080130-1, which was handed into the faculty with all other relevant forms. The Biosafety clearance certificate number is 20090704.

REFERENCES

Abrami, L., Fivaz, M., Glauser, P.E., Parton, R.G. and van der Goot, F.G. (1998) A pore-forming toxin interacts with a GPI-anchored protein and causes vacuolation of the endoplasmic reticulum. J Cell Biol 140, 525-40.

Ahmed, S.N., Brown, D.A. and London, E. (1997) On the origin of sphingolipid/cholesterol-rich detergent-insoluble cell membranes: physiological concentrations of cholesterol and sphingolipid induce formation of a detergent-insoluble, liquid-ordered lipid phase in model membranes. Biochemistry 36, 10944-53.

Alexander, M., Bor, Y.C., Ravichandran, K.S., Hammarskjold, M.L. and Rekosh, D. (2004) Human immunodeficiency virus type 1 Nef associates with lipid rafts to downmodulate cell surface CD4 and class I major histocompatibility complex expression and to increase viral infectivity. J Virol 78, 1685-96.

Alkhatib, G., Ahuja, S.S., Light, D., Mummidi, S., Berger, E.A. and Ahuja, S.K. (1997) CC chemokine receptor 5-mediated signaling and HIV-1 Co-receptor activity share common structural determinants. Critical residues in the third extracellular loop support HIV-1 fusion. J Biol Chem 272, 19771-6.

Alkhatib, G., Combadiere, C., Broder, C.C., Feng, Y., Kennedy, P.E., Murphy, P.M. and Berger, E.A. (1996) CC CKR5: a RANTES, MIP-1alpha, MIP-1beta receptor as a fusion cofactor for macrophage-tropic HIV-1. Science 272, 1955-8.

Arni, S., Ilangumaran, S., van Echten-Deckert, G., Sandhoff, K., Poincelet, M., Briol, A., Rungger-Brandle, E. and Hoessli, D.C. (1996) Differential regulation of Src-family protein tyrosine kinases in GPI domains of T lymphocyte plasma membranes. Biochem Biophys Res Commun 225, 801-7.

Arthos, J., Deen, K.C., Chaikin, M.A., Fornwald, J.A., Sathe, G., Sattentau, Q.J., Clapham, P.R., Weiss, R.A., McDougal, J.S., Pietropaolo, C. and et al. (1989)

Identification of the residues in human CD4 critical for the binding of HIV. Cell 57, 469-81.

Arya, S.K., Guo, C., Josephs, S.F. and Wong-Staal, F. (1985) Trans-activator gene of human T-lymphotropic virus type III (HTLV-III). Science 229, 69-73.

Badizadegan, K., Wolf, A.A., Rodighiero, C., Jobling, M., Hirst, T.R., Holmes, R.K. and Lencer, W.I. (2000) Floating cholera toxin into epithelial cells: functional association with caveolae-like detergent-insoluble membrane microdomains. Int J Med Microbiol 290, 403-8.

Baggiolini, M., Dewald, B. and Moser, B. (1997) Human chemokines: an update. Annu Rev Immunol 15, 675-705.

Baorto, D.M., Gao, Z., Malaviya, R., Dustin, M.L., van der Merwe, A., Lublin, D.M. and Abraham, S.N. (1997) Survival of FimH-expressing enterobacteria in macrophages relies on glycolipid traffic. Nature 389, 636-9.

Barbaro, G., Scozzafava, A., Mastrolorenzo, A. and Supuran, C.T. (2005) Highly active antiretroviral therapy: current state of the art, new agents and their pharmacological interactions useful for improving therapeutic outcome. Curr Pharm Des 11, 1805-43.

Barre-Sinoussi, F., Chermann, J.C., Rey, F., Nugeyre, M.T., Chamaret, S., Gruest, J., Dauguet, C., Axler-Blin, C., Vezinet-Brun, F., Rouzioux, C., Rozenbaum, W. and Montagnier, L. (1983) Isolation of a T-lymphotropic retrovirus from a patient at risk for acquired immune deficiency syndrome (AIDS). Science 220, 868-71.

Bavari, S., Bosio, C.M., Wiegand, E., Ruthel, G., Will, A.B., Geisbert, T.W., Hevey, M., Schmaljohn, C., Schmaljohn, A. and Aman, M.J. (2002) Lipid raft microdomains: a gateway for compartmentalized trafficking of Ebola and Marburg viruses. J Exp Med 195, 593-602.

Berger, E.A., Murphy, P.M. and Farber, J.M. (1999) Chemokine receptors as HIV-1 coreceptors: roles in viral entry, tropism, and disease. Annu Rev Immunol 17, 657-700.

Berman, P.W., Nunes, W.M. and Haffar, O.K. (1988) Expression of membrane-associated and secreted variants of gp160 of human immunodeficiency virus type 1 in vitro and in continuous cell lines. J Virol 62, 3135-42.

Berson, J.F., Long, D., Doranz, B.J., Rucker, J., Jirik, F.R. and Doms, R.W. (1996) A seven-transmembrane domain receptor involved in fusion and entry of T-cell-tropic human immunodeficiency virus type 1 strains. J Virol 70, 6288-95.

Bhattacharya, J., Peters, P.J. and Clapham, P.R. (2004) Human immunodeficiency virus type 1 envelope glycoproteins that lack cytoplasmic domain cysteines: impact on association with membrane lipid rafts and incorporation onto budding virus particles. J Virol 78, 5500-6.

Bhattacharya, J., Repik, A. and Clapham, P.R. (2006) Gag regulates association of human immunodeficiency virus type 1 envelope with detergent-resistant membranes. J Virol 80, 5292-300.

Bowerman, B., Brown, P.O., Bishop, J.M. and Varmus, H.E. (1989) A nucleoprotein complex mediates the integration of retroviral DNA. Genes Dev 3, 469-78.

Broder, S. (2010) The development of antiretroviral therapy and its impact on the HIV-1/AIDS pandemic. Antiviral Res 85, 1-18.

Brown, D.A. and London, E. (1998) Functions of lipid rafts in biological membranes. Annu Rev Cell Dev Biol 14, 111-36.

Brown, D.A. and Rose, J.K. (1992) Sorting of GPI-anchored proteins to glycolipid-enriched membrane subdomains during transport to the apical cell surface. Cell 68, 533-44.

Bukrinsky, M.I., Sharova, N., Dempsey, M.P., Stanwick, T.L., Bukrinskaya, A.G., Haggerty, S. and Stevenson, M. (1992) Active nuclear import of human immunodeficiency virus type 1 preintegration complexes. Proc Natl Acad Sci U S A 89, 6580-4.

Bukrinsky, M.I., Sharova, N., McDonald, T.L., Pushkarskaya, T., Tarpley, W.G. and Stevenson, M. (1993) Association of integrase, matrix, and reverse transcriptase

antigens of human immunodeficiency virus type 1 with viral nucleic acids following acute infection. Proc Natl Acad Sci U S A 90, 6125-9.

Buzon, V., Padros, E. and Cladera, J. (2005) Interaction of fusion peptides from HIV gp41 with membranes: a time-resolved membrane binding, lipid mixing, and structural study. Biochemistry 44, 13354-64.

Campbell, S.M., Crowe, S.M. and Mak, J. (2001) Lipid rafts and HIV-1: from viral entry to assembly of progeny virions. J Clin Virol 22, 217-27.

CDC. (1981) Pneumocystis pneumonia--Los Angeles. MMWR Morb Mortal Wkly Rep 30, 250-2.

CDC. (1982) Update on acquired immune deficiency syndrome (AIDS)--United States. MMWR Morb Mortal Wkly Rep 31, 507-8, 513-4.

Chan, A.C., Irving, B.A., Fraser, J.D. and Weiss, A. (1991) The zeta chain is associated with a tyrosine kinase and upon T-cell antigen receptor stimulation associates with ZAP-70, a 70-kDa tyrosine phosphoprotein. Proc Natl Acad Sci U S A 88, 9166-70.

Chan, D.C., Fass, D., Berger, J.M. and Kim, P.S. (1997) Core structure of gp41 from the HIV envelope glycoprotein. Cell 89, 263-73.

Chan, D.C. and Kim, P.S. (1998) HIV entry and its inhibition. Cell 93, 681-4.

Chan, W.E., Lin, H.H. and Chen, S.S. (2005) Wild-type-like viral replication potential of human immunodeficiency virus type 1 envelope mutants lacking palmitoylation signals. J Virol 79, 8374-87.

Charneau, P., Borman, A.M., Quillent, C., Guetard, D., Chamaret, S., Cohen, J., Remy, G., Montagnier, L. and Clavel, F. (1994) Isolation and envelope sequence of a highly divergent HIV-1 isolate: definition of a new HIV-1 group. Virology 205, 247-53.

Chatterjee, S., Basak, S. and Khan, N.C. (1992) Morphogenesis of human immunodeficiency virus type 1. Pathobiology 60, 181-6.

Chazal, N. and Gerlier, D. (2003) Virus entry, assembly, budding, and membrane rafts. Microbiol Mol Biol Rev 67, 226-37, table of contents.

Chen, S.S., Yang, P., Ke, P.Y., Li, H.F., Chan, W.E., Chang, D.K., Chuang, C.K., Tsai, Y. and Huang, S.C. (2009) Identification of the LWYIK motif located in the human immunodeficiency virus type 1 transmembrane gp41 protein as a distinct determinant for viral infection. J Virol 83, 870-83.

Cinek, T. and Horejsi, V. (1992) The nature of large noncovalent complexes containing glycosyl-phosphatidylinositol-anchored membrane glycoproteins and protein tyrosine kinases. J Immunol 149, 2262-70.

Clark, S.J., Jefferies, W.A., Barclay, A.N., Gagnon, J. and Williams, A.F. (1987) Peptide and nucleotide sequences of rat CD4 (W3/25) antigen: evidence for derivation from a structure with four immunoglobulin-related domains. Proc Natl Acad Sci U S A 84, 1649-53.

Clavel, F., Mansinho, K., Chamaret, S., Guetard, D., Favier, V., Nina, J., Santos-Ferreira, M.O., Champalimaud, J.L. and Montagnier, L. (1987) Human immunodeficiency virus type 2 infection associated with AIDS in West Africa. N Engl J Med 316, 1180-5.

Coffin, J., Haase, A., Levy, J.A., Montagnier, L., Oroszlan, S., Teich, N., Temin, H., Toyoshima, K., Varmus, H., Vogt, P. and et al. (1986) What to call the AIDS virus? Nature 321, 10.

Connell, B.J., Michler, K., Capovilla, A., Venter, W.D., Stevens, W.S. and Papathanasopoulos, M.A. (2008) Emergence of X4 usage among HIV-1 subtype C: evidence for an evolving epidemic in South Africa. Aids 22, 896-9.

Cordonnier, A., Montagnier, L. and Emerman, M. (1989) Single amino-acid changes in HIV envelope affect viral tropism and receptor binding. Nature 340, 571-4.

Dalgleish, A.G., Beverley, P.C., Clapham, P.R., Crawford, D.H., Greaves, M.F. and Weiss, R.A. (1984) The CD4 (T4) antigen is an essential component of the receptor for the AIDS retrovirus. Nature 312, 763-7.

De Leys, R., Vanderborght, B., Vanden Haesevelde, M., Heyndrickx, L., van Geel, A., Wauters, C., Bernaerts, R., Saman, E., Nijs, P., Willems, B. and et al. (1990) Isolation and partial characterization of an unusual human immunodeficiency retrovirus from two persons of west-central African origin. J Virol 64, 1207-16.

Deans, J.P., Robbins, S.M., Polyak, M.J. and Savage, J.A. (1998) Rapid redistribution of CD20 to a low density detergent-insoluble membrane compartment. J Biol Chem 273, 344-8.

Del Real, G., Jimenez-Baranda, S., Lacalle, R.A., Mira, E., Lucas, P., Gomez-Mouton, C., Carrera, A.C., Martinez, A.C. and Manes, S. (2002) Blocking of HIV-1 infection by targeting CD4 to nonraft membrane domains. J Exp Med 196, 293-301.

Deng, H., Liu, R., Ellmeier, W., Choe, S., Unutmaz, D., Burkhart, M., Di Marzio, P., Marmon, S., Sutton, R.E., Hill, C.M., Davis, C.B., Peiper, S.C., Schall, T.J., Littman, D.R. and Landau, N.R. (1996) Identification of a major co-receptor for primary isolates of HIV-1. Nature 381, 661-6.

Dimitrov, D.S., Golding, H. and Blumenthal, R. (1991) Initial stages of HIV-1 envelope glycoprotein-mediated cell fusion monitored by a new assay based on redistribution of fluorescent dyes. AIDS Res Hum Retroviruses 7, 799-805.

Doms, R.W. and Moore, J.P. (2000) HIV-1 membrane fusion: targets of opportunity. J Cell Biol 151, F9-14.

Doyle, C. and Strominger, J.L. (1987) Interaction between CD4 and class II MHC molecules mediates cell adhesion. Nature 330, 256-9.

Dragic, T., Litwin, V., Allaway, G.P., Martin, S.R., Huang, Y., Nagashima, K.A., Cayanan, C., Maddon, P.J., Koup, R.A., Moore, J.P. and Paxton, W.A. (1996) HIV-1 entry into CD4+ cells is mediated by the chemokine receptor CC-CKR-5. Nature 381, 667-73.

Edidin, M. (2001) Shrinking patches and slippery rafts: scales of domains in the plasma membrane. Trends Cell Biol 11, 492-6.

Eigen, M. and Nieselt-Struwe, K. (1990) How old is the immunodeficiency virus? Aids 4 Suppl 1, S85-93.

Farnet, C.M. and Haseltine, W.A. (1990) Integration of human immunodeficiency virus type 1 DNA in vitro. Proc Natl Acad Sci U S A 87, 4164-8.

Farnet, C.M. and Haseltine, W.A. (1991) Determination of viral proteins present in the human immunodeficiency virus type 1 preintegration complex. J Virol 65, 1910-5.

Fassati, A. and Goff, S.P. (2001) Characterization of intracellular reverse transcription complexes of human immunodeficiency virus type 1. J Virol 75, 3626-35.

Feinberg, M.B., Jarrett, R.F., Aldovini, A., Gallo, R.C. and Wong-Staal, F. (1986) HTLV-III expression and production involve complex regulation at the levels of splicing and translation of viral RNA. Cell 46, 807-17.

Feng, Y., Broder, C.C., Kennedy, P.E. and Berger, E.A. (1996) HIV-1 entry cofactor: functional cDNA cloning of a seven-transmembrane, G protein-coupled receptor. Science 272, 872-7.

Field, K.A., Holowka, D. and Baird, B. (1997) Compartmentalized activation of the high affinity immunoglobulin E receptor within membrane domains. J Biol Chem 272, 4276-80.

Frey, G., Peng, H., Rits-Volloch, S., Morelli, M., Cheng, Y. and Chen, B. (2008) A fusion-intermediate state of HIV-1 gp41 targeted by broadly neutralizing antibodies. Proc Natl Acad Sci U S A 105, 3739-44.

Gallaher, W.R. (1987) Detection of a fusion peptide sequence in the transmembrane protein of human immunodeficiency virus. Cell 50, 327-8.

Gallaher, W.R., Ball, J.M., Garry, R.F., Griffin, M.C. and Montelaro, R.C. (1989) A general model for the transmembrane proteins of HIV and other retroviruses. AIDS Res Hum Retroviruses 5, 431-40.

Gallo, R.C., Salahuddin, S.Z., Popovic, M., Shearer, G.M., Kaplan, M., Haynes, B.F., Palker, T.J., Redfield, R., Oleske, J., Safai, B. and et al. (1984) Frequent detection

and isolation of cytopathic retroviruses (HTLV-III) from patients with AIDS and at risk for AIDS. Science 224, 500-3.

Gallo, S.A., Clore, G.M., Louis, J.M., Bewley, C.A. and Blumenthal, R. (2004) Temperature-dependent intermediates in HIV-1 envelope glycoprotein-mediated fusion revealed by inhibitors that target N- and C-terminal helical regions of HIV-1 gp41. Biochemistry 43, 8230-3.

Gallo, S.A., Puri, A. and Blumenthal, R. (2001) HIV-1 gp41 six-helix bundle formation occurs rapidly after the engagement of gp120 by CXCR4 in the HIV-1 Env-mediated fusion process. Biochemistry 40, 12231-6.

Gao, F., Bailes, E., Robertson, D.L., Chen, Y., Rodenburg, C.M., Michael, S.F., Cummins, L.B., Arthur, L.O., Peeters, M., Shaw, G.M., Sharp, P.M. and Hahn, B.H. (1999) Origin of HIV-1 in the chimpanzee Pan troglodytes troglodytes. Nature 397, 436-41.

Gay, D., Maddon, P., Sekaly, R., Talle, M.A., Godfrey, M., Long, E., Goldstein, G., Chess, L., Axel, R., Kappler, J. and et al. (1987) Functional interaction between human T-cell protein CD4 and the major histocompatibility complex HLA-DR antigen. Nature 328, 626-9.

Gelderblom, H.R. (1991) Assembly and morphology of HIV: potential effect of structure on viral function. Aids 5, 617-37.

Gelderblom, H.R., Hausmann, E.H., Ozel, M., Pauli, G. and Koch, M.A. (1987) Fine structure of human immunodeficiency virus (HIV) and immunolocalization of structural proteins. Virology 156, 171-6.

Germain, R.N. (1997) T-cell signaling: the importance of receptor clustering. Curr Biol 7, R640-4.

Golde, T.E. and Eckman, C.B. (2001) Cholesterol modulation as an emerging strategy for the treatment of Alzheimer's disease. Drug Discov Today 6, 1049-1055.

Golding, H., Zaitseva, M., de Rosny, E., King, L.R., Manischewitz, J., Sidorov, I., Gorny, M.K., Zolla-Pazner, S., Dimitrov, D.S. and Weiss, C.D. (2002) Dissection of

human immunodeficiency virus type 1 entry with neutralizing antibodies to gp41 fusion intermediates. J Virol 76, 6780-90.

Goto, T., Ikuta, K., Zhang, J.J., Morita, C., Sano, K., Komatsu, M., Fujita, H., Kato, S. and Nakai, M. (1990) The budding of defective human immunodeficiency virus type 1 (HIV-1) particles from cell clones persistently infected with HIV-1. Arch Virol 111, 87-101.

Goto, T., Nakai, M. and Ikuta, K. (1998) The life-cycle of human immunodeficiency virus type 1. Micron 29, 123-38.

Gottlieb, M.S., Schroff, R., Schanker, H.M., Weisman, J.D., Fan, P.T., Wolf, R.A. and Saxon, A. (1981) Pneumocystis carinii pneumonia and mucosal candidiasis in previously healthy homosexual men: evidence of a new acquired cellular immunodeficiency. N Engl J Med 305, 1425-31.

Grewe, C., Beck, A. and Gelderblom, H.R. (1990) HIV: early virus-cell interactions. J Acquir Immune Defic Syndr 3, 965-74.

Gu, M., Rappaport, J. and Leppla, S.H. (1995) Furin is important but not essential for the proteolytic maturation of gp160 of HIV-1. FEBS Lett 365, 95-7.

Hart, T.K., Kirsh, R., Ellens, H., Sweet, R.W., Lambert, D.M., Petteway, S.R., Jr., Leary, J. and Bugelski, P.J. (1991) Binding of soluble CD4 proteins to human immunodeficiency virus type 1 and infected cells induces release of envelope glycoprotein gp120. Proc Natl Acad Sci U S A 88, 2189-93.

Holdorf, A.D., Lee, K.H., Burack, W.R., Allen, P.M. and Shaw, A.S. (2002) Regulation of Lck activity by CD4 and CD28 in the immunological synapse. Nat Immunol 3, 259-64.

Holm, K., Weclewicz, K., Hewson, R. and Suomalainen, M. (2003) Human immunodeficiency virus type 1 assembly and lipid rafts: Pr55(gag) associates with membrane domains that are largely resistant to Brij98 but sensitive to Triton X-100. J Virol 77, 4805-17.

http://www.hiv.lanl.gov/. (2009) Los Alamos HIV Sequence Database. In.

Huang, C.C., Tang, M., Zhang, M.Y., Majeed, S., Montabana, E., Stanfield, R.L., Dimitrov, D.S., Korber, B., Sodroski, J., Wilson, I.A., Wyatt, R. and Kwong, P.D. (2005) Structure of a V3-containing HIV-1 gp120 core. Science 310, 1025-8.

Hwang, S.S., Boyle, T.J., Lyerly, H.K. and Cullen, B.R. (1991) Identification of the envelope V3 loop as the primary determinant of cell tropism in HIV-1. Science 253, 71-4.

Ikonen, E. (2001) Roles of lipid rafts in membrane transport. Curr Opin Cell Biol 13, 470-7.

Ingallinella, P., Bianchi, E., Ladwa, N.A., Wang, Y.J., Hrin, R., Veneziano, M., Bonelli, F., Ketas, T.J., Moore, J.P., Miller, M.D. and Pessi, A. (2009) Addition of a cholesterol group to an HIV-1 peptide fusion inhibitor dramatically increases its antiviral potency. Proc Natl Acad Sci U S A 106, 5801-6.

Isakov, N. (1997) Immunoreceptor tyrosine-based activation motif (ITAM), a unique module linking antigen and Fc receptors to their signaling cascades. J Leukoc Biol 61, 6-16.

Jacobson, K. and Dietrich, C. (1999) Looking at lipid rafts? Trends Cell Biol 9, 87-91.

Jones, P.L., Korte, T. and Blumenthal, R. (1998) Conformational changes in cell surface HIV-1 envelope glycoproteins are triggered by cooperation between cell surface CD4 and co-receptors. J Biol Chem 273, 404-9.

Kabouridis, P.S., Magee, A.I. and Ley, S.C. (1997) S-acylation of LCK protein tyrosine kinase is essential for its signalling function in T lymphocytes. Embo J 16, 4983-98.

Kakio, A., Nishimoto, S., Yanagisawa, K., Kozutsumi, Y. and Matsuzaki, K. (2002) Interactions of amyloid beta-protein with various gangliosides in raft-like membranes: importance of GM1 ganglioside-bound form as an endogenous seed for Alzheimer amyloid. Biochemistry 41, 7385-90.

Kakio, A., Nishimoto, S.I., Yanagisawa, K., Kozutsumi, Y. and Matsuzaki, K. (2001) Cholesterol-dependent formation of GM1 ganglioside-bound amyloid beta-protein, an endogenous seed for Alzheimer amyloid. J Biol Chem 276, 24985-90.

Keller, P. and Simons, K. (1998) Cholesterol is required for surface transport of influenza virus hemagglutinin. J Cell Biol 140, 1357-67.

Klatzmann, D., Champagne, E., Chamaret, S., Gruest, J., Guetard, D., Hercend, T., Gluckman, J.C. and Montagnier, L. (1984) T-lymphocyte T4 molecule behaves as the receptor for human retrovirus LAV. Nature 312, 767-8.

Klein, T.R., Kirsch, D., Kaufmann, R. and Riesner, D. (1998) Prion rods contain small amounts of two host sphingolipids as revealed by thin-layer chromatography and mass spectrometry. Biol Chem 379, 655-66.

Kliger, Y., Aharoni, A., Rapaport, D., Jones, P., Blumenthal, R. and Shai, Y. (1997) Fusion peptides derived from the HIV type 1 glycoprotein 41 associate within phospholipid membranes and inhibit cell-cell Fusion. Structure-function study. J Biol Chem 272, 13496-505.

Kliger, Y., Gallo, S.A., Peisajovich, S.G., Munoz-Barroso, I., Avkin, S., Blumenthal, R. and Shai, Y. (2001) Mode of action of an antiviral peptide from HIV-1. Inhibition at a post-lipid mixing stage. J Biol Chem 276, 1391-7.

Kolchinsky, P., Kiprilov, E., Bartley, P., Rubinstein, R. and Sodroski, J. (2001) Loss of a single N-linked glycan allows CD4-independent human immunodeficiency virus type 1 infection by altering the position of the gp120 V1/V2 variable loops. J Virol 75, 3435-43.

Konig, R., Huang, L.Y. and Germain, R.N. (1992) MHC class II interaction with CD4 mediated by a region analogous to the MHC class I binding site for CD8. Nature 356, 796-8.

Konig, R., Shen, X. and Germain, R.N. (1995) Involvement of both major histocompatibility complex class II alpha and beta chains in CD4 function indicates a role for ordered oligomerization in T cell activation. J Exp Med 182, 779-87.

Korazim, O., Sackett, K. and Shai, Y. (2006) Functional and structural characterization of HIV-1 gp41 ectodomain regions in phospholipid membranes suggests that the fusion-active conformation is extended. J Mol Biol 364, 1103-17.

Koshiba, T. and Chan, D.C. (2003) The prefusogenic intermediate of HIV-1 gp41 contains exposed C-peptide regions. J Biol Chem 278, 7573-9.

Kozak, S.L., Heard, J.M. and Kabat, D. (2002) Segregation of CD4 and CXCR4 into distinct lipid microdomains in T lymphocytes suggests a mechanism for membrane destabilization by human immunodeficiency virus. J Virol 76, 1802-15.

Krell, T., Greco, F., Engel, O., Dubayle, J., Dubayle, J., Kennel, A., Charloteaux, B., Brasseur, R., Chevalier, M., Sodoyer, R. and El Habib, R. (2004) HIV-1 gp41 and gp160 are hyperthermostable proteins in a mesophilic environment. Characterization of gp41 mutants. Eur J Biochem 271, 1566-79.

Kwong, P.D., Wyatt, R., Desjardins, E., Robinson, J., Culp, J.S., Hellmig, B.D., Sweet, R.W., Sodroski, J. and Hendrickson, W.A. (1999) Probability analysis of variational crystallization and its application to gp120, the exterior envelope glycoprotein of type 1 human immunodeficiency virus (HIV-1). J Biol Chem 274, 4115-23.

Kwong, P.D., Wyatt, R., Robinson, J., Sweet, R.W., Sodroski, J. and Hendrickson, W.A. (1998) Structure of an HIV gp120 envelope glycoprotein in complex with the CD4 receptor and a neutralizing human antibody. Nature 393, 648-59.

Leis, J., Baltimore, D., Bishop, J.M., Coffin, J., Fleissner, E., Goff, S.P., Oroszlan, S., Robinson, H., Skalka, A.M., Temin, H.M. and et al. (1988) Standardized and simplified nomenclature for proteins common to all retroviruses. J Virol 62, 1808-9.

Leitner, T., Foley, B., Hahn, B., Marx, P., McCutchan, F., Mellors, J., Wolinsky, S., Korber, B. and Eds. (2005) HIV Sequence Compendium 2005 Theoretical Biology and Biophysics Group, Los Alamos National Laboratory, NM, LA-UR 03-3564.

Leonard, C.K., Spellman, M.W., Riddle, L., Harris, R.J., Thomas, J.N. and Gregory, T.J. (1990) Assignment of intrachain disulfide bonds and characterization of potential glycosylation sites of the type 1 recombinant human immunodeficiency virus envelope glycoprotein (gp120) expressed in Chinese hamster ovary cells. J Biol Chem 265, 10373-82.

Levy, J.A., Hoffman, A.D., Kramer, S.M., Landis, J.A., Shimabukuro, J.M. and Oshiro, L.S. (1984) Isolation of lymphocytopathic retroviruses from San Francisco patients with AIDS. Science 225, 840-2.

Li, M., Yang, C., Tong, S., Weidmann, A. and Compans, R.W. (2002) Palmitoylation of the murine leukemia virus envelope protein is critical for lipid raft association and surface expression. J Virol 76, 11845-52.

Lifson, J.D., Feinberg, M.B., Reyes, G.R., Rabin, L., Banapour, B., Chakrabarti, S., Moss, B., Wong-Staal, F., Steimer, K.S. and Engleman, E.G. (1986) Induction of CD4-dependent cell fusion by the HTLV-III/LAV envelope glycoprotein. Nature 323, 725-8.

Lineberger, J.E., Danzeisen, R., Hazuda, D.J., Simon, A.J. and Miller, M.D. (2002) Altering expression levels of human immunodeficiency virus type 1 gp120-gp41 affects efficiency but not kinetics of cell-cell fusion. J Virol 76, 3522-33.

Liu, S., Zhao, Q. and Jiang, S. (2003) Determination of the HIV-1 gp41 fusogenic core conformation modeled by synthetic peptides: applicable for identification of HIV-1 fusion inhibitors. Peptides 24, 1303-13.

Lu, M., Blacklow, S.C. and Kim, P.S. (1995) A trimeric structural domain of the HIV-1 transmembrane glycoprotein. Nat Struct Biol 2, 1075-82.

Lu, Z., Berson, J.F., Chen, Y., Turner, J.D., Zhang, T., Sharron, M., Jenks, M.H., Wang, Z., Kim, J., Rucker, J., Hoxie, J.A., Peiper, S.C. and Doms, R.W. (1997) Evolution of HIV-1 coreceptor usage through interactions with distinct CCR5 and CXCR4 domains. Proc Natl Acad Sci U S A 94, 6426-31.

Luster, A.D. (1998) Chemokines--chemotactic cytokines that mediate inflammation. N Engl J Med 338, 436-45.

Maddon, P.J., Dalgleish, A.G., McDougal, J.S., Clapham, P.R., Weiss, R.A. and Axel, R. (1986) The T4 gene encodes the AIDS virus receptor and is expressed in the immune system and the brain. Cell 47, 333-48.

Maddon, P.J., Littman, D.R., Godfrey, M., Maddon, D.E., Chess, L. and Axel, R. (1985) The isolation and nucleotide sequence of a cDNA encoding the T cell surface protein T4: a new member of the immunoglobulin gene family. Cell 42, 93-104.

Maddon, P.J., Molineaux, S.M., Maddon, D.E., Zimmerman, K.A., Godfrey, M., Alt, F.W., Chess, L. and Axel, R. (1987) Structure and expression of the human and mouse T4 genes. Proc Natl Acad Sci U S A 84, 9155-9.

Manes, S., del Real, G., Lacalle, R.A., Lucas, P., Gomez-Mouton, C., Sanchez-Palomino, S., Delgado, R., Alcami, J., Mira, E. and Martinez, A.C. (2000) Membrane raft microdomains mediate lateral assemblies required for HIV-1 infection. EMBO Rep 1, 190-6.

Manie, S.N., de Breyne, S., Vincent, S. and Gerlier, D. (2000) Measles virus structural components are enriched into lipid raft microdomains: a potential cellular location for virus assembly. J Virol 74, 305-11.

Markosyan, R.M., Cohen, F.S. and Melikyan, G.B. (2003) HIV-1 envelope proteins complete their folding into six-helix bundles immediately after fusion pore formation. Mol Biol Cell 14, 926-38.

Marlink, R., Kanki, P., Thior, I., Travers, K., Eisen, G., Siby, T., Traore, I., Hsieh, C.C., Dia, M.C., Gueye, E.H. and et al. (1994) Reduced rate of disease development after HIV-2 infection as compared to HIV-1. Science 265, 1587-90.

Marx, P.A., Munn, R.J. and Joy, K.I. (1988) Computer emulation of thin section electron microscopy predicts an envelope-associated icosadeltahedral capsid for human immunodeficiency virus. Lab Invest 58, 112-8.

McDonald, D., Vodicka, M.A., Lucero, G., Svitkina, T.M., Borisy, G.G., Emerman, M. and Hope, T.J. (2002) Visualization of the intracellular behavior of HIV in living cells. J Cell Biol 159, 441-52.

McDougal, J.S., Kennedy, M.S., Sligh, J.M., Cort, S.P., Mawle, A. and Nicholson, J.K. (1986) Binding of HTLV-III/LAV to T4+ T cells by a complex of the 110K viral protein and the T4 molecule. Science 231, 382-5.

Melikyan, G.B., Egelhofer, M. and von Laer, D. (2006) Membrane-anchored inhibitory peptides capture human immunodeficiency virus type 1 gp41 conformations that engage the target membrane prior to fusion. J Virol 80, 3249-58.

Melikyan, G.B., Markosyan, R.M., Hemmati, H., Delmedico, M.K., Lambert, D.M. and Cohen, F.S. (2000) Evidence that the transition of HIV-1 gp41 into a six-helix bundle, not the bundle configuration, induces membrane fusion. J Cell Biol 151, 413-23.

Miyauchi, K., Kim, Y., Latinovic, O., Morozov, V. and Melikyan, G.B. (2009) HIV enters cells via endocytosis and dynamin-dependent fusion with endosomes. Cell 137, 433-44.

Mkrtchyan, S.R., Markosyan, R.M., Eadon, M.T., Moore, J.P., Melikyan, G.B. and Cohen, F.S. (2005) Ternary complex formation of human immunodeficiency virus type 1 Env, CD4, and chemokine receptor captured as an intermediate of membrane fusion. J Virol 79, 11161-9.

Modrow, S., Hahn, B.H., Shaw, G.M., Gallo, R.C., Wong-Staal, F. and Wolf, H. (1987) Computer-assisted analysis of envelope protein sequences of seven human immunodeficiency virus isolates: prediction of antigenic epitopes in conserved and variable regions. J Virol 61, 570-8.

Moebius, U., Clayton, L.K., Abraham, S., Harrison, S.C. and Reinherz, E.L. (1992) The human immunodeficiency virus gp120 binding site on CD4: delineation by quantitative equilibrium and kinetic binding studies of mutants in conjunction with a high-resolution CD4 atomic structure. J Exp Med 176, 507-17.

Moore, J.P., McKeating, J.A., Weiss, R.A. and Sattentau, Q.J. (1990) Dissociation of gp120 from HIV-1 virions induced by soluble CD4. Science 250, 1139-42.

Moreno, M.R., Guillen, J., Perez-Berna, A.J., Amoros, D., Gomez, A.I., Bernabeu, A. and Villalain, J. (2007) Characterization of the interaction of two peptides from the N terminus of the NHR domain of HIV-1 gp41 with phospholipid membranes. Biochemistry 46, 10572-84.

Muesing, M.A., Smith, D.H., Cabradilla, C.D., Benton, C.V., Lasky, L.A. and Capon, D.J. (1985) Nucleic acid structure and expression of the human AIDS/lymphadenopathy retrovirus. Nature 313, 450-8.

Munoz-Barroso, I., Durell, S., Sakaguchi, K., Appella, E. and Blumenthal, R. (1998) Dilation of the human immunodeficiency virus-1 envelope glycoprotein fusion pore revealed by the inhibitory action of a synthetic peptide from gp41. J Cell Biol 140, 315-23.

Nabel, G. and Baltimore, D. (1987) An inducible transcription factor activates expression of human immunodeficiency virus in T cells. Nature 326, 711-3.

Naslavsky, N., Shmeeda, H., Friedlander, G., Yanai, A., Futerman, A.H., Barenholz, Y. and Taraboulos, A. (1999) Sphingolipid depletion increases formation of the scrapie prion protein in neuroblastoma cells infected with prions. J Biol Chem 274, 20763-71.

Naslavsky, N., Stein, R., Yanai, A., Friedlander, G. and Taraboulos, A. (1997) Characterization of detergent-insoluble complexes containing the cellular prion protein and its scrapie isoform. J Biol Chem 272, 6324-31.

Nguyen, D.H., Giri, B., Collins, G. and Taub, D.D. (2005) Dynamic reorganization of chemokine receptors, cholesterol, lipid rafts, and adhesion molecules to sites of CD4 engagement. Exp Cell Res 304, 559-69.

Nguyen, D.H. and Hildreth, J.E. (2000) Evidence for budding of human immunodeficiency virus type 1 selectively from glycolipid-enriched membrane lipid rafts. J Virol 74, 3264-72.

Nguyen, D.H. and Taub, D. (2002) CXCR4 function requires membrane cholesterol: implications for HIV infection. J Immunol 168, 4121-6.

Nguyen, D.H. and Taub, D.D. (2003) Inhibition of chemokine receptor function by membrane cholesterol oxidation. Exp Cell Res 291, 36-45.

Nieva, J.L., Bron, R., Corver, J. and Wilschut, J. (1994) Membrane fusion of Semliki Forest virus requires sphingolipids in the target membrane. Embo J 13, 2797-804.

Noah, E., Biron, Z., Naider, F., Arshava, B. and Anglister, J. (2008) The membrane proximal external region of the HIV-1 envelope glycoprotein gp41 contributes to the stabilization of the six-helix bundle formed with a matching N' peptide. Biochemistry 47, 6782-92.

Ochsenbauer-Jambor, C., Miller, D.C., Roberts, C.R., Rhee, S.S. and Hunter, E. (2001) Palmitoylation of the Rous sarcoma virus transmembrane glycoprotein is required for protein stability and virus infectivity. J Virol 75, 11544-54.

Olive, S., Dubois, C., Schachner, M. and Rougon, G. (1995) The F3 neuronal glycosylphosphatidylinositol-linked molecule is localized to glycolipid-enriched membrane subdomains and interacts with L1 and fyn kinase in cerebellum. J Neurochem 65, 2307-17.

Olshevsky, U., Helseth, E., Furman, C., Li, J., Haseltine, W. and Sodroski, J. (1990) Identification of individual human immunodeficiency virus type 1 gp120 amino acids important for CD4 receptor binding. J Virol 64, 5701-7.

Ono, A. and Freed, E.O. (2001) Plasma membrane rafts play a critical role in HIV-1 assembly and release. Proc Natl Acad Sci U S A 98, 13925-30.

Ono, A., Waheed, A.A. and Freed, E.O. (2007) Depletion of cellular cholesterol inhibits membrane binding and higher-order multimerization of human immunodeficiency virus type 1 Gag. Virology 360, 27-35.

Palca, J. (1986) Virus nomenclature: controversy over AIDS virus extends to name. Nature 321, 3.

Peeters, M., Honore, C., Huet, T., Bedjabaga, L., Ossari, S., Bussi, P., Cooper, R.W. and Delaporte, E. (1989) Isolation and partial characterization of an HIV-related virus occurring naturally in chimpanzees in Gabon. Aids 3, 625-30.

Penn-Nicholson, A., Han, D.P., Kim, S.J., Park, H., Ansari, R., Montefiori, D.C. and Cho, M.W. (2008) Assessment of antibody responses against gp41 in HIV-1-infected patients using soluble gp41 fusion proteins and peptides derived from M group consensus envelope. Virology 372, 442-56.

Percherancier, Y., Lagane, B., Planchenault, T., Staropoli, I., Altmeyer, R., Virelizier, J.L., Arenzana-Seisdedos, F., Hoessli, D.C. and Bachelerie, F. (2003) HIV-1 entry into T-cells is not dependent on CD4 and CCR5 localization to sphingolipid-enriched, detergent-resistant, raft membrane domains. J Biol Chem 278, 3153-61.

Pereira, F.B., Goni, F.M., Muga, A. and Nieva, J.L. (1997) Permeabilization and fusion of uncharged lipid vesicles induced by the HIV-1 fusion peptide adopting an extended conformation: dose and sequence effects. Biophys J 73, 1977-86.

Peterlin, B.M. and Luciw, P.A. (1988) Molecular biology of HIV. Aids 2 Suppl 1, S29-40.

Phalen, T. and Kielian, M. (1991) Cholesterol is required for infection by Semliki Forest virus. J Cell Biol 112, 615-23.

Popik, W. and Alce, T.M. (2004) CD4 receptor localized to non-raft membrane microdomains supports HIV-1 entry. Identification of a novel raft localization marker in CD4. J Biol Chem 279, 704-12.

Popik, W., Alce, T.M. and Au, W.C. (2002) Human immunodeficiency virus type 1 uses lipid raft-colocalized CD4 and chemokine receptors for productive entry into CD4(+) T cells. J Virol 76, 4709-22.

Popovic, M., Sarngadharan, M.G., Read, E. and Gallo, R.C. (1984) Detection, isolation, and continuous production of cytopathic retroviruses (HTLV-III) from patients with AIDS and pre-AIDS. Science 224, 497-500.

Premack, B.A. and Schall, T.J. (1996) Chemokine receptors: gateways to inflammation and infection. Nat Med 2, 1174-8.

Profy, A.T., Salinas, P.A., Eckler, L.I., Dunlop, N.M., Nara, P.L. and Putney, S.D. (1990) Epitopes recognized by the neutralizing antibodies of an HIV-1-infected individual. J Immunol 144, 4641-7.

Qiao, Z.S., Kim, M., Reinhold, B., Montefiori, D., Wang, J.H. and Reinherz, E.L. (2005) Design, expression, and immunogenicity of a soluble HIV trimeric envelope fragment adopting a prefusion gp41 configuration. J Biol Chem 280, 23138-46.

Rao, Z., Belyaev, A.S., Fry, E., Roy, P., Jones, I.M. and Stuart, D.I. (1995) Crystal structure of SIV matrix antigen and implications for virus assembly. Nature 378, 743-7.

Raport, C.J., Gosling, J., Schweickart, V.L., Gray, P.W. and Charo, I.F. (1996) Molecular cloning and functional characterization of a novel human CC chemokine receptor (CCR5) for RANTES, MIP-1beta, and MIP-1alpha. J Biol Chem 271, 17161-6.

Ratner, L., Haseltine, W., Patarca, R., Livak, K.J., Starcich, B., Josephs, S.F., Doran, E.R., Rafalski, J.A., Whitehorn, E.A., Baumeister, K. and et al. (1985) Complete nucleotide sequence of the AIDS virus, HTLV-III. Nature 313, 277-84.

Riddell, D.R., Christie, G., Hussain, I. and Dingwall, C. (2001) Compartmentalization of beta-secretase (Asp2) into low-buoyant density, noncaveolar lipid rafts. Curr Biol 11, 1288-93.

Rietveld, A. and Simons, K. (1998) The differential miscibility of lipids as the basis for the formation of functional membrane rafts. Biochim Biophys Acta 1376, 467-79.

Robertson, D.L., Anderson, J.P., Bradac, J.A., Carr, J.K., Foley, B., Funkhouser, R.K., Gao, F., Hahn, B.H., Kalish, M.L., Kuiken, C., Learn, G.H., Leitner, T., McCutchan, F., Osmanov, S., Peeters, M., Pieniazek, D., Salminen, M., Sharp, P.M., Wolinsky, S. and Korber, B. (2000) HIV-1 nomenclature proposal. Science 288, 55-6.

Rodgers, W. and Rose, J.K. (1996) Exclusion of CD45 inhibits activity of p56lck associated with glycolipid-enriched membrane domains. J Cell Biol 135, 1515-23.

Ryu, S.E., Kwong, P.D., Truneh, A., Porter, T.G., Arthos, J., Rosenberg, M., Dai, X.P., Xuong, N.H., Axel, R., Sweet, R.W. and et al. (1990) Crystal structure of an HIV-binding recombinant fragment of human CD4. Nature 348, 419-26.

Samson, M., Labbe, O., Mollereau, C., Vassart, G. and Parmentier, M. (1996) Molecular cloning and functional expression of a new human CC-chemokine receptor gene. Biochemistry 35, 3362-7.

Sanchez-Pescador, R., Power, M.D., Barr, P.J., Steimer, K.S., Stempien, M.M., Brown-Shimer, S.L., Gee, W.W., Renard, A., Randolph, A., Levy, J.A. and et al. (1985) Nucleotide sequence and expression of an AIDS-associated retrovirus (ARV-2). Science 227, 484-92.

Sandvig, K., Garred, O., van Helvoort, A., van Meer, G. and van Deurs, B. (1996) Importance of glycolipid synthesis for butyric acid-induced sensitization to shiga toxin and intracellular sorting of toxin in A431 cells. Mol Biol Cell 7, 1391-404.

Sattentau, Q.J. and Moore, J.P. (1991) Conformational changes induced in the human immunodeficiency virus envelope glycoprotein by soluble CD4 binding. J Exp Med 174, 407-15.

Sattentau, Q.J., Moore, J.P., Vignaux, F., Traincard, F. and Poignard, P. (1993) Conformational changes induced in the envelope glycoproteins of the human and simian immunodeficiency viruses by soluble receptor binding. J Virol 67, 7383-93.

Scholz, C., Schaarschmidt, P., Engel, A.M., Andres, H., Schmitt, U., Faatz, E., Balbach, J. and Schmid, F.X. (2005) Functional solubilization of aggregation-prone HIV envelope proteins by covalent fusion with chaperone modules. J Mol Biol 345, 1229-41.

Schroeder, R.J., Ahmed, S.N., Zhu, Y., London, E. and Brown, D.A. (1998) Cholesterol and sphingolipid enhance the Triton X-100 insolubility of glycosylphosphatidylinositol-anchored proteins by promoting the formation of detergent-insoluble ordered membrane domains. J Biol Chem 273, 1150-7.

Shu, W., Ji, H. and Lu, M. (2000) Interactions between HIV-1 gp41 core and detergents and their implications for membrane fusion. J Biol Chem 275, 1839-45.

Simon, F., Mauclere, P., Roques, P., Loussert-Ajaka, I., Muller-Trutwin, M.C., Saragosti, S., Georges-Courbot, M.C., Barre-Sinoussi, F. and Brun-Vezinet, F. (1998) Identification of a new human immunodeficiency virus type 1 distinct from group M and group O. Nat Med 4, 1032-7.

Simons, K. and Ikonen, E. (1997) Functional rafts in cell membranes. Nature 387, 569-72.

Singer, S.J. and Nicolson, G.L. (1972) The fluid mosaic model of the structure of cell membranes. Science 175, 720-31.

Skehel, J.J. and Wiley, D.C. (2000) Receptor binding and membrane fusion in virus entry: the influenza hemagglutinin. Annu Rev Biochem 69, 531-69.

Sleckman, B.P., Peterson, A., Jones, W.K., Foran, J.A., Greenstein, J.L., Seed, B. and Burakoff, S.J. (1987) Expression and function of CD4 in a murine T-cell hybridoma. Nature 328, 351-3.

Speck, R.F., Wehrly, K., Platt, E.J., Atchison, R.E., Charo, I.F., Kabat, D., Chesebro, B. and Goldsmith, M.A. (1997) Selective employment of chemokine receptors as human immunodeficiency virus type 1 coreceptors determined by individual amino acids within the envelope V3 loop. J Virol 71, 7136-9.

Stefanova, I. and Horejsi, V. (1991) Association of the CD59 and CD55 cell surface glycoproteins with other membrane molecules. J Immunol 147, 1587-92.

Stein, B.S., Gowda, S.D., Lifson, J.D., Penhallow, R.C., Bensch, K.G. and Engleman, E.G. (1987) pH-independent HIV entry into CD4-positive T cells via virus envelope fusion to the plasma membrane. Cell 49, 659-68.

Suomalainen, M. (2002) Lipid rafts and assembly of enveloped viruses. Traffic 3, 705-9.

Tan, K., Liu, J., Wang, J., Shen, S. and Lu, M. (1997) Atomic structure of a thermostable subdomain of HIV-1 gp41. Proc Natl Acad Sci U S A 94, 12303-8.

Taraboulos, A., Scott, M., Semenov, A., Avrahami, D., Laszlo, L. and Prusiner, S.B. (1995) Cholesterol depletion and modification of COOH-terminal targeting

sequence of the prion protein inhibit formation of the scrapie isoform. J Cell Biol 129, 121-32.

Thompson, T.E. and Tillack, T.W. (1985) Organization of glycosphingolipids in bilayers and plasma membranes of mammalian cells. Annu Rev Biophys Biophys Chem 14, 361-86.

Tong-Starksen, S.E., Luciw, P.A. and Peterlin, B.M. (1987) Human immunodeficiency virus long terminal repeat responds to T-cell activation signals. Proc Natl Acad Sci U S A 84, 6845-9.

Tran, D., Carpentier, J.L., Sawano, F., Gorden, P. and Orci, L. (1987) Ligands internalized through coated or noncoated invaginations follow a common intracellular pathway. Proc Natl Acad Sci U S A 84, 7957-61.

Triantafilou, M., Morath, S., Mackie, A., Hartung, T. and Triantafilou, K. (2004) Lateral diffusion of Toll-like receptors reveals that they are transiently confined within lipid rafts on the plasma membrane. J Cell Sci 117, 4007-14.

Trkola, A., Dragic, T., Arthos, J., Binley, J.M., Olson, W.C., Allaway, G.P., Cheng-Mayer, C., Robinson, J., Maddon, P.J. and Moore, J.P. (1996) CD4-dependent, antibody-sensitive interactions between HIV-1 and its co-receptor CCR-5. Nature 384, 184-7.

Turpin, J.A. (2003) The next generation of HIV/AIDS drugs: novel and developmental antiHIV drugs and targets. Expert Rev Anti Infect Ther 1, 97-128.

Valentin, A., Albert, J., Fenyo, E.M. and Asjo, B. (1994) Dual tropism for macrophages and lymphocytes is a common feature of primary human immunodeficiency virus type 1 and 2 isolates. J Virol 68, 6684-9.

Varmus, H. (1988) Retroviruses. Science 240, 1427-35.

Veronese, F.D., DeVico, A.L., Copeland, T.D., Oroszlan, S., Gallo, R.C. and Sarngadharan, M.G. (1985) Characterization of gp41 as the transmembrane protein coded by the HTLV-III/LAV envelope gene. Science 229, 1402-5.

Vey, M., Pilkuhn, S., Wille, H., Nixon, R., DeArmond, S.J., Smart, E.J., Anderson, R.G., Taraboulos, A. and Prusiner, S.B. (1996) Subcellular colocalization of the cellular and scrapie prion proteins in caveolae-like membranous domains. Proc Natl Acad Sci U S A 93, 14945-9.

Viard, M., Parolini, I., Sargiacomo, M., Fecchi, K., Ramoni, C., Ablan, S., Ruscetti, F.W., Wang, J.M. and Blumenthal, R. (2002) Role of cholesterol in human immunodeficiency virus type 1 envelope protein-mediated fusion with host cells. J Virol 76, 11584-95.

Wain-Hobson, S., Sonigo, P., Danos, O., Cole, S. and Alizon, M. (1985) Nucleotide sequence of the AIDS virus, LAV. Cell 40, 9-17.

Wang, J.H., Yan, Y.W., Garrett, T.P., Liu, J.H., Rodgers, D.W., Garlick, R.L., Tarr, G.E., Husain, Y., Reinherz, E.L. and Harrison, S.C. (1990) Atomic structure of a fragment of human CD4 containing two immunoglobulin-like domains. Nature 348, 411-8.

Weiss, C.D., Barnett, S.W., Cacalano, N., Killeen, N., Littman, D.R. and White, J.M. (1996) Studies of HIV-1 envelope glycoprotein-mediated fusion using a simple fluorescence assay. Aids 10, 241-6.

Weiss, C.D., Levy, J.A. and White, J.M. (1990) Oligomeric organization of gp120 on infectious human immunodeficiency virus type 1 particles. J Virol 64, 5674-7.

Weissenhorn, W., Dessen, A., Harrison, S.C., Skehel, J.J. and Wiley, D.C. (1997) Atomic structure of the ectodomain from HIV-1 gp41. Nature 387, 426-30.

Weissenhorn, W., Wharton, S.A., Calder, L.J., Earl, P.L., Moss, B., Aliprandis, E., Skehel, J.J. and Wiley, D.C. (1996) The ectodomain of HIV-1 env subunit gp41 forms a soluble, alpha-helical, rod-like oligomer in the absence of gp120 and the N-terminal fusion peptide. Embo J 15, 1507-14.

Wild, C.T., Shugars, D.C., Greenwell, T.K., McDanal, C.B. and Matthews, T.J. (1994) Peptides corresponding to a predictive alpha-helical domain of human

immunodeficiency virus type 1 gp41 are potent inhibitors of virus infection. Proc Natl Acad Sci U S A 91, 9770-4.

Wingfield, P.T., Stahl, S.J., Kaufman, J., Zlotnick, A., Hyde, C.C., Gronenborn, A.M. and Clore, G.M. (1997) The extracellular domain of immunodeficiency virus gp41 protein: expression in Escherichia coli, purification, and crystallization. Protein Sci 6, 1653-60.

Wu, H., Kwong, P.D. and Hendrickson, W.A. (1997) Dimeric association and segmental variability in the structure of human CD4. Nature 387, 527-30.

Wyatt, R., Kwong, P.D., Desjardins, E., Sweet, R.W., Robinson, J., Hendrickson, W.A. and Sodroski, J.G. (1998) The antigenic structure of the HIV gp120 envelope glycoprotein. Nature 393, 705-11.

Yoshie, O., Imai, T. and Nomiyama, H. (1997) Novel lymphocyte-specific CC chemokines and their receptors. J Leukoc Biol 62, 634-44.

Yu, J., Fischman, D.A. and Steck, T.L. (1973) Selective solubilization of proteins and phospholipids from red blood cell membranes by nonionic detergents. J Supramol Struct 1, 233-48.

Zisch, A.H., D'Alessandri, L., Amrein, K., Ranscht, B., Winterhalter, K.H. and Vaughan, L. (1995) The glypiated neuronal cell adhesion molecule contactin/F11 complexes with src-family protein tyrosine kinase Fyn. Mol Cell Neurosci 6, 263-79.

Zlotnik, A., Morales, J. and Hedrick, J.A. (1999) Recent advances in chemokines and chemokine receptors. Crit Rev Immunol 19, 1-47.

Zurcher, T., Luo, G. and Palese, P. (1994) Mutations at palmitylation sites of the influenza virus hemagglutinin affect virus formation. J Virol 68, 5748-54.